Mathematical Modelling of Tumour-Immune Interactions and Cancer Therapy

by

Khaphetsi Joseph Mahasa
Supervisor: Dr. Rachid Ouifki
Co-supervisor: Prof. Amina Eladdadi

Dissertation presented at the University of Stellenbosch for the degree of

Doctor of Philosophy

Department of Mathematical Sciences
University of Stellenbosch

December **2017**

Declaration

I, the undersigned, hereby declare that the work contained in this thesis is my own original work and has not previously, in its entirety or in part, been submitted at any university for a degree.

December 2017

Khaphetsi Joseph Mahasa

Date

Abstract

The immune system plays a key role against the development and progression of tumor cells mainly because of its capability of recognizing and destroying cancerous cells. While incredible research efforts have been made over the past decades to decipher the complexity of the tumor-immnue interactions, there is still a lack of a definite and complete picture of these interactions. This may be attributed to the fact that tumor cells develop intricate mechanisms to evade detection and control by the immune system and resist treatments.

Although this has been attributed to tumor escape from the immune system, no quantitative studies have been made to precisely characterize key tumor evasion mechanisms from immune surveillance. There is a growing need for new modeling approaches that take into account the complexity of immune system response and/or tumor escape mechanisms, and the recent advances in cancer therapy. This lack has motivated the work in this thesis. We focused our research on addressing the following three scientific questions: (1) How do tumors evolve by escaping immune surveillance? (2) How can oncolytic virus infection of some normal cells in the vicinity of tumor cells enhance oncolytic virotherapy? (3) How can the use of cell carriers for the delivery of oncolytic virus particles to tumor sites affect the outcomes of oncolytic virotherapy in the presence of active immune response?

To address these major questions, we have devised three novel mathematical models to study the behaviour of tumor cells following their interactions with key cytotoxic immune cells and oncolytic viruses. The results herein this thesis show the development of immunoresistant phenotype by tumor cells to effectively evade the immune system. This thesis supports the natural killer (NK) cell-based immunotherapeutic approaches that are aimed at enhancing the immune surveillance of tumors. Our work also highlights an interesting possibility of infecting some normal cells in the vicinity of tumor cells to increase the oncolytic infectious titers within tumor microenvironment. Additionally, our findings provide pertinent information on how the use of certain cell carriers may enhance oncolytic virotherapy in the presence of effective immune response within the tumor microenvironment.

Opsomming

Die immuunstelsel speel 'n sleutelrol om die ontwikkeling en groei van tumor selle teen te werk, hoofsaaklik as gevolg van die vermoë om kanker selle te herken en te vernietig. Terwyl ongelooflike navorsing oor die afgelope dekades gedoen is om die kompleksiteit van die tumor-immuun interaksies te ontleed, is daar nog nie 'n definitiewe en volledige beeld van hierdie interaksies nie. Dit kan toegeskryf word aan die feit dat tumorselle ingewikkelde meganismes ontwikkel om opsporing en beheer deur die immuunstelsel te ontduik en behandelings te weerstaan. Alhoewel dit toegeskryf word aan tumors wat van die immuunstelsel onsnap, is geen kwantitatiewe studies gedoen om die belangrikste ontduikingsmeganismes teen immuniteitswaarneming presies te karakteriseer nie. Daar is 'n toenemende behoefte aan nuwe modelleringsbenaderings wat die kompleksiteit van die immuunstelselrespons en / of tumor-ontsnappingsmeganismes in ag neem, asook die onlangse vordering in kankerterapie. Hierdie gebrek het die werk in hierdie proefskrif gemotiveer. Ons navorsing is gefokus daarop om die volgende drie vrae aan te spreek: (1) Hoe verander of ontwikkel die gewasse deur die immuunstelsel se toesig vry te spring? (2) Hoe kan onkolitiese virusinfeksie van sommige normale selle in die omtrek van tumor selle onkolitiese viroterapie verbeter? (3) Watter invloed kan die gebruik van seldraers vir die toediening van onkolitiese virusdeeltjies na die omgewing van die gewas h op die resultaat van onkolitiese virapie in die teenwoordigheid van aktiewe immuunrespons? Om hierdie hoofvrae aan te spreek, het ons drie wiskundige modelle opgestel om die gedrag van tumorselle te ondersoek deur hul interaksies met belangrike sitotoksiese immuunselle en onkolitiese virusse te volg. Die resultate in hierdie proefskrif toon die ontwikkeling van immunoresistante fenotipe deur tumorselle om die immuunstelsel doeltreffend te ontduik. Hierdie proefskrif ondersteun die natuurlike uitwisser (NK) se selgebaseerde immunoterapeutiese benaderings wat daarop gemik is om die immuunstelsel se opsporing van gewasse te verbeter. Ons werk beklemtoon ook die interessante moontlikheid om sommige normale selle in die omgewing van tumorselle te besmet om die onkolitiese infeksie tellings binne die mikro-omgewing van die tumor te verhoog. Daarbenewens verskaf ons bevindings relevante inligting oor hoe die gebruik van sekere seldraers onkolitiese viroterapie kan verbeter in die teenwoordigheid van effektiewe immuunrespons binne die gewas se mikro-omgewing.

Dedication

This thesis is dedicated to my beautiful wife, Macharles Anastasia Mahasa (Ntsoaki A. Rabele). She had always motivated and supported me during this PhD journey. Her genuine unconditional love gave me an indispensable surge of energy to accomplish this thesis.

Acknowledgments

First and foremost, I would like to thank the Almighty God for granting me with all the necessary and sufficient strength to accomplish this thesis. Without His endless mercy the mission would have been impossible. I would like to wholeheartedly thank my supervisor, Dr. Rachid Ouifki, for his endless and constructive support he gave me throughout this journey. He continually challenged me to think and rationalize everything from a mathematical and modeling perspective. I will always remember his guidance and encouragement to keep moving even during difficult times in my PhD voyage.

I would like to profoundly thank my co-supervisor, Prof. Amina Eladdadi of the College of Saint Rose, Albany NY, for her indescribable and unprecedented supervision and mentoring throughout the years of this study. At first, I could not understand what she demanded of me. She would always question every biological blurb I put forward in my research and vehemently emphasize that I should dig deep into the biology behind my ideas before I come with my beautiful mathematics. At first, I saw that as a punishment, only to be discover later that was a blessing in disguise. Throughout all the years of my thesis, I had her view of keeping up the good work rammed down my throat.

I will forever be indebted to Prof. Lisette de Pillis of Harvey Mudd College, Claremont, CA for her involvement in my thesis. She humbly and kindly nurtured me to grow in the field of mathematical oncology. Her reviews, comments and technical suggestions had vastly improved every part of my work in this thesis. She made me find an appropriate balance between mathematics and the biology of the complex field of tumour-immune dynamics. Her world-renowned expertise in the field of mathematical modeling of the tumor-immune dynamics set the foundation for many of the researchers and made it possible for me to develop the work in my thesis. Thank you Prof. Lisette de Pillis ! We're very grateful for that.

I also greatly thank Prof. Chae-Ok Yun and Prof. Arum Yoon for their collaborative support and provision of new experimental data.

I pass my thanks to the administrators of SACEMA, the former director, Dr. Alex Welte, the current director, Prof. Juliet Pulliam, for their supportive and constructive questions he made during my research presentations at SACEMA seminars. I also like to extend my sincere thanks to all SACEMA folks who had always emotionally and academically supported me. Above all, I would like to thank SACEMA stirring committee for granting me the financial support for my PhD study and conference travels. I also take this moment to thank all of my friends who contributed positively to my PhD journey. Your true friendship means a lot to me.

I would like to acknowledge and thank the Society for Mathematical Biology (SMB) for granting me the SMB Landahl-Busenberg Award not once but twice to present my research at the 2016 SMB/ECMT annual meeting in Nottingham and at the SMB2017 in Salt Lake City in Utah, USA.

The list is endless of the people who supported and touched my heart during my PhD journey. I thank everyone not mentioned here, but who played a great part in my life in general. A special thankfulness goes to my family. My parents played a central role in every part of my life. My profound thankfulness goes to my mother, Mamolefi Lucy Mahasa, for her intricate and passionate love she has shown me from my birth. Your everlasting love has given me a hope in life and has guided me in righteous paths. I am very indebted to my grandmother, Maliako Matete, who brought me up and encouraged me to never cease schooling. She fought all the financial battles I unavoidably faced since my childhood. She had always wanted me to become a "Doctor" so that I can attend her when she is "sick" in her old ages. Her unconditional love and endless support paved every path to my success. I would like to thank my brothers: Molefi Mahasa (and his wife, Maneo Mahasa) and Kekeletso Mahasa ($1988 - 2017$. May his soul rest in peace), and my sister, Ntsoaki Mahasa, who continually supported and prayed for me in all of my ventures. You have all individually played a special part in my life. Above all, I would like to pass my deepest gratitude to my lovely wife, Macharles Anastasia Mahasa, who had been my walking stick in this PhD journey, and supported me in everything I do in life. I would have not made it to this far without your unwavering and unconditional love. My special thanks goes to my

parents-in-law: Lekhetho Rabele and Mamolise Rabebe, for being there in every part of my life. Your parental love to me has been far more than just being a son-in-law. I would also like to acknowledge my brothers-in-law: Raboshabane Rabele and Molise Liphapang for their supportive love in life. In particular, I truly thank Molise Liphapang for his motivational support and encouragement to become a great mathematical oncologist. Your amicable and sincere love is greatly appreciated. I also thank my sister-in-law, Mpolokeng Liau, for her support and care to my son when I and wife have come to South Africa during my PhD research. Last, but not least, I would like to thank my children: Charles Katleho Mahasa and Lerato Mildred Mahasa, for always coming to play with me when I am very stressed with my research work. Your playful, yet absolutely necessary, moments had always refreshed my mind and prompted me to resume with energized effort.

List of Publications

The work in this thesis resulted in two publications. We are working on the third and fourth manuscripts that we plan to submit very soon.

1. Mahasa KJ, Ouifki R, Eladdadi A, de Pillis L. Mathematical model of tumor–immune surveillance. Journal of Theoretical Biology. 2016; 404:312–330.
2. Mahasa KJ, Eladdadi A, de Pillis L, Ouifki R. Oncolytic Potency and Reduced Virus Tumor-specificity in Oncolytic Virotherapy. A Mathematical Modelling Approach. PloS one. 2017; 12(9):e0184347.
3. **Mathematical Model of Oncolytic Virus Delivery By Cell Carriers**. Letters in Biomathematics (Submitted)
4. **A computational model for targeting tumor vasculature endothelium collapse with oncolytic virus therapy: Implications for the design of immunovirotherapies**. (In preparation)

Contents

List of Figures

List of Tables

Chapter 1

Introduction and Thesis Overview

In this chapter, we present the motivation and the rationale behind our mathematical modeling of tumour-immune system interactions and the effects of oncolytic virotherapy in maintaining tumor control. We also present a short review of immune surveillance of tumors and the mechanisms that tumors often engage to escape immune response.

1.1 Preview of thesis contributions

This research has three main aims which are:

1. To formulate a novel differential-equation based mathematical model for the immune surveillance of tumors. The model describes how tumor cells evolve and survive the brief encounter with the immune system mediated by natural killer (NK) cells and the activated $CD8^+$ cytotoxic T lymphocytes (CTLs).
2. To develop an original delay differential equation mathematical model describing the interactions between the oncolytic virus, the tumor cells, the normal cells, and the antitumoral and antiviral immune responses. We derive the model's basic reproductive number within tumor and normal cell populations and use their ratio as a metric for virus tumor-specificity.
3. To construct a new differential-equation based mathematical model that describes the use of the mesenchymal stem cell-based and T cell-based therapies for the delivery of oncolytic viruses to tumor site. We use the model to simulate and compare the

efficacy of delivering oncolytic viruses by either type of therapy. This comparison is essential for understanding the possible treatment benefits of each therapy.

1.2 Motivation

The motivation for this mathematical modeling of tumor-immune interactions and cancer therapy stems from the lack of a quantitative framework to precisely predict how certain types of tumors evolve to elude active immune system and some cancer treatments, particularly immunotherapy and oncolytic virotherapy. The hypothesis of immune surveillance (defined as the ability of the immune system to recognize and destroy neoplastic cells before they develop into clinically detectable tumors) has led to the evolution and development of immunotherapies. The immunotherapies are currently being utilised in isolation or in combination with conventional chemotherapy. Despite these great advances, tumors however often display a wide variety of complex mechanisms to evade immune system recognition and control. Thus, this suggests that there is a clear need for new cancer research which may be appropriate for eradicating tumors or at least bring them to a controllable state. Before we describe such modeling attempts in the next chapters, we first give a brief overview of immune surveillance of tumors.

1.2.1 Immune surveillance

In the early 20^{th} century, Paul Ehrlich, a German scientist, proposed a theory of tumor immune surveillance [2]. Following his studies about the roles of immune response in controlling infections caused by microorganisms, he investigated if the same observations exist in cancer [3]. An immune surveillance is an effective host defence against formation and progression of tumor cells. According to immune surveillance hypothesis, immune effector cells orchestrate the host body like sentinels in attempt to recognize and eliminate the incipient cancer cells and nascent tumors [2, 4, 5]. An existence and importance of immune surveillance of tumors in both mice and humans was experimentally and epidemiologically elucidated by Dunn et al. [2]. The findings of Dunn et al. [2] showed that:

(i) Immune system has capacity to recognise and destroy nascent transformed cells (Elim-

ination phase (immunosurveillance))

(ii) Some tumor cells may survive immune destruction and become dormant for certain period of time (Equilibrium phase (i.e., the phase where immuno-editing occurs)

(iii) After some time, selected tumor cell variants from the equilibrium phase can now grow into clinically detectable tumors.

Importantly, Dunn et al. [2] showed that the host immune system does not only protect the host organism, but also "sculpts" tumor phenotype. An overwhelming body of research suggests that tumor cells express surface molecules that render them as "non-self" or "foreign" to the immune system [4–10]. These surface molecules are known as tumor antigens. Expression of theses antigens can trigger reactions from both the innate and the adaptive immune system [2, 11, 12]. More recently, an accumulating evidence from genetically engineered mice suggests that the host immune surveillance, at least to some certain types of tumors, provides a significant shield against tumor development and progression [13–15]. In particular, mice with deficiencies in the functionality of activated $CD8^+$ cytotoxic T lymphocytes (CTLs), $CD4^+$ T_h^1 helper T cells, or natural killer (NK) cells showed an increased incidence of tumorigenesis [15].

Additionally, evidence from clinical epidemiology also confirm and support the existence of host immune surveillance against human tumors [16]. High infiltration of activated CTLs and NK cells to patients with colon and ovarian tumors lead to improved prognosis than those who lacked such immune killer lymphocytes [17–19]. This further shows that host immune surveillance serves an effective barrier to tumorigenesis and tumor progression. Additionally, importance of tumor immunosurveillance in humans has been observed in patients with immunosuppressed transplant organs, where the development and progression of tumor growth was kept in dormant state by the immune system [20]. The presence of activated $CD8^+$ cytotoxic T lymphocytes (CTLs) at the tumor site has been shown to provide an improved prognosis for patients with colorectal tumors [21]. An illustration of cancer "immunoediting" by Dunn et al. [2] provides additional viable evidence of a key function of immune surveillance in controlling tumorigenesis (i.e., formation of tumors) and tumor progression [22–24].

Although immune surveillance of tumor is an essential host first line of defence, accumulating evidence, however, suggests that highly immunogenic tumor cells may employ a

variety of mechanisms to evade immune destruction and control [2, 13, 23, 25]. Such escape mechanism are discussed in the next section.

1.2.2 Tumor-immune evasion mechanisms

Evasion of tumor cells from immune system control is currently considered as a second emerging hallmark of cancer [25]. Emerging evidence indicates that tumors are not passive targets of host immune lymphocytic cells [26]; instead, they actively display a wide variety of mechanisms to avoid immune system recognition and control. Such mechanisms are listed in Table 1.1.

TABLE. 1.1: Tumor escape mechanisms from immune surveillance

Strategy	Mechanism	References
Impaired antigen expression	Downregulation of tumor antigens	[22, 27, 28]
	Downregulation of MHC molecules	[22, 29–32]
Expression of Immunosuppressive factors	Cytokines (Interleukin 10 (IL-10), Transforming Growth Factor (TGF)-β), vascular endothelial growth factor (VEGF)	[22, 27, 32–34]
Ignorance	Lack of danger signals (or "pathogenic-associated molecular patterns" (PAMPs))	[35–37]
Apoptosis resistance	Downregulation of pro-apoptotic molecules or up-regulation of anti-apoptotic molecules (such FLICE-inhibitory proteins, surface protein B7-H1)	[29, 36–40]
Counterattack	Expression of Fas ligand (FasL)	[29, 36, 41–44]

	Expression of TRAIL [tumor necrosis factor (TNF)-related apoptosis-inducing ligand]	[26, 36]
Immune tolerance	Lack of costimulatory molecules	[29, 36, 45]
	Inadequate or inappropriate antigen (Ag) processing and presentation of tumor-associated antigens (TAA) by antigen-presenting cells (APCs)	[26, 29]
	Immunesupression by Regulatory T cells (such as $CD4^+$ $CD25^+$ T cells)	[26, 46, 47]

To date, tumor escape from host immune surveillance presents a major obstacle for immunotherapies [44, 47–51]. Molecular and clinical tumor escape mechanisms that enhance tumorigenesis and tumor progression are now known and have been progressively reviewed by Whiteside and colleagues [26, 47]. This thesis is concerned with elucidating how some of these tumor escape hall-marks can be abrogated from a qualitative point of view.

1.3 Thesis outline

The primary contributions to the field of research in this thesis are presented in Chapters 3, 4 and 5. In these chapters, we describe three novel mathematical models that take into account different aspects of tumor-immune interactions and oncolytic virotherapy. The structure of this thesis is as follows:

Chapter 2: Background. We present the relevant biological background on tumor formation and the commonly used cancer treatment procedures. We then give a brief survey of the relevant mathematical models that directly or indirectly influenced the development of the novel models in presented in this thesis. At the end of this chapter, we reiterate the research problem definition and thesis statement.

Chapter 3: Mathematical Model of Tumor-Immune Surveillance. We develop a novel differential-equation based mathematical model that describes how tumor cells evolve

and survive the brief encounter with the immune system mediated by natural killer (NK) cells and the activated $CD8^+$ cytotoxic T lymphocytes (CTLs). We carry out numerical simulations and discuss the results obtained from the model. Numerical simulations of the model are comparable with previously published models of tumor-immune interactions. The model successfully predicts how a low number of key immune cells might lead to tumor escape. We further illustrates some plausible immunotherapeutic approaches to endeavor to minimize tumor evasion from immune surveillance.

Chapter 4: Oncolytic Potency and Reduced Virus Tumor-specificity in Oncolytic Virotherapy. A Mathematical Modeling Approach. In this chapter, we formulate a new delay differential equation mathematical model describing the interactions between the oncolytic virus, the tumor cells, the normal cells, and the antitumoral and antiviral immune responses. Therein, we also present a complete and thorough mathematical analysis of the model and discuss its implications for oncolytic virotherapy. Moreover, we derive the model's basic reproduction number, R_0, and use it in the model simulation as a therapeutic index of oncolytic potency and tumor-specificity. This chapter contains pertinent information on tolerable depletion of normal cells, within tumor vicinity, that favours significant reduction of tumor burden and/or tumor eradication.

Chapter 5: Mathematical Model of Oncolytic Virus Delivery By Cell Carriers. In this chapter, we devise a new mathematical model to study the comparative efficacy of delivering oncolytic viruses by either T cells or mesenchymal stem cells (MSC). The model consists of a coupled system of ordinary differential equations that elucidate the impact of delivering oncolytic viral particles by a certain type of a carrier cell to tumor site. Numerical simulations are carried out to assess the therapeutic benefits of each carrier cell. The effect of antitumoral and antiviral immune responses within tumor microenvironment before and after the delivery of oncolytic viruses at tumor site is also investigated.

Chapter 6: Conclusions. We present a conclusion of this thesis, highlight the major scientific contributions of our work to the field of mathematical oncology, and suggest plausible future directions.

Chapter 2

Background

In this chapter, we present a succinct review of some of the relevant biology and mathematical modeling approaches that have been used to describe various aspects of the tumor-immune system dynamics. Observations from the biological experiments and mathematical modeling of tumor, immune system and oncolytic viruses interactions, motivate the choice of modeling techniques described in the next chapters of this thesis.

2.1 Biology background

In this section, we review the relevant biological literature pertaining to tumor development and progression. We also survey the commonly used cancer treatment treatment modalities.

2.1.1 Tumor formation

A tumor is a mass of masses of proliferating cells that originated from a single normal cell that underwent cellular alterations [52, 53] and began to proliferate uncontrollably [29, 54]. For a given time period, these tumors accumulate more changes that enable them to progressively acquire attributes that would help them to survive within tissues [55, 56]. Recent evidence indicates that tumor is far more than a mass of proliferating cell, but rather a complex tissue composed of multiple distinct cell types [25, 57]. These subpopulations

within the tumor, all contribute distinct, but complementary capabilities that support overall tumor growth in various ways [25]. Hanahan and Weinberg [52] articulated six key phenotypic differences called "hallmarks" of cancer, which distinguish tumor cells from normal cells. These are:

1. Activation of tissue invasion and metastasis
2. Evasion of growth suppressors
3. Resistance to cell death
4. induction and sustenance of angiogenesis
5. Sustenance of proliferative signaling
6. Support of replicative immortality

Recently, low level of oxygen, *hypoxia*, was has been added as a new hallmark of cancer [58]. Hypoxia, usually expressed by advanced solid tumors, results from defective vascularization of oxygen to a tumor site [59, 60].

An increasing body of research supports inclusion of two additional hallmarks of cancer, yet not generalized and fully validated, which are involved in the tumorigenesis of some and perhaps all cancerous cells [25, 61, 62]. Such new hallmarks involve deregulations of cellular energy metabolism in order to support progressive tumor cell growth and proliferation, and active tumor cells evasion from immune surveillance [25]. In the next section, we present a succinct review of current treatment modalities available to cancer patients.

2.2 The immune system

The immune system plays unprecedented role in protecting the body against pathogens such as bacteria or viruses, and elimination of transformed cells in the body. It has two major constituents, namely an innate and adaptive immunities. A central difference in these components lies in their abilities to recognise "non-self" (foreign) cells or transformed cells, such as a tumor cell. The innate immune cells are capable of recognizing a foreign cell without being primed (i.e., being trained to recognise) about such foreign cells, while the adaptive immune cells need to be primed about the existence of the foreign cell or a transformed cell in the body [4, 5, 7].

The Natural Killer (NK) cells constitute an important cytotoxic component of the innate immunity. The NK cells serve as sentinels in the body against pathogens or transformed cells, and play a crucial role in immunosurveillance of tumors [2, 7, 8, 63]. To identify abnormal cells or virus infected cells, NK cells use a broad spectrum of "missing self" signals [10] that help them to distinguish if a target cell should be destroyed or not. After identifying the target cell to destroy, NK cells may secrete lethal chemicals, such as perforin which binds to the cell membrane of a target cell, and form lytic pores through which they send deadly cytokines into the target cell [64, 65]. Serving as a specific part of the adaptive immunity, the activated $CD8^+$ Cytotoxic T Lymphocytes (CTL) play a crucial role in controlling the development of tumor cells. The $CD8^+$ CTLs also use similar cytotoxic pathways to kill the target cells [4, 37]. The $CD8^+$ CTLs are, however, known to mount a more robust attack against transformed cells than NK cells [4, 64].

As another means of evading the immune system destruction, tumor may usurp the immune checkpoints expressed on activated T cells [66]. The immune checkpoints are inhibitory pathways that often reduce the strength and duration of immune responses [67]. The immune checkpoints inhibitors are drugs that help to block the immune checkpoints by targeting the blockage of the cytotoxic T-lymphocyte-associated protein 4 (CTLA-4) or programmed cell death protein 1 (PD-1) expressed by T cells. The Clinical clinical research is now focusing on combination therapy of immune checkpoint inhibitors with other therapies, such as oncolytic virotherapy [66, 68]. Even though the immunological activation induced by the checkpoint inhibitors is non-specific, clinical evidence indicates that the checkpoint blockade therapy has often resulted in unprecedented enhancement and durability of the immune responses in some cancer patients [69, 70].

2.3 Cancer treatment modalities

A variety of treatment modalities, such as surgery, chemotherapy and radiotherapy, have been used to treat different types of cancers over the past decades. Surgery is used where a tumor can be easily accessed and removed directly. Chemotherapy involves utilization of chemical drugs that aim at destroying fast replicating cells, which is a typical characteristic of cancerous cells. Radiotherapy attempts to kill and destroy cancerous cells via a direct

application of radiation on the affected area. Despite their individual successes, most of these therapeutics are often combined to achieve results. However, a commonly reported limitation of these therapeutics is their relative low efficacy and high toxicity to non-cancerous, healthy cells. There are other emerging novel therapeutics, like gene therapy, angiogenetic inhibitors, immunotherapy and oncolytic virotherapy, that are in clinical trials to treat certain types of cancers. A major aim of all these new treatment modalities is to minimize unwanted toxicities on normal healthy tissues, while simultaneously maximizing tumor targeting. In this review, we only provide recent review of therapeutics that are purported to have better treatment outcomes in clinics.

2.3.1 Chemotherapy

In cancer research, chemotherapy is a treatment modality that involves use of chemical drugs to combat cancer. Chemotherapeutic agents are usually classified into two broad categories: "targeted" and "cytotoxic" drugs [71]. Targeted drugs are designed to distract cancer-specific pathways, for instance, by blocking a kinase oncogene [72]. Cytotoxic drugs work by directing damaging ribonucleic acid (RNA) or deoxyribonucleic acid (DNA), or microtubules, and in human body they are believed to preferentially destroy fast proliferating cells [71, 73]. These cytotoxic drugs target rapidly replicating cells, which is a common attribute of all cancerous cells [74, 75]. Thus, they kill target cells by halting cell division, facilitating a damage of RNA or DNA. Chemotherapeutic drugs are delivered via direct injection into a bloodstream (intravenous injection) [76], hepatic arterial infusion pumps [77], clinical drips (intravenous infusion) [78], or orally as chemotherapy tablets [79]. These drugs are assumed to circulate through the blood to annihilate rapidly dividing cells or at least prohibit them from spreading from their primary sites. In this manner, chemotherapeutic drugs are often considered to be the prime candidates for treating metastatic tumors. A major outstanding challenge with chemotherapeutic drugs is that they only target rapidly replicating cells. Thus, they do not distinguish between fast replicating cancerous and non-cancerous cells. Evidence indicates that there are other non-cancerous cells, such as bone marrow cells, immune cells and hair follicle cells, that are know to be fast replicating [73] and such cells, are also destroyed by chemotherapeutic drugs [71, 73]. Chemotherapeutic agents are usually administered in cycles ranging one to eight cycles, where one cycle may last between $1 - 5$ days [80].

Currently, there are many approved distinct types of chemotherapeutic agents, which are either administered in isolation or in combinations. It is important to note that chemotherapeutic drug administration varies from patient to patient. They may be given based on the type of cancer, its size and stage (i.e., whether is a benign tumor or metastatic tumor). In clinics, currently there is no unequivocal consent on the optimal chemotherapeutic regimes [81]. Thus, there is a need for further biological, mathematical and clinical research to address this issue.

2.3.2 Radiotherapy

Depending on the type of cancer, its resident location, stage and grade, patients may receive beams of ionising radiation, including X-rays, gamma rays, and heavy ions, that pierce tumor host tissue and distract the DNA of the cell. This method of cancer treatment is called Radiotherapy. Damage generated by ionising radiation usually alter the growth and division patterns of the affected cell. Thus, depending on the extent of damage of DNA damage, affected cells may undergo either a transient or permanent cell cycle arrest, and/or cell death [82]. On the other hand, depending on the extent of ionising radiation, healthy cells can be rapidly regenerated, but tumor cells cannot [83]. However, it is important to note that if cell is not aligned for apoptosis (i.e., programmed cell death), its survival depends diametrically on DNA repair [82]. Sometimes, radiotherapy can be administered prior to clinical surgery in order to reduce tumor burden, thus improving the success of the surgery. Similar to chemotherapy, a major limitation of radiotherapy is toxicity to healthy tissue surrounding a tumor [84].

2.3.3 Immunotherapy

Recent evidence indicates a great advancement in field of immunology. Molecular and cellular understanding of functionality and control of immune system in response to “non-self” or “foreign” cells in the body has widely opened new promising cancer therapies that augment the ability of immune response. For instance, recent evidence shows that toll-like receptor agonists can be used to boost immune responses to combat tumors [85]. Furthermore, major advances in cell-based immunotherapies such as adoptive T cell therapy

(ACT) [86], NK cell-based immunotherapy [87], and dendritic cell immunotherapy [88] have been established. Furthermore, an emerging evidence shows that a large numbers of monoclonal antibodies (mAbs) has recently being developed to treat tumors, and many of the available antibodies have shown a positive clinical responses. A succinct review of the current immunotherapies is given by Galluzzi et al. [89]. These immunotherapies are attractive because they enhance immune surveillance through activation and proliferation of endogenous cells in cancer patients [87].

2.3.4 Oncolytic virotherapy

Oncolytic virotherapy is a treatment modality that uses viruses that are capable of replicating in, and killing tumor cells with little or no harm to normal cells [66, 90–95]. Oncolytic viruses (OVs) either have a natural tumor tropism or are genetically engineered to target tumor cells [96–100]. Tumor targeting is achieved by deleting and/or inserting specific genes, potentiating viral replication within tumors while having attenuated replication in normal cells, in the genome of the oncolytic virus [101, 102]. One of the approaches fostering oncolytic virus to target tumor cells is transductional targeting (sometimes called oncoselectivity targeting) [91, 103]. If an oncolytic virus shows an increased potency in replicating within and destroying tumor cells over non-cancerous cells, it is said to be oncoselective or tumor-specific [104]. There are two approaches for increasing oncoselectivity for a given virus [104]:

(i) Changing of virus entry tropism. This approach involves changing of the cell type to which the oncolytic virus often enters most efficiently so that the virus can only bind and enter into the targeted tumor cell via some specific receptors at its surface.
(ii) Increasing of viral replication. This approach involves increasing of virus replication in tumor cells or reducing viral replication in healthy non-cancerous cells, or both.

Since neither approach has been employed independently and has shown perfect tumor-specificity [104], these two approaches are often combined to enhance tumor targeting. Tumor-specificity, however, remains a complex and challenging multistep process in oncolytic virotherapy [91, 105, 106].

Oncolytic viruses (OV) are often injected directly into a tumor (i.e., intratumoral administration) or they are injected into the blood (i.e., intravenous administration), where the virons diffuse to tumor sites. Recent research in cancer virology indicates that although intratumoral virus administration minimizes virus loss and maximizes viral load within a tumor, intravenous administration offers better treatment protocol [107, 108]. This is mainly because viruses administered intravenously can reach disseminated metastasis which cannot otherwise be reached directly. Administering OVs through bloodstream is currently considered to be a promising treatment option for treating metastatic tumors [109, 110]. On the other hand, a compelling body of evidence indicates that administration of OVs systemically has many obstacles [111]. The systemically administered naked OVs are susceptible to neutralization by circulating anti-bodies, inactivation by complement proteins and clearance by virus-specific immune cells [66, 109, 112]. In the recent years, much attention has been paid predominantly on mechanisms of virus interaction with tumor cells rather than on processes of oncolytic delivery and entry upon arrival at tumor sites. A new emerging era of oncolytic virotherapy research now focuses on methods that can effectively protect the OVs from immune response. This includes the use of engineered nanoparticles [113] or carrier cells [114] to effectively deliver OVs to tumor sites. Many challenges, however, remain to be addressed before these therapies can be routinely applied in clinical settings. As part of this research, we address some of these systemic delivery challenges from a qualitative point view. It is interesting to note that some few of oncolytic viruses, such as T-VEC [115], are now FDA approved, while others are in their phase II/III of clinical trials [116].

2.3.5 Targeted therapies with tyrosine kinase inhibitors

In the recent years, enormous efforts have been made to tailor treatments to individual patients or tumor cells. The targeted therapies are aimed at blocking certain molecular genes or pathways that increase the spread (metastasis) or growth of tumor cells without harming healthy cells. It is important to note that these therapies target the molecules which may be present in normal cells, but are abundantly expressed on tumor cells [117]. Of particular interest, are the targeted therapies that uses tyrosine kinase inhibitor domain, such as ibrutinib, gefitinib and erlotinib. These drugs target the epidermal growth factor

receptor-(EGFR-) which is often expressed tumors of neck, head or chronic myelogenous leukemia [118]. These drugs are often taken orally as form of pills, and known to be less cytotoxic to normal cells than traditional chemotherapy [117, 119]. There exists an ample clinical evidence that the tyrosine kinase inhibitors are very effective against a number of cancer types, including the chronic lymphocytic leukemia (CLL) [119, 120] and mantle cell lymphoma (MCL) [121]. These drugs have been approved by the US Food and Drug Administration (FDA) for patients with relapsed CLL and MCL.

2.4 Mathematical models of tumor-immune dynamics

In this section, we provide a brief review of appropriate existing mathematical models that incorporate the dynamics of tumor cell interactions with immune system, normal cells, and/or oncolytic viruses. Mathematical models reviewed in this chapter provide a basic understanding of various dynamics of tumor response to treatments, particularly immunotherapy and oncolytic virotherapy. The non-spatial modeling approaches and assumptions reviewed in this section lay a fundamental understanding for the novel mathematical models contained in Chapters $3-5$.

Currently, a considerable number of mathematical models of tumor-immune interactions have been developed, using a variety of differential equations based approaches and individual-based cell techniques. The majority of these models focus on role of immune system against the growth of a solid tumor prior to tumor escape [122]. In the recent decades, a great breadth of detailed molecular mechanisms underlying tumor growth and progression enabled development of a new generation of mathematical models that are specific and data-oriented [123, 124]. Despite the overwhelming evidence of molecular mechanisms of tumor development and progression, a comprehensive knowledge of tumor-immune interactions is still limited. An understanding of immune system response to tumors is essential for development of new, and/or refinement of existing therapeautic approaches.

2.4.1 Models of the tumor and immune cells interactions

In the recent decades, many mathematical models describing the interactions of immune system with tumors have been developed [125–130]. Most of these model are reviewed in [123, 124, 131–134]. Of particular interest in this thesis are the models that illustrate the engagement of immune system in controlling tumor growth and evasion. We present a review and discussion of some of these models that consider immune surveillance of tumors. We only present a review of the mathematical models that provided a profound understanding of the key interactions between tumor cells and immune cells.

Immune surveillance of tumors is considered to be a key host defense mechanism through which the body attempts to inhibit tumor progression and to retain cellular homeostasis. A mathematical model describing how tumors expressing Fas ligand (FasL) may induce an apoptosis on activated lymphocytes via corresponding Fas receptor (Fas) was developed in [135]. An important immune escape mechanism modeled in this model is the expression of death ligand, FasL, by tumor cells. Evidence shows that certain types of tumors constitutively express FasL which might induce apoptosis on activated lymphocytes which express Fas in response to tumor antigen. The model is constructed to illustrate the following molecular interactions between tumor cells and activated T-cells: (a) Tumors often exhibit down-regulated levels of Fas receptor compared to activated T-cells; (b) tumor cells constitutively express the death ligand, FasL, whereas T-cells only express FasL upon activation. The model predicted that by neutralising the expression of Fas ligand or receptor on the cell surface, production of soluble forms of Fas and FasL may enable tumors to evade immune-mediated apoptosis. Through numerical simulations, authors confirmed that MMP inactivation increases Fas-mediated apoptosis for T-cells than for tumor cells. Although the model illustrated most important dynamics of the combat between tumor and T cells, it did not include the possibility of the apoptosis resulting from T-cell-to-T-cell interactions with up-regulated FasL and Fas receptor expression, and tumor-to-tumor cell apoptosis. The latter case may be clinically favourable, as it may contribute to tumor destruction, whereas the apoptosis resulting from T-cell-to-T-cell interactions may promote tumor evasion from immune surveillance.

Another interesting mathematical model describing how cancer immune surveillance is maintained by different immune cells of innate and adaptive immunities was developed

in [126]. The model focused mainly on different roles played by NK and $CD8^+$ T cells in battle against tumor development and progression. Using an experimental data from mouse models, authors investigated parameter estimation and explored model validation. Sensitivity analysis, a procedure for identifying most important parameters in the model in regard to tumor treatment, was also performed. From sensitivity analyses, it was found that the intrinsic tumor cell growth rate and the parameter which indicates how the lysis rate depends on the $CD8^+$ T cell/tumor ratio, were the most significant parameters in the model. This model provides a basic understanding about the distinct key roles played by the natural killer and $CD8^+$ T cells in inhibiting tumor growth and progression. Indeed, the immune system is undoubtedly known to play an important role against the development and progression of neoplasm cells [2, 22, 24, 29, 49, 50, 136, 137]. The model, however, did not illustrate which tumor evasion mechanism do tumor cells evade the immune surveillance. In Chapter 3, we will present and discuss a mathematical modeling framework that addresses to this aspect of tumor escape from the immune surveillance.

2.4.2 Models of the oncolytic viruses, tumor and immune cells interactions

One of the promising therapeutic approaches in treating certain cancers involves the use of virus particles, called oncolytic viruses (OVs). These viruses are capable of infecting and replicating within tumor cells, and have no or less harm to normal non-cancerous cells [93, 96–100, 138–140]. The OVs can also be used to boost the antitumor immune response by expressing pro-inflammatory cytokines and co-stimulatory molecules that are capable of invoking a targeted immune attack against the infected and uninfected tumor cells [141, 142]. Over the past decades, several mathematical models that provide insights into the complex mechanisms inducing the immune response against tumor cells have been developed. The effects of oncolytic virus infection on tumor and normal cell populations, prior to adaptive immune response, have been investigated in [143]. The model focused on elucidating how allowing oncolytic viruses to infect a limited number of normal cells can be of great benefit to oncolytic virotherapy. In particular, the model showed how apparent competition mediated by OVs on tumor-normal cell interactions may contribute to tumor elimination while minimizing the loss of normal cells. Using a combination of analytical and numerical solutions, it was shown that apparent competition can drive tumor to extinction

when there is a small number of surviving tumor cells. Additionally, it was elucidated that the virus burst size and infection rate of tumor cells can have a significant effect in facilitating tumor clearance within a short time frame. Although this model provides a fundamental understanding on how the infection of normal cells can enhance oncolytic virotherapy, it did not fully demonstrate to what extend should normal cells be depleted to achieve the targeted therapeutic outcome. Most importantly, the model did not show how to avoid unwanted endemic infections on normal cell population. These two challenges are fully addressed in the new mathematical model developed in 4.

In another study, the immune response was found to be an indispensable factor that could influence tumor elimination in oncolytic virotherapy [144]. The effects of the immune response triggered by sequential virus administration, an adenovirus (Ad) followed by the oncolytic vesicular stomatitis virus (VSV), were investigated in [144]. The model is based on the experimental settings in [145]. An ordinary differential equations model was constructed to describe the dynamics of the tumor-immune interactions in the experiments in [145]. By considering two biological phenomena, namely multi-stability and multi-instability, it is illustrated that these phenomena equally influence tumors to change their states. That is to change from tumor-free state to tumor-present state, or vice-versa. More importantly, it is indicated that multi-instability can be attributed to an unexpected switch from the tumor-free state to the tumor-present state. Additionally, it is shown that multi-stability is driven by immune response, while multi-instability is driven by the presence of the oncolytic virus.

2.4.3 Models of the delivery of therapeutic agents to tumor sites

Over the past few decades, a considerable number of both experimental and mathematical models have been developed to address a challenge of low delivery of therapeutic agents to tumor sites. These includes use of nanoparticles [113, 146, 147] and macrophages [148, 149] to deliver therapeutic drugs to tumor sites. In this section, we only present a short review of mathematical models that describe the application of cell-based delivery approaches. In [148], a simple mathematical model that describes the growth of tumor spheroids in hypoxic regions was proposed. Since hypoxic regions are known to have low rates of cell proliferation and poor chemotherapeutic drug permeability, authors proposed the model that uses

macrophage infiltration capability into early avascular solid tumors. In particular, they investigated how chemotaxis and chemokine production at tumor sites influence macrophage trafficking, and also how macrophages can be used as cell carriers of chemotherapeutic drugs to the hypoxic tumor sites. Through model simulations, a traditional chemotherapy and a chemotherapy coupled with engineered macrophages (which are used to deliver therapeutic agents to hypoxic tumor sites) were compared. The model predicted that a combination of the standard chemotherapy and macrophage-based therapies is more synergistic, with regard to antitumor efficacy, than the additive impact of each of treatment protocol. The model also predicted that timing of the combined treatment protocol is an important factor which determines the outcome of the treatment. Additionally, the model indicated that the greatest outcome can be achieved when the macrophage-based therapy is carried out shortly before or simultaneously with conventional chemotherapy.

Another intriguing mathematical model for delivery of therapeutic genes within tumor microenvironment by engineered macrophages was developed in [149]. This model is an extension of previous multiphase models developed in [148, 150, 151]. The model is based on *in vitro* growth of tumor spheroids. Through numerical simulations, two modes of drug action in the multicellular tumor spheroids were investigated: either the engineered macrophages delivered the enzyme which is aimed at activating an externally applied prodrug (this was referred as a bystander model) or they delivered cytotoxic drugs directly to tumor spheroids (this was referred to as a local model). Authors found out that the bystander model resulted in similar outcomes to conventional chemotherapy due to poor targeting of hypoxic tumor spheroid regions (i.e., at the center of the spheroid). The local model, however, indicated high sensitivity of the hypoxic tumor regions. Therefore, the authors suggested that in order to precisely target tumor hypoxic regions, it is important to use a chemotherapeutic drug with limited mobility or whose action of mode does not depend on proliferating cells.

Despite the great therapeutic insights unravelled by the above models, they did not consider the impact of immune response within tumor sites upon successful delivery of therapeutic agents, particularly when the macrophages are used to deliver oncolytic viruses. Understanding the influence of immune response is vital for designing effective treatment protocols that are applicable in immunocompetent hosts. This lack of research in this direction motivates the development of the original research contained in Chapter 5.

2.5 Summary

In this chapter, in addition to a brief review of commonly used cancer treatment modalities, we presented a brief literature review of some of the key mathematical models of tumor-immune interactions, and tumor response to treatments, particularly immunotherapy and oncolytic virotherapy. This short literature review does indeed indicate that there has been a substantial advancement in tumor biology and mathematical biology, as well as an increase in the understanding of complex tumor-immune interactions.

Over the past decades, mathematical modeling of tumor-immune interactions has increased our understanding of the tumor progression and response to treatments. In some models discussed above, however, the precise mechanisms by which tumors escape from immune surveillance have not yet been fully studied. In Chapter 3, we will provide a more closer relevant look at some of these tumor-immune interactions which might lead to tumor escape from immune system. In Chapter 4, we will then turn our attention to address some of the outstanding challenges in oncolytic virotherapy, such as lack of sufficient oncolytic viruses at tumor site when administering viruses systemically and inappropriate dosing scheme. Although some of the models discussed above have indicated how cell carriers, such as engineered macrophages, can be used to deliver therapeutic agents to tumor sites, the effect of local immune response within tumor microenvironment has not yet been investigated. The immune system is a major obstacle that can limit the success of oncolytic virotherapy after the cell carriers have successfully delivered their therapeutic payloads. In Chapter 5, in addition to determining the efficacy of two carrier cell-based treatments, we investigate the long-term impact of the immune response within tumor microenvironment.

In the recent decades, many mathematical models describing the interactions of immune system with tumors have been developed [125–130, 152]. Most of these model are reviewed in [123, 124, 131–134]. The mathematical models, developed in this thesis are ordinary differential- and delay-based models. It is worthwhile to note that in the literature, there exists a wide variety of mathematical methods used to describe various dynamics of effective therapeutic protocols. The models range from deterministic ODEs models [11, 153], stochastic process models [154, 155], agent-based models [156, 157], and multiscale models [158–160]. The agent-based models represent each cell as a separate entity that functions as an independent agent in accord with some predefined set of cellular rules. The general

cell behavior is, however, defined by its interactions with other cells and with the host cell microenvironment. The multiscale models are formulated in lattice-based formulations, to account for cell-cell interactions and motions. The diffusion of chemicals and small molecules (virotherpies) among cells are often explicitly described by partial differential equation (PDE) formulations.

In a nut shell, mathematical and computational models have vastly improved our understanding of various biological phenomena and cancer biology. In combination with data, mathematical models can shed light on the underlying mechanisms during cancer treatment [161]. Moreover, in accord with certain biological assumptions, mathematical models can provide a valuable information, and generate new predictions about different treatment aspects, which would otherwise be difficult to make by experimental and clinical studies only.

2.6 Problem definition and thesis statement

As indicated in the above mathematical background discussion, it is obvious that no attempt has been made to precisely characterize key tumor evasion mechanisms from immune surveillance, though some models have illustrated a possibility of tumor evasion from immune system. Currently, there is still a limited understanding of how various tumors evolve to evade immune system detection and control due to complex cellular interactions between individual tumor cells and immune cells. Thus, there is a growing need for new modeling approaches that take into account the complexity of immune system response and/or tumor escape mechanisms, and the recent advances in cancer therapy. As part of this research, we formulate and develop a quantitative framework that provides a complete picture of the complex interactions between the growing tumors and immune system, with particular focus on how individual tumor cells elude immune cells. Additionally, we also provide a succinct quantitative framework that indicates how tumor burden can be reduced, if not completely eliminated, with immunotherapy and oncolytic virotherapy. Herein, we report the development of three novel mathematical models that account for distinct interaction dynamics between tumor cells, normal cells, immune cells, and oncolytic viruses.

Through mathematical modeling, analysis and simulations, the overall goal of this research

is to address the following major scientific questions:

1. How do tumors evolve by escaping immune surveillance?
2. How can oncolytic virus infection of some normal cells in the vicinity of tumor cells enhance oncolytic virotherapy?
3. How can the use of cell carriers for the delivery of oncolytic virus particles to tumor sites affect the outcomes of oncolytic virotherapy in the presence of active immune response?

We tackle these three major scientific questions in Chapters 3, 4 and 5 respectively.

Chapter 3

Mathematical Model of Tumor-Immune Surveillance

We present a novel mathematical model involving various immune cell populations and tumor cell populations to address the following scientific question: ***How do tumors evolve by escaping immune surveillance?*** The model describes how tumor cells evolve and survive the brief encounter with the immune system mediated by natural killer (NK) cells and the activated $CD8^+$ cytotoxic T lymphocytes (CTLs). The model is composed of ordinary differential equations describing the interactions between these important immune lymphocytes and various tumor cell populations. Based on up-to-date knowledge of immune evasion and rational considerations, the model is designed to illustrate how tumors evade both arms of host immunity (i.e. innate and adaptive immunity). The model predicts that: (a) An influx of an external source of NK cells might play a crucial role in enhancing NK-cell immune surveillance; (b) The host immune system alone is not fully effective against progression of tumor cells; (c) The development of immunoresistance by tumor cells is inevitable in tumor immune surveillance. Our model also supports the importance of infiltrating NK cells in tumor immune surveillance, which can be enhanced by NK cell-based immunotherapeutic approaches.

3.1 Introduction

Cancer is still one of the major causes of death worldwide. According to the World Health Organization (WHO), the number of new cancer cases is expected to increase by 70% over the next two decades [162]. Despite substantial advances in the treatment of certain types of cancer over the last few years, a definite cure for cancer is still difficult to find. Of particular importance is the immune system's ability to destroy cancer cells before they can cause harm to the body, a function known as immune surveillance. Studies show that the host immune system can recognize and eliminate cancerous cells [2, 22, 24, 29, 136, 137], and that immunosurveillance mainly acts as a component of a more general process of cancer immunoediting through which neoplastic progression may be inhibited [2, 163]. Research also indicates that, despite immune surveillance, tumors do develop in the presence of a functioning immune system [4, 5, 36, 87]. Additionally, studies suggest that tumor cells quickly acquire various mechanisms to "*escape*" immune surveillance and successfully grow into clinically apparent neoplasms [2, 163–167]. Recent findings also report that tumor escape mechanisms from host immune surveillance present a major impediment for successful immunotherapy [44, 47–51].

3.1.1 Tumor-immune interactions

The Natural Killer (NK) cells are part of the innate immune-effector cells that provide a first line of defense in the body against pathogens, and crucially contribute to the immunosurveillance of tumors [2, 7, 8]. The NK cells have different cytotoxic properties and cytokine-production capacities that enable them to eliminate transformed cells (i.e, tumor cells and viral-infected cells). The NK cells can lyse tumor cells in a variety of distinct ways by exocytosis of perforin, subsequent binding of perforin to the target tumor cell membrane and formation of lytic pores or even by cytokine secretion [64, 65]. Some NK cells can also lyse tumor cells through the expression of the death-inducing ligands Fas ligand (FasL) and tumor necrosis factor (TNF)-related apoptosis inducing ligand (TRAIL). These ligands can induce tumor-cell apoptosis by binding to respective receptors, Fas and TRAILR on the tumor cell surface [168–172]. Tumor cells could also be killed by TNF-

α produced by NK cells [87, 173]. Moreover, some natural killer cells, particularly the natural killer T (NKT) cells [174], secrete various pro-inflammatory cytokines, such as interferon (IFN)-γ and nitric oxide (NO) which act as danger signals, to inhibit tumor development and growth [174–176]. Natural killer cells can also lyse tumor cells through antibody-dependent cellular cytotoxicity (ADCC) which involves binding of antibodies to the FcγRIIIa receptor (CD16) on the NK cells [177, 178].

As part of the adaptive immunity, the activated $CD8^+$ Cytotoxic T Lymphocytes (CTL) play a crucial role in controlling the development of tumor cells. Activation of T cells occurs when the T cell receptors bind to the antigen peptides, on the major histocompatibility complex (MHC) class molecules, presented to them by the antigen presenting cells, such dendritic cells or macrophages [179–182]. Upon recognition of antigen peptides on MHC class I molecules, the activated CTLs can directly kill tumor cells via death cell ligands such as TRAIL or by secreting cytotoxic granules such as perforin or granzyme [175, 183, 184]. The success of immune surveillance in controlling tumor development and growth may also depend on the number of cytotoxic T lymphocytes primed to combat the target cancerous cell. Therefore, another type of T cells called $CD4^+$ T cells become activated and secrete cytokines, such as interleukin-2 (IL-2), which help in the clonal expansion of the cytotoxic T lymphocytes [185–187]. The more the cytotoxic T lymphocytes are produced, the better are the chances of immune surveillance of tumors [185]. Additionally, experimental studies by Gulubova et al. [188] suggest that a low NK cell number could be attributed to escape of metastatic cancer cells from the mechanisms of immune surveillance. Thus, the number of immune cells during the evolution of tumor cells may determine if the host immune system can effectively control tumor growth [185–188].

In this study, we are interested in the long-time dynamics between tumor cells and the host immune cells, and only consider the interplay of a tumor cells with natural killer (NK) cells and cytotoxic T lymphocytes (CTLs). In our modeling framework, we propose that the tumor cells that survived (through genetic mutations or epigenetic changes) a brief attack by either NK or CTLs, or both, have higher chances of acquiring resistance to future attacks by one or both types of immune cells. In fact, a tumor that has survived a lethal encounter with immune cells, usually develops a variety of defensive mechanisms to avoid future destruction by immune cells [29, 36, 136]. In turn, after surviving each encounter with either a NK or CTL, tumor apoptotic resistance to immune system control

increases further via secretion of chemicals that diminish effectiveness of immune cells in the subsequent attacks [136], or by developing mechanisms that down-regulate or inactivate pro-apoptotic molecules, and up-regulate anti-apoptotic molecules [36, 38]. Tumor cells that escaped the initial interactions with immune cells are "wild-type" tumor cells because they are aware of the lethal presence of the immune effectors, and as such, they posses some defensive mechanism from the immune cell types that attacked them [13, 36, 87, 179, 189]. Therefore, after a finite number of encounters with either NK or CTL, or both, a complete or maximal resistance to NK-CTL based immunity is acquired [164].

3.1.2 Previous mathematical models

Several mathematical models of tumor-immune system interactions have been developed by various researchers over the past decades [125–130]. For a comprehensive review of these models, the reader is referred to excellent review articles in [123, 131–134].

Here, we review some of the key papers in the mathematical modeling of tumor-immune interactions. We focus specifically on these papers because we have used them in our model since they mathematically model evasion of tumors from immunosurveillance.

In [126], de Pillis et al. proposed a cancer immunosurveillance model system that considered different immune responses of innate and adaptive immunities to tumors recognition: the natural killer (NK) and $CD8^+$ T cells responses. The model tracked the different roles played by NK and $CD8^+$ T cells on tumor destruction. Based on experimental data, authors developed an innovative functional form to represent the interaction between tumor cells and the $CD8^+$ T cells. This functional form represents a percentage lysis of $CD8^+$ T cells to tumor cells. Their model did indeed set the stage for the cancer immunosurveillance modeling. Details of the hypothesis, such as why the functional form did not work for the natural killer dynamics was kind of lacking. Since in our model we assume that the tumour cells survive an attack by $CD8^+$ CTLs, we have not used this functional form in [126]; instead, we follow the dynamics of binding/detachment of $CD8^+$ CTLs to tumor cells, which lead to tumor escape from immune system, as in [164, 190, 191].

Webb et al. [135] proposed a mathematical model that represented tumor cell-lymphocyte interactions and the cell surface expression of Fas and FasL. The model was based upon the fact that certain types of human cancers produce functional FasL and hence can introduce an apoptosis on activated lymphocytes in vitro. This model by Webb et al. [135] showed how tumor cells evade immune surveillance using the FasL/Fas system and their secreted soluble forms (i.e. the matrix metalloproteinase (MMP) catalyzed soluble degradation product of the ligand (sFasL)); however it did not show how tumor cells escape from one or both arms of immune system (i.e. adaptive and innate immunity) and how tumor cells evolve after evading one or both arms of the host immune system. These shortcomings from Webb et al. [135] models are of particular interest to our model because tumors need to circumvent either one or both arms of immunity to maintain progressive growth [2]. More importantly, our proposed model considers the fact that the innate and adaptive immunities perform complementary functions. One of the most common mechanism by which tumors evade the host immune surveillance is by loss of MHC class I molecule expression on their cell surfaces. This mechanism only renders T cell responses ineffective. However, evidence shows that tumor cells that evade the $CD8^+$ T cell-mediated killing by down-regulation of MHC class I molecules become potential targets for NK cell-mediated killing [32, 192] via "missing self" signals [10]. If the NK cell is unable to bind to MHC class I on the target cell, then NK-cell killing signal is triggered [10, 193, 194]. Therefore, it is important to show how tumor cells evolve and survive from both cytotoxic arms of immune system.

In [1], de Pillis et al. proposed a mathematical model that tracks the effect of multiple immune cells, $CD8^+$ T and NK cells, on tumor regression. The model focused on the interaction of the $CD8^+$ T and NK cells with various tumor cell lines: NKG2D ligand transduced and control-transduced (non-ligand) tumor cells. From the simulations, it was shown that ligand transduced cells can stimulate protective immunity against tumor growth, while the control-transduced tumor cells can escape immune surveillance. Additionally, it was shown that the immune system provide better protection against tumors if it is primed with ligand-transduced cells than with non-ligand tumor cells. These simulations were in agreement with experimental data by Diefenbach et al. [195] which provided information

on mouse immune response to the presence of a tumor. This model by de Pillis et al. [1] provided a baseline framework for our model. In comparison to our proposed model, ligand transduced tumor cells can be described as those tumor cells which are attacked by activated $CD8^+$ cytotoxic T lymphocytes (CTLs) (i.e. tumor cells with high expression of MHC class I molecules in attempt to hide from NK cell-mediated killing [196, 197]) and the control-transduced tumor cells can be described as those tumor cells which are potential targets for NK cells (i.e. tumor cells with down-regulated MHC class I molecules on their cell surfaces in attempt to evade the $CD8^+$ T cell-mediated killing [32, 192]).

Despite major advances in the fight against cancer, the mechanisms by which tumors escape the immune system's recognition and control are still not well understood. Our aim in this work is to gain insight into these dynamics of tumor-immune surveillance via a mathematical model employing a system of nonlinear ordinary differential equations. To the best of our knowledge, this is the first attempt to mathematically model how tumor cell populations escape and acquire resistance to multiple immune cell populations resulting from their several cell-cell encounters. In this study, we extend recent literature on tumor-immune surveillance [1, 126, 135] and present a unique study that proposes a predictive understanding of how tumor cells elude key immune system cells that provide robust host immune surveillance.

3.2 Model formulation

3.2.1 Model description

To describe how some immunogenic tumors (i.e. tumors that can be recognized by immune-effector cells), escape from the host immune surveillance, we first differentiate between the distinct interaction kinetics between natural killer (NK) cells, and the activated $CD8^+$ cytotoxic T lymphocytes (CTLs) with immunogenic tumors. Since both NK cells and CTLs can employ similar apoptosis mechanisms, we consider Fas/FasL binding between either type of immune system with the tumor cell. Fas is a 45-kDa type I membrane protein, and Fas-ligand (FasL) is a 37- to 40-kDa type II membrane protein which are members of the tumor necrosis factor receptor and ligand families [198, 199].

A Fas ligand (FasL) is present on cell surface of either an NK cell [168, 169, 172] or an activated $CD8^+$ CTL [200]. When an immune cell employs a Fas/FasL binding mechanism to lyse tumor cell, the FasL binds with its cell surface-bound receptor Fas on tumor cell [201]. This binding results in a complex through which apoptosis signals are sent into the target tumor cell.

The attachment and detachment between tumor and NK cells via Fas/FasL binding are depicted in Figure 3.1.

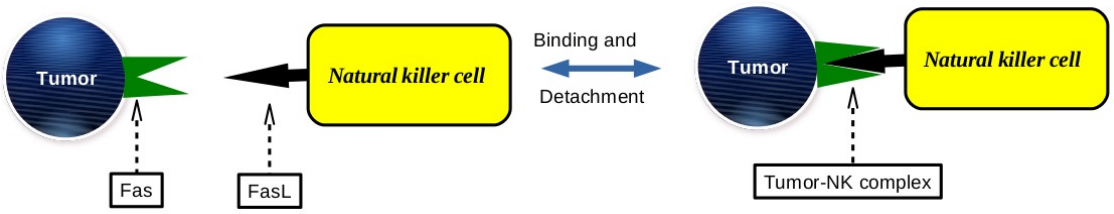

FIG. 3.1. A schematic view of the binding and detachment of a tumor cell to a natural killer (NK) cell.

The formed complex enables the NK cell or CTL to induce the apoptosis signals to the bound tumor cell. Binding of Fas on a tumor cell with FasL triggers a cascade of sub-cellular events that result in apoptosis [202, 203]. Some tumors, however, avoid the apoptosis through several mechanisms, including down-regulation of death receptors [36, 41, 204] or expression of anti-apoptotis proteins like B7-H1 [205, 206], Phosphatidylinositol 3′-kinase (PI3 K) and Akt (protein kinase B) [207] on their cell surface. The evolution of these mechanisms may ultimately lead to tumor evasion from immune surveillance mediated by either natural killer cells or activated $CD8^+$ cytotoxic T lymphocyte [2, 196, 208].

A partial schematic interaction dynamics which lead to tumor escape are depicted in Figure 3.2.

Figure 3.2 indicates the interaction dynamics between a population of natural killer cells, denoted by N, the population of activated $CD8^+$ cytotoxic T lymphocytes, denoted by L, and the population of "naive" tumor cells (i.e. tumor cells that have not yet developed any

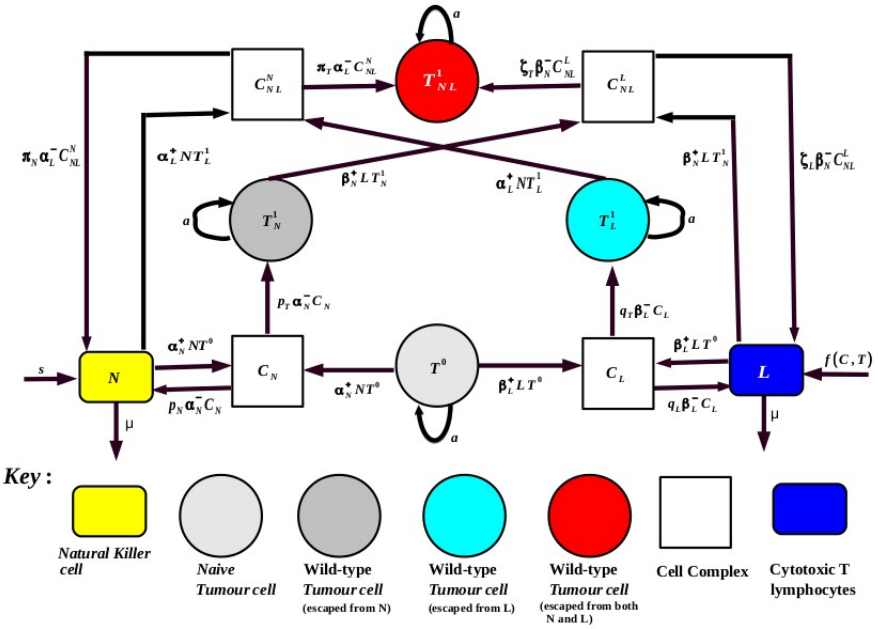

FIG. 3.2. A schematic diagram of the interactions between tumor cells, natural killer cells and the activated CD8$^+$ cytotoxic T lymphocytes. Parameters and variables appearing on this schematic diagram are summarized in Tables 3.1 & 3.2.

escape mechanism to immune cells), denoted by T^0, and the population of tumor cells that have escaped immune surveillance once, T_N^1 and T_L^1, or twice T_{NL}^1. Note, the superscript 0 appearing in T^0 denotes "naiveness" (i.e. tumor cells that have not yet developed any escape mechanism to immune cells), while the superscript 1 appearing in T_N^1, T_L^1 and T_{NL}^1 denotes "wildness" of tumor cells (i.e. tumor cells that can hide from the specific immune attack, and develop resistance to that specific immune cell). The subscripts, N, L and NL appearing in T_N^1, T_L^1 and T_{NL}^1, respectively denote the type of immune cell that interacted with the tumor cell.

Accumulating evidence indicates that tumor cells, after surviving an immune attack, they can either mount a "counter-attack" or develop resistance to immune cells [2, 26, 47]. Our model does not account for a direct tumor counterattack, as was done in [190, 191]. In our model, upon surviving their brief encounter with the tumor cells, the immune cells die to natural cell death, not as a consequence of tumor counterattack. In Matzavinos et al. [190] a spatio-temporal model of the interactions between tumor cells and tumor-infiltrating cytotoxic lymphocytes (TICLs) was proposed. The model included the spatial motility of

both TICLs and tumor cells via a combination of random motility and chemotactic motion of the TICLs in response to the presence of chemokines. Authors focused mainly on the role of the immune system in determining dormant states of the tumor. Similar to our model, the TICLs are assumed to migrate into the tumor site and interact with the tumor cells in such a way that TICL-tumor cell complexes are formed. The outcome of these complexes was two fold: the death of the tumor cells or the inactivation (sometimes even the death) of the immune lymphocytes. The direct tumor counterattack was attributed to the death of the immune lymphocytes, TICLs. In Joshi et al [191], a mathematical model of immunotherapy and cancer vaccination was proposed. The model focused on the role of antigen presentation and co-stimulatory signaling pathways in cancer immunology. The direct tumor counterattack against effector immune cells was ascribed by the death of effector immune cells as one of the outcomes of the effector-tumor cell complexes. Counter-intuitively to these models, our model accounts for the development of resistance to immune cell-mediated killings as a result of one or multiple encounters of tumor cells with certain immune cells, as was done in [164]. In Al-Tameemi et al [164], a mathematical model that describes a solid tumor growth in the presence of the immune system response was presented. The model focused on the spatio-temporal interactions of the immunogenic tumor cells and cytotoxic T-lymphocytes (CTLs) in the presence of chemokines and "chemorepellents". In [164], as well as in our model, tumor cells and CTLs are assumed to interact in such a way that CTL-tumor cell complexes are formed. After some time, the formed CTL-tumor cell complex breaks up. This break-up of complex can lead to a situation in which both the tumor cell and the CTL are alive, and either the CTL or the tumor cell survives their brief encounter [164].

In order for the adaptive immunity to mount a specific anti-tumor response, there has to be a variety of alarming activities from innate immune response that activate the adaptive immunity [4, 209]. We, however, have not included this step in our model since the focus is on the interaction dynamics of the activated $CD8^+$ cytotoxic T lymphocytes with tumor cells.

The kinetic parameters α_N^+ and β_L^+ represent respective initial rates of attachment of NK cells and CTLs to naive tumor cells. Rates of tumor escape following its first brief encounter with NK or CTL, with no damage on the cells, are denoted by α_N^- and β_L^-, respectively. Since the interaction between tumor cells and immune cells may inactivate some immune

cells, we consider only the immune cells that posses a certain effector fitness (i.e. immune cytotoxic capacity similar to the one immune cells posses prior to their entanglement with tumor cells) after their interaction with tumor cells. The quantities, p_N and p_L, represent the respective proportions of NK cells and CTLs that are detached, with no damage on the cells, from complexes formed when tumor cells bound with NK cells and CTLs. Similarly, the quantities, π_N and ζ_L, denote the respective proportions of NK cells and CTLs that are detached, with no damage on the cells, from complexes formed when "wild-type" tumors, T_N^1 and T_L^1, bound with NK cells and CTLs.

It is known that almost all kinds of tumor cells express Fas [202], and some may express a Fas ligand, FasL, which might bind with its receptor, Fas, on the activated immune cell [37]. Through this engagement of Fas receptor with its ligand FasL, tumor cell may directly lyse the immune cell [29, 36, 135, 207, 210]. Thus, the quantities p_T and q_T represent the proportions of tumor cells that escaped (i.e. via tumor "counterattack") from the surveillance mediated by NK cells and CTLs, respectively. Therefore, the Fas/FasL complex constitutes an important role in controlling survival or growth of tumor cells [202, 211].

Tumor cells interact with NK cell or CTL in such a way that complexes are formed as shown in Figure 3.1. The complex resulting from binding of natural killer cell or activated $CD8^+$ cytotoxic T lymphocytes to naive tumor cell is denoted by C_N and C_L, respectively. If a tumor has survived a brief encounter with either a NK cell or CTL then such tumor develops, via mutations or epigenetic changes, a variety of mechanisms that might enable it to avoid future attacks by the encountered type(s) of immune system [164].

Since we are considering the tumor-immune interactions under immune surveillance, tumor cell that has once survived its encounter with NK cell is still susceptible to further attacks by CTLs, and vice-versa. Since "wild-type" tumor cells usually develop immune resistance to a type of immune cell that it has encountered [164], in this study, we assume that subsequent interactions between that particular "wild-type" tumor with the same type of immune cell is unlikely. Thus, we are only considering susceptibility of such tumor cell to other different types of immune cell to illustrate how tumors may ultimately elude overlapping attacks of distinct immune cells participating in tumor surveillance.

Tumors do indeed develop complex mechanisms to evade various activities of immune system recognition and control [2]. Here, we denote by C_{NL}^{N} and C_{NL}^{L} complexes formed from the interaction of such "wild-type" tumor cells with NK cell and CTLs, respectively. Rate of binding of NK cells to "wild-type" tumor cell that escaped from CTL surveillance is denoted by α_L^+, and the rate of detachment of NK cells from the complex C_{NL}^{N} formed with such tumor cell is denoted by α_L^-. Similarly, the respective rates of binding and detachment of CTLs from "wild-type" tumor cell that escaped from NK-cell surveillance are denoted by β_N^+ and β_N^-.

The parameters and variables described in this section are summarized in Tables 3.1 & 3.2.

3.2.2 Model assumptions

We make the following assumptions for our model based on the discussion above and the scientific literature on the immune system [1, 30–32, 35, 38, 122, 164, 192, 212, 213]:

(i) All tumors are immunogenic to trigger an immune response, and grow logistically in the absence of immune response [1].

(ii) If a tumor has escaped from NK-cell surveillance, then the tumor resistance to NK-mediated killing increases after its brief encounter with NK cell; the same analogy is also true for the CTL surveillance. This resistance to NK-mediated killing is considered to occur as a result of up-regulation of MHC class I molecules [38]. Consequently, up-regulation of these MHC class I molecules renders tumor cells more susceptible to CTL-mediated killing [30–32, 192, 213]. Thus, phenotypically, the "wild-type" tumors are different from the naive tumor cells.

(iii) The probability of "wild-type" tumor cell, that escaped NK-mediated killing, being recognized and also of forming a complex with a NK cell (implicitly embedded in the parameter α_L^+) is small or zero. The same assumption applies to "wild-type" tumor cell that escaped CTL-mediated killing [164].

(iv) As part of the innate system, natural killer cells (N) are always present [1, 212] in the host immune system, but cytotoxic T lymphocytes (L) are only present when tumor is present [1].

(v) Both NK cells and activated CD8$^+$ CTLs eventually become less effective after the first encounter with tumor cells [1, 122].

(vi) Both NK and CTLs can lyse tumor cells [1, 35].

3.2.3 Terms used for growth, death and recruitment

We adapt a logistic growth for naive tumor cell, $aT^0(1-bT^0)$, as well as wild-type tumor cells that have survived the encounter with immune cells, $aT^i_j(1-bT^i_j)$ with $j = N, L, NL$ and $i = 1$. The rate of tumor growth is denoted by a, which includes both cell multiplication (mitosis) and death, and the maximum carrying capacity of the tumor cells is represented by the parameter b. Since we have assumed that CTLs are only present in the host immune system only when the tumor is present, the growth term for the activated CD8$^+$ CTLs consists only of natural cell death. Thus, we have $\mu_2 L$ as the growth term for the activated CD8$^+$ CTLs. The NK cells are produced from an external source, s, as in [1]. The constant parameter, s, accounts for the fact that that NK cells, as part of the innate immune, are always present in the host body, even when no tumor is present. We assume that NK cells and CTLs die at different constant rates μ_1 and μ_2, respectively.

The recruitment term, $f(C,T)$ where $C = (C_L, C^L_{NL})$ and $T = (T^0, T^1_N)$, denotes proliferation function of CTLs due to signals, such as released cytokines, produced in an autocrine manner by the CTLs in CTL-tumor cell complexes [190, 214]. The function f reaches some saturation at certain point since the immune system cannot produce activated CD8$^+$ CTLs indefinitely. Thus, the function f can be written as $f(C,T) = r_1 C_L/(g+T^0) + r_2 C^L_{NL}/(g+T^1_N)$, where r_1 and r_2 are constant rates at which CTLs are recruited due to the formation of the complexes with "naive" and "wild-type" tumor cell populations, respectively. Note $r_1 \geq r_2 \geq 0$ because after each brief encounter with immune cells, the tumor cell develops some resistance towards subsequent interaction or potential killing of each type of immune system encountered. Model variables are summarized in Table 3.1.

TABLE. 3.1. Model Variables

Variables	Description
L	Activated $CD8^+$ cytotoxic T lymphocytes (CTLs)
N	Natural killer (NK) cells
T^0	Naive tumor cells
T_N^1	Wild-type tumor cells that escaped from NK cells
T_L^1	Wild-type tumor cells that escaped from activated $CD8^+$ CTLs
T_{NL}^1	Wild-type tumor cells that escaped from both NK cells and activated $CD8^+$ CTLs
C_N	Complex formed by NK cell and naive tumor cell
C_L	Complex formed by CTL and naive tumor cell
C_{NL}^N	Complex formed by NK cell and wild-type tumor cell that escaped from activated $CD8^+$ CTLs
C_{NL}^L	Complex formed by CTL and wild-type tumor cell that escaped from NK cells

3.2.4 Model equations

Assuming mass action kinetics, the model describing the interactions between various immune cells and tumor cells is given by the following system of nonlinear ordinary differential equations:

$$\frac{dN}{dt} = \underbrace{s}_{\text{supply}} - \underbrace{\mu_1 N}_{\text{natural death}} - \underbrace{\alpha_N^+ N T^0 + p_N \alpha_N^- C_N}_{\text{local kinetics, with } T^0} - \underbrace{\alpha_L^+ N T_L^1 + \pi_N \alpha_L^- C_{NL}^N}_{\text{local kinetics, with } T_L^1} \tag{3.1}$$

$$\frac{dL}{dt} = \underbrace{f(C,T)}_{\text{recruitment}} - \underbrace{\mu_2 L}_{\text{natural death}} - \underbrace{\beta_L^+ L T^0 + q_L \beta_L^- C_L}_{\text{local kinetics, with } T^0} - \underbrace{\beta_N^+ L T_N^1 + \zeta_L \beta_N^- C_{NL}^L}_{\text{local kinetics, with } T_N^1} \tag{3.2}$$

$$\frac{dT^0}{dt} = \underbrace{aT^0(1-bT^0)}_{\text{logistic growth}} - \underbrace{\alpha_N^+ N T^0}_{\text{local kinetics, with } N} - \underbrace{\beta_L^+ L T^0}_{\text{local kinetics, with } L} \tag{3.3}$$

$$\frac{dT_N^1}{dt} = \underbrace{aT_N^1(1-bT_N^1)}_{\text{logistic growth}} + \underbrace{p_T \alpha_N^- C_N}_{\text{escaped, from } N} - \underbrace{\beta_N^+ L T_N^1}_{\text{local kinetics, with } L} \tag{3.4}$$

$$\frac{dT_L^1}{dt} = \underbrace{aT_L^1(1-bT_L^1)}_{\text{logistic growth}} + \underbrace{q_T \beta_L^- C_L}_{\text{escaped, from } L} - \underbrace{\alpha_L^+ N T_L^1}_{\text{local kinetics, with } N} \tag{3.5}$$

$$\frac{dT_{NL}^1}{dt} = \underbrace{aT_{NL}^1(1-bT_{NL}^1)}_{\text{logistic growth}} + \underbrace{\zeta_T \beta_N^- C_{NL}^L}_{\text{escaped, from } L} + \underbrace{\pi_T \alpha_L^- C_{NL}^N}_{\text{escaped, from } N} \tag{3.6}$$

where

$$f(C,T) = \underbrace{r_1 C_L/(g+T^0)}_{\substack{\text{Proliferation of CTLs in response} \\ \text{to the naive tumors}}} + \underbrace{r_2 C_{NL}^L/(g+T_N^1)}_{\substack{\text{Proliferation of CTLs in response} \\ \text{to the wild-type tumors}}} \tag{3.7}$$

The parameters $\alpha_N^+, \alpha_N^-, \alpha_L^+, \alpha_L^-, \beta_L^+, \beta_L^-, \beta_N^+, \beta_N^-, \pi_T, \pi_N, \zeta_T, \zeta_L, p_N, p_T, q_L, q_T, r_1, r_2$, s, r_1, r_2, g, μ_1 and μ_2, summarized in Table 3.2, are all positive constants. Note, $f(C,T)$ denotes activation of the CTLs due to signals from binding of the activated $CD8^+$ CTLs with the tumor cells. Here, p_T and q_T denotes the proportions of initial tumor cell populations that escaped the local interactions with NK cells and CTLs, respectively. Similarly, π_T and ζ_T represent the proportions of the "wild-type" tumor cell populations that escaped local interactions with NK cells and CTLs, respectively.

The tumor-immune interactions resulting in cell-complexes are governed by the kinetics

derived in Figure 3.2. Therefore, the equations for the complexes are given by:

$$\frac{dC_N}{dt} = \underbrace{\alpha_N^+ NT^0}_{\substack{\text{Complex formation}\\ \text{between } N \text{ \& } T^0}} - \underbrace{\alpha_N^- C_N}_{\substack{\text{Complex detachment}\\ \text{between } N \text{ \& } T^0}} \tag{3.8}$$

$$\frac{dC_L}{dt} = \underbrace{\beta_L^+ LT^0}_{\substack{\text{Complex formation}\\ \text{between } L \text{ \& } T^0}} - \underbrace{\beta_L^- C_L}_{\substack{\text{Complex detachment}\\ \text{between } L \text{ \& } T^0}} \tag{3.9}$$

$$\frac{dC_{NL}^N}{dt} = \underbrace{\alpha_L^+ NT_L^1}_{\substack{\text{Complex formation}\\ \text{between } L \text{ \& } T_L^1}} - \underbrace{\alpha_L^- C_{NL}^N}_{\substack{\text{Complex detachment}\\ \text{between } N \text{ \& } T_L^1}} \tag{3.10}$$

$$\frac{dC_{NL}^L}{dt} = \underbrace{\beta_N^+ LT_N^1}_{\substack{\text{Complex formation}\\ \text{between } L \text{ \& } T_N^1}} - \underbrace{\beta_N^- C_{NL}^L}_{\substack{\text{Complex detachment}\\ \text{between } N \text{ \& } T_N^1}} \tag{3.11}$$

In this model, if either the tumor cell or attacking immune cell does not posses a ligand, then the variables $C_N(t),\ C_L(t), C_{NL}^N(t)$ and $C_{NL}^L(t)$ are zero because the formation of complexes requires the ligand to be present. The initial conditions for the model are:

$$\begin{aligned} &N(0) = N_0,\ L(0) = L_0,\ T^0(0) = T_0,\ T_N^1(0) = T_L^1(0) = T_{NL}^1(0) = 0, \\ &C_N(0) = C_L(0) = C_{NL}^N = C_{NL}^L = 0. \end{aligned} \tag{3.12}$$

For simplicity, we do not model successive multiple encounters between one immune cell type and the same tumor cell that survived the first brief encounter. We only consider the case where the target tumor cells have evaded the NK and/ or CTL surveillance once. This is to illustrate how tumors acquire resistance to immune surveillance, and ultimately proliferate without bound or get to equilibrium state of immunoediting as suggested by Dunn et al. [2]. This model (3.1) – (3.11) can easily be extended to the setup of n tumor escapes from immune surveillance mediated by NK cells and CTLs. Thus we have omitted this case in this study. We now present a detailed explanation of each term involved in each model equation.

In equation 3.1, the first term, s, represents a constant background source rate for natural killer cells. The second term, $-\mu_1 N$, represents natural cell death of the NK cell population. The third term, $(-\alpha_N^+ NT^0 + p_N \alpha_N^- C_N)$, represents the local interaction dynamics between NK cells and naive tumor cells, resulting in binding of NK cells to naive

tumor cells, $-\alpha_N^+ NT^0$, and detachment of NK cells from tumor cells, $p_N\alpha_N^- C_N$, without damaging cells. Here, we assume that the NK cells that are detached from NK cell-tumor complex maintained a high level of effectiveness as before the interaction with tumor cells. This assumption is usually made when there is no cell damage resulting from detachment of cells from the complexes [164]. Similarly, the fourth term, $(-\alpha_L^+ NT_L^1 + \pi_N\alpha_L^- C_{NL}^N)$, represents the local interaction kinetics between NK cells and the wild-type tumor cells that survived their brief encounters with the CTLs. The term $-\alpha_L^+ NT_L^1$ represent binding of NK cells to tumor cells, while the term $\pi_N\alpha_L^- C_{NL}^N$ represents detachment of NK cells from the NK cell-tumor complex. Recently, it has been shown that NK/CTLs can rapidly attack other target cells after their detachment from tumor cells [215]. This later interaction of NK cells and wild-type tumors may be important and is therefore included in the model.

In equation 3.2, the first term, $f(C,T)$, denotes recruitment of CTLs in response to the presence to tumor cells. That is, $r_1 C_L/(g+T^0)$, represents CTL proliferation in response to naive tumor cells, and $r_2 C_{NL}^L/(g+T_N^1)$ represents the CTL proliferation in response to wild-type tumor cells that escaped their brief encounter with the natural killer cells. This functional form is borrowed from the simplified activated $CD8^+$ T-cell recruitment term from de Pillis et al [216]. Moreover, this CTL recruitment has been used by Matzavinos et al. [190] and Joshi et al [191]. This functional form is usually employed when one assumes that the recruitment of CTLs is due to signals, such as released cytokines (signaling molecules that mediate and regulate immune system), produced by immune cells in tumor-CTL complexes [190, 191]. The second term, $-\mu_2 L$, represents natural death of the activated $CD8^+$ CTLs, as in de Pillis et al [1, 131, 212]. Since we have assumed that activated $CD8^+$ CTLs are only present when the tumor is present, then the activated $CD8^+$ CTLs do not have an intrinsic growth. This third term, $(-\beta_L^+ LT^0 + q_L\beta_L^- C_L)$, represents binding $-\beta_L^+ LT^0$, of activated $CD8^+$ CTLs to the naive tumor cells, and detachment, $q_L\beta_L^- C_L$, of activated $CD8^+$ CTLs from the naive tumor cells. Similar to NK cell, activated $CD8^+$ CTLs are susceptible to interactions with the wild-type tumor. Hence, the last term, $(-\beta_N^+ LT_N^1 + \zeta_L\beta_N^-\ C_{NL}^L)$, represents the local interactions of the activated $CD8^+$ CTLs with the wild-type tumors that escaped from NK cell surveillance. The term $-\beta_N^+ LT_N^1$ represents binding of the activated $CD8^+$ CTLs to wild-type tumor cells, and $\zeta_L\beta_N^-\ C_{NL}^L$ represents detachment of the activated $CD8^+$ CTLs from wild-type tumor cells.

In equation 3.3, the intrinsic growth dynamics of the naive tumor cells is represented by logistic growth, $aT^0(1 - bT^0)$. The logistic growth laws are consistent with models fitted to real tumor growth data [1, 126, 131]. Since naive tumor cells are immunogenic to all immune cells, the local interactions of the naive tumour cells with NK cells and activated $CD8^+$ CTLs is represented by $-\alpha_N^+ NT^0$ and $-\beta_L^+ LT^0$, respectively.

In equation 3.4, similar to equation (3.3), the first term represents a logistic growth of the wild-type tumor cells which survived and escape their brief encounters with the NK cells. The number of escaped tumor cells are represented by the second term, $p_T \alpha_N^- C_N$. However, since tumor cells which evade NK cell surveillance (i.e. tumor cells with up-regulated expression of major histocompatibility complex (MHC) class I molecules [38]) are susceptible to CTL-mediated killing [30–32, 192, 213], their local interaction with the activated $CD8^+$ CTLs is represented by the last term, $-\beta_N^+ LT_N^1$.

In equation 3.5, the equation for wild-type tumor cells discussed is similar to the above equation. The first term, $aT_L^1(1 - bT_L^1)$, represents logistic growth of the wild-type tumor cells that survived and escaped their brief encounter with activated $CD8^+$ CTLs. The second term, $q_T \beta_L^- C_L$, represents tumor cells that escaped CTL surveillance (i.e. tumor cells with down-regulated MHC class I molecules). Down-regulation of MHC class I molecule is known to be one of the escape mechanisms of tumor cells to evade CTL-mediated killing [30–32, 192, 213]. However, down-regulation of these MHC class I molecules renders tumor cells more susceptible to NK cell-mediated killing [32, 192]. Furthermore, evidence shows that NK cells can recognize tumors that might evade the activated $CD8^+$ CTL-mediated killing by aberrant human leukocyte antigen (HLA) expression [217].

In equation 3.6, the first term represents logistic growth of the wild-type tumor cells that are resistant to immune surveillance mediated by both NK cell and activated $CD8^+$ CTLs. We note that these tumor cells are "*multi-immunoresistant*" to both cytotoxic immune cells, and therefore present a major impediment to successful immunotherapy [44, 48–51].

3.2.5 The reduced model

The intrinsic growth of tumors involves multiple time scales: the proliferation of tumor cells normally occurs on a time interval of months to years *in vivo*, while *in vitro* takes weeks to months [218]. A complex formed between a NK cell or CTL and tumor cell occurs on a small time scale (i.e. from several minutes to a few hours [214]). Moreover, the recruitment of CTLs as well as the influx of NK cells to a tumor site usually occurs on a much slower time scale (i.e. tens of hours [214]). In order to account for these differences in the time scales, we adopt a quasi-steady-state analysis on the cell complexes $\left(\text{i.e. } \frac{dC_N}{dt} = \frac{dC_L}{dt} = \frac{dC^N_{NL}}{dt} = \frac{dC^L_{NL}}{dt} \approx 0\right)$. More importantly, we are interested in the interaction between tumor cell populations and the immune system; hence we simplify the model's equations (3.1) – (3.11), by using quasi-steady-state approximations for the complexes. By this approach, we obtain the following relations for the cell complexes:

$$C_N = \left(\frac{\alpha_N^+}{\alpha_N^-}\right) NT^0; \quad C_L = \left(\frac{\beta_L^+}{\beta_L^-}\right) LT^0; \tag{3.13}$$

$$C^N_{NL} = \left(\frac{\alpha_L^+}{\alpha_L^-}\right) NT^1_L; \quad C^L_{NL} = \left(\frac{\beta_N^+}{\beta_N^-}\right) LT^1_N. \tag{3.14}$$

By substituting these expressions into the system equations (3.1) – (3.6), we obtain the following simplified system for the tumor-immune dynamics:

$$\frac{dN}{dt} = s - \mu_1 N - (1-p_N)\alpha_N^+ NT^0 - (1-\pi_N)\alpha_L^+ NT^1_N \tag{3.15}$$

$$\frac{dL}{dt} = \frac{r_1\beta_L^+ LT^0}{\beta_L^-(g+T^0)} + \frac{r_2\beta_N^+ LT^1_N}{\beta_N^-(g+T^1_N)} - \mu_2 L - (1-q_L)\beta_L^+ LT^0 - (1-\zeta_L)\beta_N^+ LT^1_N \tag{3.16}$$

$$\frac{dT^0}{dt} = aT^0(1-bT^0) - \alpha_N^+ NT^0 - \beta_L^+ LT^0 \tag{3.17}$$

$$\frac{dT^1_N}{dt} = aT^1_N(1-bT^1_N) + p_T\alpha_N^+ NT^0 - \beta_N^+ LT^1_N \tag{3.18}$$

$$\frac{dT^1_L}{dt} = aT^1_L(1-bT^1_L) + q_T\beta_L^+ LT^0 - \alpha_L^+ NT^1_L \tag{3.19}$$

$$\frac{dT^1_{NL}}{dt} = aT^1_{NL}(1-bT^1_{NL}) + \zeta_T\beta_N^+ LT^1_N + \pi_T\alpha_L^+ NT^1_L \tag{3.20}$$

Followings are the positive initial conditions of the system:

$$N(0) = N_0,\ L(0) = L_0,\ T^0(0) = T_0,\ T^1_N(0) = T^1_L(0) = T^1_{NL}(0) = 0,\ s(0) = s_0. \tag{3.21}$$

The system of equations (3.15) – (3.20) along with the initial conditions (3.21) constitute a reduced model of the immune surveillance of tumors that we use to explain how tumor cells evade immune surveillance in the next section.

3.3 Model simulations and results

In this section, we discuss the numerical simulations of our mathematical model and give plausible explanations of the proposed model results. The model enables us to simulate tumor evasion based on various influx of the NK cells and the activated $CD8^+$ CTLs. An enhanced understanding of how tumors evade immune surveillance may help to identify which components of host immune-effector forces that need to be augmented to boost natural protection against tumors [2]. The major goal of this computational study is to quantitatively elucidate how tumor cells escape from immune surveillance based on the findings by Dunn et al. [2]:

(i) The immune system has capacity to recognize and destroy nascent transformed cells (Elimination phase (immunosurveillance)).

(ii) Some tumor cells may survive immune destruction and become dormant (Equilibrium phase (i.e. the phase where immuno-editing occurs).

(iii) After some time, selected tumor cell variants from the equilibrium phase can now grow into clinically detectable tumors.

Of particular interest to our model framework is to elucidate how tumor cells most likely circumvent either one or both arms of host immunity (i.e. innate and adaptive immunity) in order to maintain progressive growth. A thorough understanding of plausible escape mechanisms employed by tumor cells is a first necessary step towards the development of successful strategies for immunotherapy [37, 48, 219].

3.3.1 Model baseline parameters

To quantitatively analyze our model, we first need to determine the model baseline parameter values or at least a reasonable physiological range for them. We use data from the available literature where possible and for other parameters we consider different value ranges and their impact on the model outputs. A summary of the parameter descriptions and their numerical values is given in table 3.2. We used most of the baseline parameter values reported in [1, 164, 190, 191, 212, 214].

We now outline our approach to estimating numerical values for each model parameter. To date, there is still a lack of quantitative data for Fas/FasL system between tumor cells and immune system. We determined our model parameter estimates based on a variety of approaches. First, we sourced all available parameter values from biological literature, particularly parameter values related to activated $CD8^+$ CTLs. To the best of our knowledge, most of the available estimates of Fas/FasL system is based on the interactions of activated $CD8^+$ CTLs with tumor cells. However, since the engagement of Fas/FasL system in activated $CD8^+$ CTLs is similar to NK cells [220], we held most of the unknown parameter estimates of binding and detachment of NK cells to tumor cells same as those of activated $CD8^+$ CTLs with tumor cells. Second, for some parameters, there is no relevant information available regarding their numerical ranges, we chose parameter values which confirmed the model's behavior with biological realism.

Even though the parameter estimates provided in this section are baseline estimates taken from a variety of sources, model sensitivity to changes in parameter values has been explored (see Section 3.4). In the following sections, we discuss in detail how numerical values for each model parameter were estimated.

The natural killer cells

For numerical ranges of source of NK cells, s, we used values within biological ranges stated in [214]. The death rate of NK cells, $\mu_1 = 4.12 \times 10^{-2} cell^{-1}\ day^{-1}$, is obtained from de

Pillis et al. [212]. We use same rate of binding of NK cells to tumor, $\alpha_N^+ = 1.3\times10^{-7}\ day^{-1}$, as activated CD8$^+$ CTLs binding rate reported in [164, 191]. The proportion of NK cells that survived from NK-naive tumor complex and maintained high level of effectiveness, $p_N = 0.94$, is an *ad hoc* value and has been chosen to give biologically feasible outcomes. The value of this proportion is not available in the literature. The formed complexes between NK cells and tumor cells, may result in inactivation of some the NK cells and consequently further chances of survival of the tumor cells [164, 190]. Since there is no information in the literature on the proportion of NK cells that survived from NK-tumor complex formed with wild-type tumor cell that escaped from CTL and maintained high level of effectiveness, we chose a value of $\pi_N = 0.80$ in order to obtain a biologically relevant outcome from the model. The binding rate of NK cells to tumor cell that escaped from CTLs, $\alpha_L^+ = 1.2\times10^{-9} day^{-1}\ cells^{-1}$, is also an *ad hoc* value that is chosen to give the biologically reasonable model results. Since the NK cells are capable of lysing tumor cells via Fas/FasL system [168–172], the chosen value of α_L^+ was motivated from the magnitude of the values of CTL Fas/FasL binding as considered in [191]. The Fas/FasL system is in the same family as tumour necrosis factor (TNF) and the extracellular domains of members of the TNF family are known to be well conserved [135]. That means, the order of magnitude of the values of Fas/FasL system should not change very much as of those values of TNF family.

The activated CD8$^+$ cytotoxic T lymphocytes

The rate of activated CD8$^+$ CTLs recruitment due to signals resulting from CTL-naive tumor interaction, $r_1 = 0.2988\times10^8\ day^{-1}\ cells$, is left unchanged from Al-Tameemi et al [164], Matzavinos et al [190] and Joshi et al [191]. The rate of binding of activated CD8$^+$ CTLs to naive tumor cells, $\beta_L^+ = 1.3\times10^{-7}\ day^{-1}\ cells^{-1}$, and rate of detachment of CTLs from naive tumor cells, $\beta_L^- = 24\ day^{-1}$, are taken from Al-Tameemi et al [164] and Joshi et al [191]. The constant appearing in recruitment function of the activated CD8$^+$ CTLs, g, is obtained from Al-Tameemi et al [164], Matzavinos et al [190] and Joshi et al [191].

The recruitment rate of activated CD8$^+$ CTLs recruitment due to the presence of wild-type tumor cells is given by $r_2 = 0.2755\times10^6\ day^{-1}\ cells$. Since there is no data measuring the relevant recruitment kinetics of activated CD8$^+$ CTLs to wild-type tumor cells, this value

is chosen to maintain model consistency with biological expectations. Since the activated $CD8^+$ CTLs binds to tumor cells via the Fas/FasL system, we used same binding and detachment rates of activated $CD8^+$ CTLs to/from wild-type tumor cells as those of CTL-naive tumor interactions: $\beta_N^+ = 1.3 \times 10^{-7}\ day^{-1}\ cells^{-1}$, and $\beta_N^- = 24\ day^{-1}$, respectively. This was motivated by the fact that the Fas/FasL system is in the same family as tumour necrosis factor (TNF) and the extracellular domains of members of the TNF family are known to be well conserved [135].

The natural death of the activated $CD8^+$ CTLs, $\mu_2 = 2.0 \times 10^{-2}\ cell^{-1}\ day^{-1}$, is taken from de Pillis et al. [212]. The proportion of activated $CD8^+$ CTLs that survived from CTL-naive tumor complex and maintained high level of effectiveness, $q_L = 0.94$, as well as the proportion of activated $CD8^+$ CTLs that survived from CTL-tumor complex formed with "wild-type" tumor cell that escaped from NK cells and maintained high level of effectiveness, $\zeta_L = 0.85$, are *ad hoc* values that are chosen to obtain the model consistency with biological expectations.

The naive tumor cells

The tumor growth rate, $a = 0.5822\ day^{-1}$, and the inverse of the tumor carrying capacity, $b = 2.33 \times 10^{-8}\ cells^{-1}$, were left unchanged from the values found by the de Pillis et al. [1], who derived them by using MATLAB's *least-squares distance* to tumor growth data in mice from Diefenbach et al. [195]. Interestingly, these same values from de Pillis et al. [1] provide a best fit to our model for naive tumor cell population, equation (3.15), in the presence of weak immune system. The fitting was done by minimizing the sum of square errors between observed data points and values of model solutions using the MATLAB function *lsqnonlin*, and obtained Figure 3.3. Other parameters, α_N^+ and β_L^+, were discussed above.

The wild-type tumor cells

Estimation of most the parameters in these tumor cell populations was discussed in the previous sub-sections, except for the proportion of tumor cells that survived from NK/CTL-tumor complex and maintained high level of effectiveness: $p_T = 0.05$ from a complex

between NK cells, N, and naive tumor cells, T^0; $q_T = 0.05$ from the complex formed by activated CD8$^+$ CTLs, L, and naive tumor cells, T^0; $\zeta_T = 0.13$ from the complex between activated CD8$^+$ CTLs, L, and wild-type tumor cells that escaped from NK cell surveillance, T_N^1, and $\pi_T = 0.18$ from the complex formed between NK cells, N, and the wild-type tumor cells that escaped from NK cell surveillance, T_L^1. These parameter values are chosen to ensure that the model operates within a biologically reasonable regime.

TABLE. 3.2: Tumor-Immune Model Baseline Parameters: Their Definition and Sources

Parameter	Definition	Value	Source
s	External influx of NK cells	$3.2 \times 10^3 - 3.2 \times 10^4\ day^{-1}\ cells$	[214]
μ_1	per capita death rate of NK cells	$4.12 \times 10^{-2}\ cell^{-1}\ day^{-1}$	[212]
μ_2	per capita death rate of CTLs	$2.0 \times 10^{-2}\ cell^{-1}\ day^{-1}$	[212]
a	The per capita growth rate of tumor cells	$0.5822\ day^{-1}$	[1]
b	The reciprocal carrying capacity of the tumor cells	$2.33\times10^{-8}\ cells^{-1}$	[1]
α_N^+	Rate of binding of NK cells to naive tumor cell	$1.3 \times 10^{-7}\ day^{-1}\ cells^{-1}$	Estimate
α_N^-	Rate of detachment of NK cells from NK-tumor cell complex	$24\ day^{-1}$	Estimate
β_L^+	Rate of binding of CTLs to naive tumor cell	$1.3 \times 10^{-7}\ day^{-1}\ cells^{-1}$	[164, 191]
β_L^-	Rate of detachment of CTLs from CTL-tumor complex	$24\ day^{-1}$	[164, 191]

α_L^+	Rate of binding of NK cells to tumor cell that escaped from CTL	$1.2 \times 10^{-9}\ day^{-1}\ cells^{-1}$	Estimate
α_L^-	Rate of detachment of NK cells from tumor cell that escaped from CTL	$24\ day^{-1}$	Estimate
β_N^+	Rate of binding of CTLs to tumor cell that escaped from NK cell	$1.3 \times 10^{-7}\ day^{-1}\ cells^{-1}$	[164, 191]
β_N^-	Rate of detachment of CTLs from tumor cell that escaped from NK cells	$24\ day^{-1}$	[164]
p_N	Proportion of NK cells that survived from NK-naive tumor complex & maintained high level of effectiveness	0.94	Estimate
p_T	Proportion of naive tumor cells that survived from NK-naive tumor complex & maintained high level of effectiveness	0.05	Estimate
q_L	Proportion of CTLs that survived from CTL-naive tumor complex & maintained high level of effectiveness	0.94	Estimate
q_T	Proportion of naive tumor cells that survived from CTL-naive tumor complex & maintained high level of effectiveness	0.05	Estimate

π_N	Proportion of NK cells that survived from NK-tumor complex formed with "wild-type" tumor cell that escaped from CTL & maintained high level of effectiveness	0.80	Estimate
π_T	Proportion of "wild-type" tumor cells that escaped from NK cells	0.18	Estimate
ζ_L	Proportion of CTLs that survived from CTL-tumor complex formed with "wild-type" tumor cell that escaped from NK cells & maintained high level of effectiveness	0.85	Estimate
ζ_T	Proportion of "wild-type" tumor cells that escaped from CTLs	0.13	Estimate
r_1	Rate of CTLs recruitment due to CTL-"naive" tumor complex	$0.2988 \times 10^8\ day^{-1}\ cells$	[164, 190, 191]
r_2	Rate of CTLs recruitment due to CTL-"wild-type" tumor complex	$0.2755 \times 10^6\ day^{-1}\ cells$	Estimate
g	Maximum CTL recruitment by immunogenic tumor cells	$2.02 \times 10^7\ cells$	[164, 190, 191]

3.3.2 Simulations and results

The numerical solutions of our model equations (3.15) – (3.20), along with the initial conditions (3.21) are carried out using MATLAB *ode23s*. This stiff ODE solver, *ode23s*, was used in this simulation in order to appropriately handle the differing time scales in the system. In this simulation, the initial value set for strong immune system consists of 10^5 NK cells and 10^2 activated $CD8^+$ lymphocytes as considered by Mamat et al [221]. The low influx of natural killer (NK) cells, is $s = 3.2 \times 10^3\ day^{-1}\ cells$ [214] and the low recruitment of activated $CD8^+$ cytotoxic T lymphocytes (CTLs), is $r_1 = 0.2988 \times 10^8\ day^{-1}\ cells$ [164, 190, 191] and $r_2 = 0.2755 \times 10^8\ day^{-1}\ cells$ - estimate.

Comparing with previous studies

Using key model parameters, we started our simulation by comparing our results to a previously published model by de Pillis et al. [1] who also investigated the interactions of the NK and $CD8^+$ cells with various tumor cell lines. It is important to emphasize here that the study in [1] is based on assuming that tumor cells are a homogeneous population, while in this study tumor cells are considered to be a heterogeneous (i.e. different tumor cell lines: naive and wild-type tumors) population. This is motivated by the evidence that tumor cells develop certain immunoresistance to a specific immune cell after surviving their brief encounters [164]. During tumor cell development, tumor cells mutate in such a way that they are not all identical [222]. This usually results in heterogeneous tumor cell sub-populations [222, 223]. Recent evidence shows that tumors cells that survive immune surveillance usually develop complex mechanisms that enable them to evade the immune system [25]. By considering different tumor cell populations, our model shows that tumor escape from immune surveillance may be attributed to evolution and development of these heterogeneous tumor cell populations. In addition, this model successfully indicates the advantage of following different tumor populations to reduce tumor escape from immune surveillance.

Figure 3.3 indicates that naive tumor cells grow logistically in the presence of a weak

immune response, not only in the absence of the immune response as done in [1]. More importantly, since NK cells are always present in the body [1, 212], this figure shows that the fact that tumor cells develop and grow in the presence of functioning immune surveillance [4].

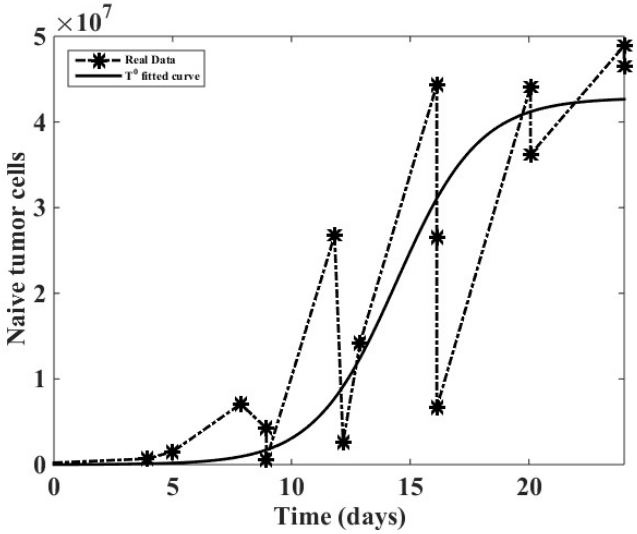

FIG. 3.3. Plot shows fitting of naive tumor cell population of the model (3.15) – (3.20) to the real data of tumor growth used by De Pillis et al [1].

Investigating the effects of the weak immune system on tumor evasion

The simulations, as indicated in Figure 3.4 suggest that the model, with the parameter assumptions and values we used, is capable of reproducing tumor escape from immune surveillance in a biologically realistic time frame.

It is known that the immune system is capable of recognising and eradicating small tumors, though some tumor cells can slip through the immune system net [4, 36, 224, 225]. Figure 3.4 indicates that tumor cells usually escape immunosurveillance when the immune system is depleted [1]. Here, by depleted immune system we mean the case when there are few cytotoxic immune cells at the tumor site. More apparent growth dynamics of each cell population are given in Figure 3.5(a) – 3.5(b).

The results in Figure 3.5(a) could describe a case where immune system cells are out-

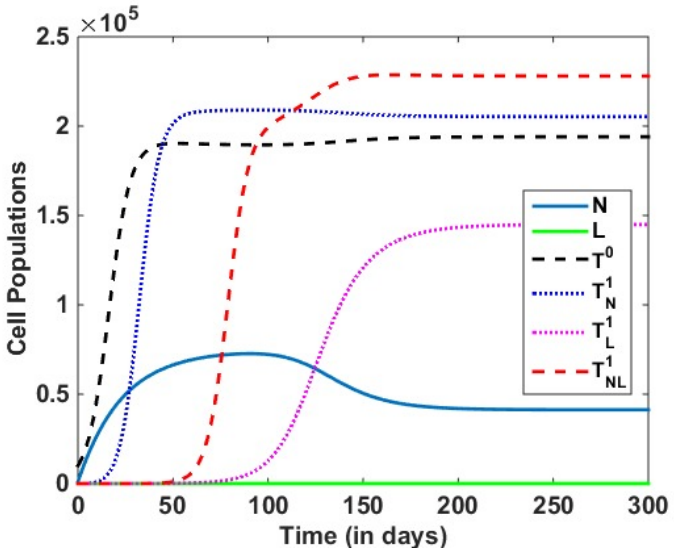

FIG. 3.4. Plots indicating the growth of the tumor cell populations and immune cells over time in the instance where there is low influx of natural killer (NK) cells, $s = 3.2 \times 10^3\ day^{-1}\ cells$ and low recruitment of activated CD8$^+$ cytotoxic T lymphocytes (CTLs), $r_1 = 0.2988 \times 10^{-8}\ day^{-1}\ cells$ and $r_2 = 0.2755 \times 10^{-8}\ day^{-1}\ cells$. The plot shows that all the "wild-type" tumors, T_N^1, T_L^1 and T_{NL}^1, are capable of evading the immune system.

competed by tumor cells in the search of necessary nutrients required to maintain their survival. Note that the CTLs are continually declining because we have assumed that they are only present when the tumor is present, hence they have a negative growth rate. Thus, we observe in Figure 3.5(b) that all tumor populations are growing when the immune system is weak (i.e. when there is low influx of natural killer (NK) cells, $s = 3.2 \times 10^3\ day^{-1}\ cells$ and low recruitment of activated CD8$^+$ cytotoxic T lymphocytes (CTLs), $r_1 = 0.2988 \times 10^{-8}\ day^{-1}\ cells$ and $r_2 = 0.2755 \times 10^{-8}\ day^{-1}\ cells$).

However, if the immune system is strong (i.e., when there are 10^5 NK cells and 10^2 activated CD8$^+$ lymphocytes), and high influx of NK cells, $s = 3.2 \times 10^4\ day^{-1}\ cells$, we obtain Figure 3.6.

Figure 3.6 demonstrates that the fact that an effective immune surveillance, mediated by NK cells and activated CD8$^+$ CTLs, is capable of controlling tumor growth [2]. We further investigate how tumor may evolve if the immune system is weak. Here, a weak immune system initially consists of 10^3 NK cells and 10 activated CD8$^+$ cytotoxic T lymphocytes

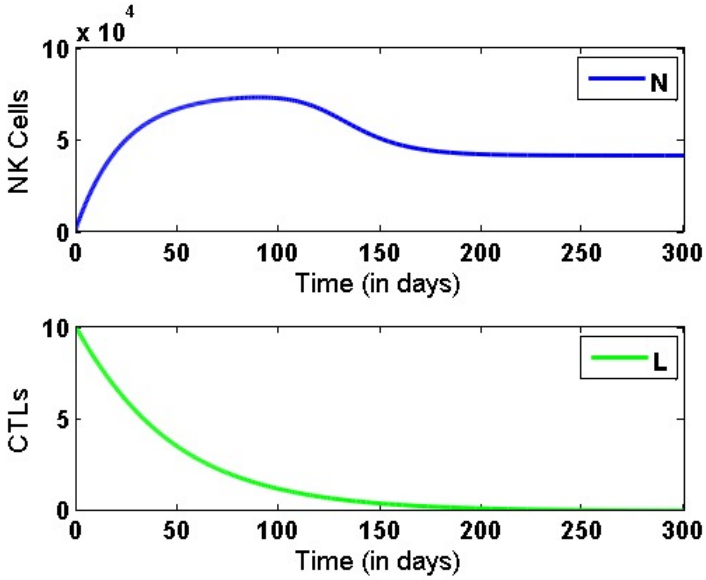

(a) Immune cells.

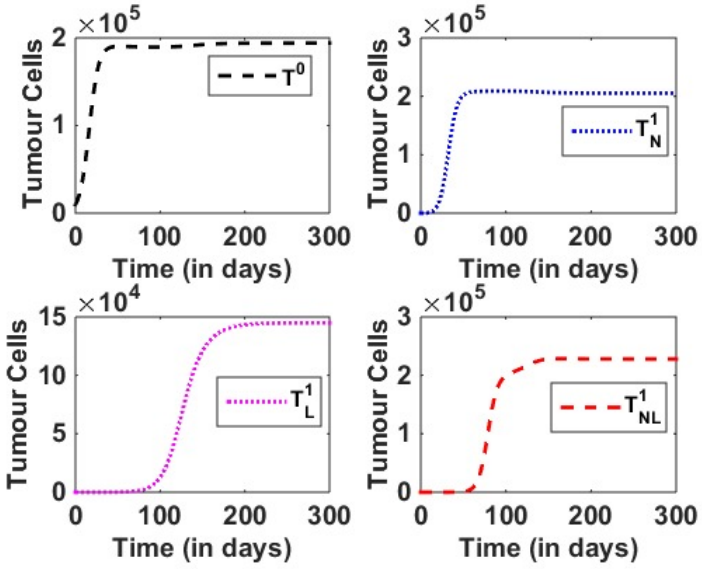

(b) tumor cells.

FIG. 3.5. Plots of individual tumor and immune cell populations when there is low influx of natural killer (NK) cells and low recruitment of activated $CD8^+$ cytotoxic T lymphocytes (CTLs). Figure 3.5(a) indicates a natural response of NK cells to the presence of the tumor, followed by decline to a non-zero level of NK cells. Figure 3.5(b) shows how each tumor sub-population is growing over time in the case when the immune system is weak.

for the same initial naive tumor cell of 10^4 cells. More interestingly, by following indi-

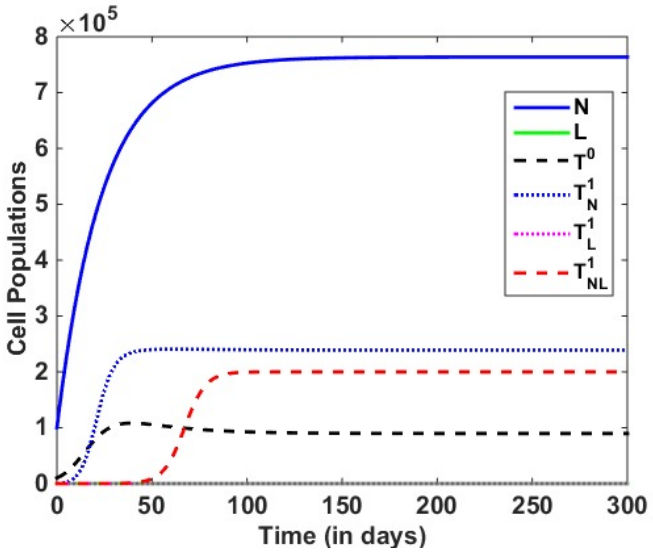

FIG. 3.6. Plots indicating the growth of the tumor cell populations and immune cells over time in case where there is high influx of natural killer (NK) cells, $s = 3.2\times10^4\ day^{-1}\ cells$. The plot indicates that immune system is capable of eliminating some "wild-type" tumor cells, particularly T_L^1, or reducing growth of other "wild-type" tumor cells, T_N^1 and T_{NL}^1.

vidual plots of each population, we obtain Figure 3.7(a) − 3.7(b). Figure 3.7(a) − 3.7(b) indicates that even-though the immune system is able to eradicate or reduce some tumor sub-populations, an evolution of multi-immunoresistant tumors cells, denoted by T_{NL}^1, that escaped from both arms of immune systems continue increasing. This simulation demonstrates the fact that tumors do develop in the presence of a functioning immune system [4, 5, 36, 87].

3.4 Sensitivity analysis

We now explore the sensitivity analysis of the model output to parameter values. We carry out two standard procedures of evaluating model sensitivity to changes in the parameter values, namely global sensitivity analysis (GSA) and local sensitivity analysis (LSA).

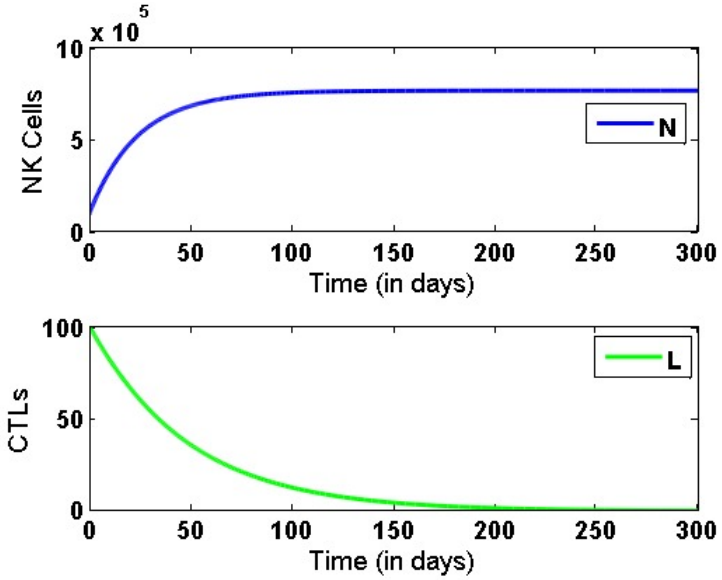

(a) Immune cells.

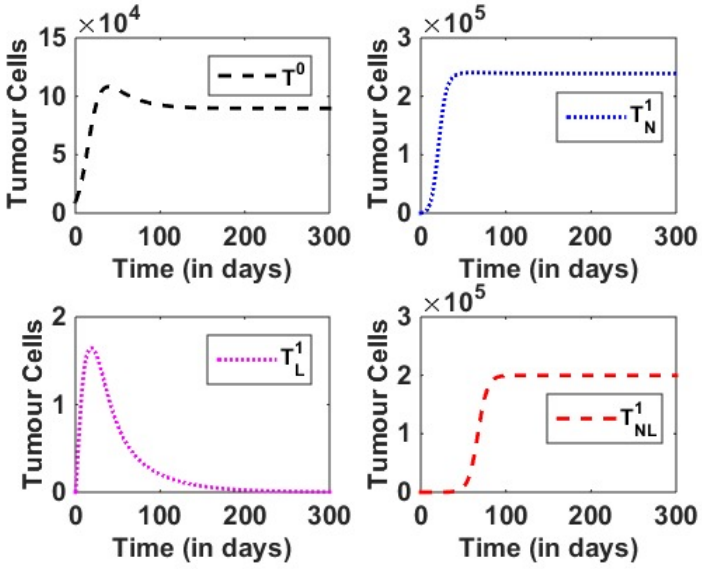

(b) tumor cells.

FIG. 3.7. Plots of individual tumor and immune cell populations when there is high influx of natural killer (NK) cells and high recruitment rate of activated $CD8^+$ cytotoxic T lymphocytes (CTLs). Figure 3.7(a) shows a rapid growth of NK cells in response to the presence of the tumors, followed by saturation because there cannot be an unbounded supply of NK cells in a realistic biological setting. Figure 3.7(b) shows how each tumor sub-populations eradicated or reduced over time.

3.4.1 Global sensitivity analysis (GSA)

We performed a global sensitivity analysis (GSA), where all 22 model parameters are varied simultaneously, to investigate how variations in all model parameters influence the model outcome. In particular, we consider one of the most reliable and efficient types of global sensitivity analysis indexes, namely partial rank correlation coefficient (PRCC) [226]. PRCC measures the relationship (specifically monotonicity) between a model variable of interest and each model parameter. Results of PRCC help to identify which key input parameters contribute most to model variability. PRCC takes values between -1 and $+1$. The sign of PRCC indicates how the model variable of interest is qualitatively related to each model parameters. The absolute value of PRCC determines the degree of monotonicity between the model variable of interest and the specific parameter.

Using the weak immune system baseline conditions, (i.e. 10^3 NK cells and 10 activated $CD8^+$ CTLs), we first computed the time to equilibrium (tumor free equilibrium) before performing the global sensitivity analysis. Here, time to equilibrium is the time immune system requires to eradicate or at least bring the tumor to a controlled state without any treatment or boosting. For our model, time to equilibrium is 60 days. After 60 days, most of the naive tumor growth dynamics have already been established. That means, either the tumor has been eliminated by the immune system or escaped the immune surveillance. Of particular interest, are the intermediate time points prior to dynamical equilibrium. These time points may represent the time periods whose effect in tumor-immune interactions may be altered through specific immunotherapies to inhibit tumor escape or prolong immune system control on tumor populations.

We performed PRCC analyses for four different time points in order to investigate which parameters consistently influence each model cell population in time. The indexes are evaluated at the following time points $15, 30, 45$ and 60 days prior to equilibrium state, and the model variable chosen for sensitivity analysis is natural killer cells (Equation (3.15)). For each of the four time points, denoted by $1, 2, 3$ and 4, PRCC results are shown in Figure 3.8. From the PRCCs results presented in Figure 3.8, we conclude that the parameters for NK source, s, natural death of NK cells, μ_1, and the binding rate, α_L^+, of NK cells to the "wild-type" tumours, T_L^1, account for most uncertainty for NK cell population.

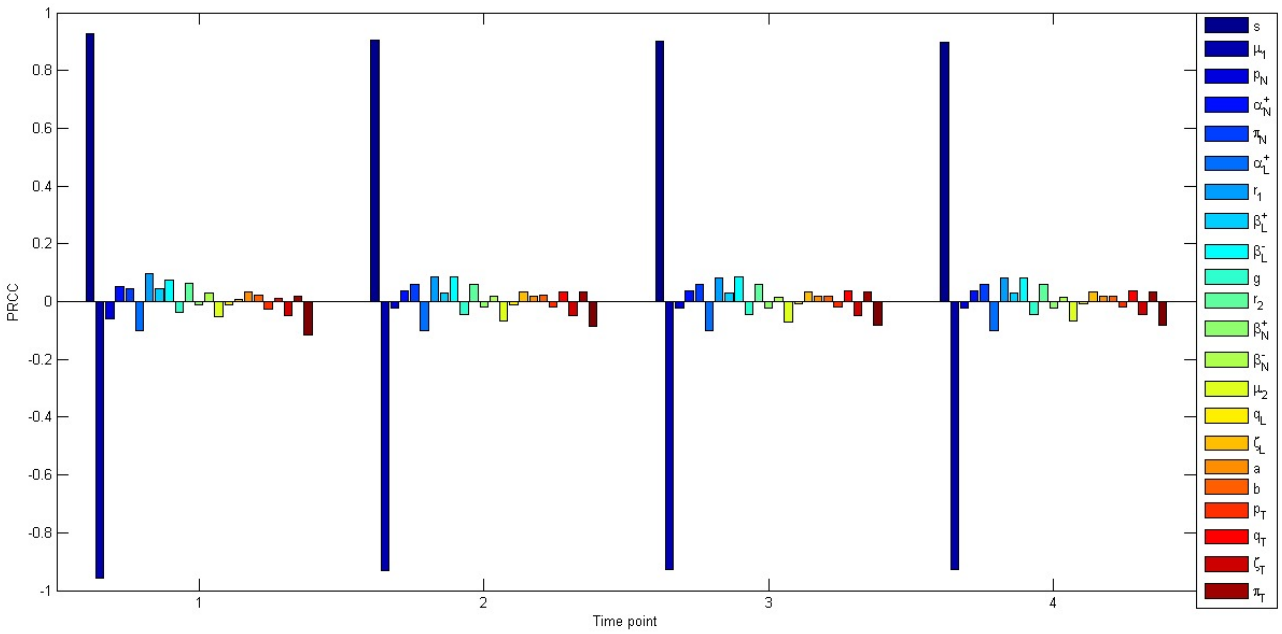

FIG. 3.8. PRCC results showing sensitivity indices of the model parameters with naive tumor cell population chosen as a baseline PRCC analysis variable.

Figure 3.8 indicates PRCC results which show how parameters s, μ_1 and α_L^+ are consistently significant and the most important parameters accountable for most of the variability NK cells. The PRCC results suggest that the NK cell population over time is mainly affected by variations in the parameters s, μ_1 and α_L^+. PRCC scatter plots of the NK cell population versus each parameter have been obtained, but we provide only scatter plots of these three important parameters in Figure $3.9(a) - 3.9(c)$, where the strong correlations are confirmed. Note that although the scatter plot for the parameter α_L^+ shows weak correlation, parameter α_L^+ is found to be consistently significant with the PRCC analysis.

In all figures in Figure $3.9(a) - 3.9(c)$, the axes indicate the residuals of the linear regression between the rank-transformed values of the NK cell population against the rank-transformed values of each the parameter. Note, Figure 3.9(a) and Figure 3.9(b) are statistically significant even at 0.001 level, while Figure 3.9(c) is significant at 0.05 level of significance. The source of NK cells has a strong positive, with PRCC of 0.92697, correlation with NK cell population, while the death rate of NK cells has a strong negative, with

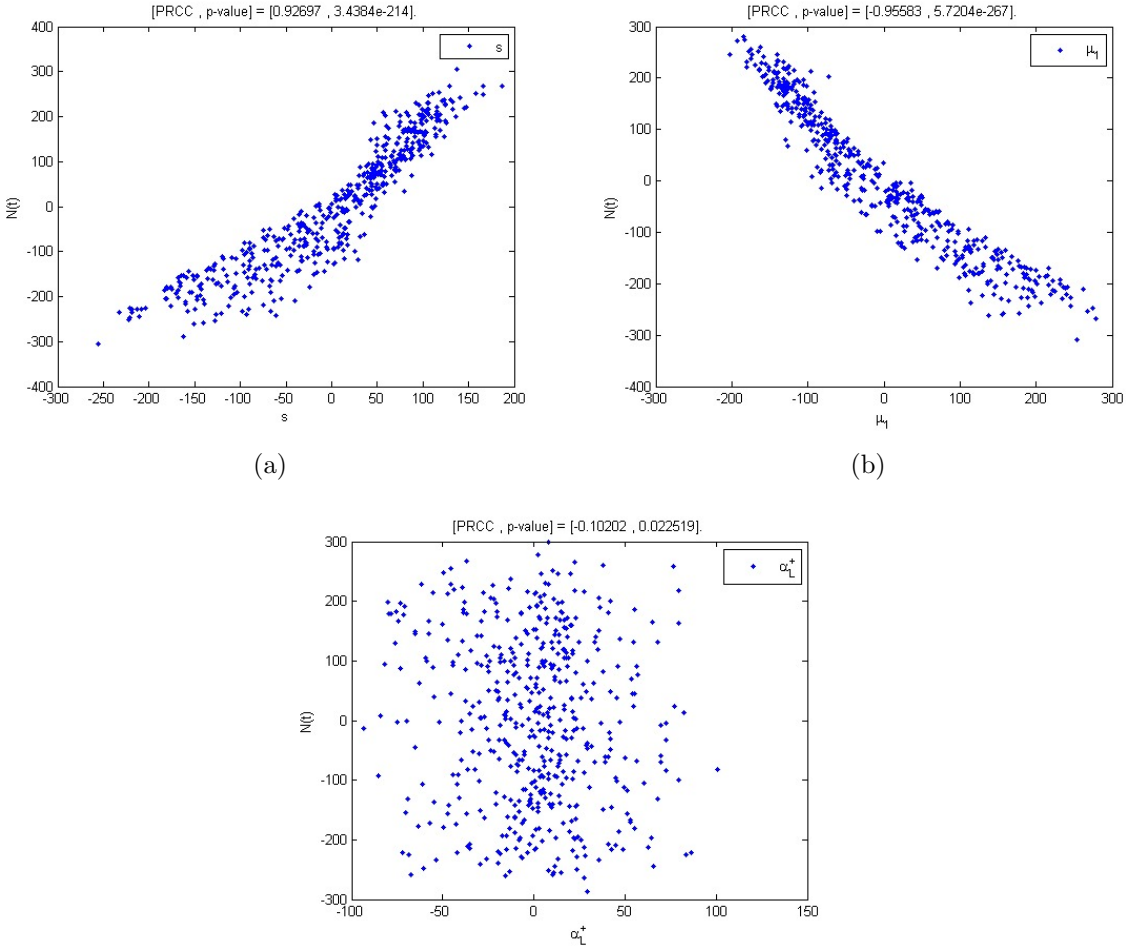

(a) (b) (c)

FIG. 3.9. PRCC scatter plots of the most significant parameters s, μ_1 and α_L^+ (computed at the last time point, day 60). The title of each plot provides the PRCC value with the corresponding p-value. The results are significant at the 0.05 level.

PRCC of -0.95583, correlation with NK cell population. The absolute value of the PRCC value of 0.5 indicates no correlation between the input variable (i.e. parameters in this case) and the outcome variable (i.e. the NK cell population). Thus, from Figure 3.9(c) we note that the binding rate of NK cell to tumor cell has a moderate negative correlation, with the PRCC value of -0.10202 and a small p-values $0.022519 < 0.05$, with the NK cell population. The parameters with large absolute PRCC values, PRCC $> |0.5|$, with corresponding small p-values < 0.05, are considered to be the most important parameters [227]. These scatter plots illustrate how significant is PRCC analysis in determining monotonic

relationships between model variables and parameters using rank-transformation method.

Most interestingly, we performed PRCC analysis with regard to naive tumor cells in order to investigate which parameters have significant variations in naive tumor population. This is important because parameters with high influence on naive tumor cell population may be accountable for tumor escape, leading to a new generation of wild-type tumor, $T_i^1, i = N, L, NL$. Identification of these parameters can help to design treatment strategies that specifically target those factors that augment tumor escape from immune surveillance. The results of the PRCCs are presented in Figure 3.10.

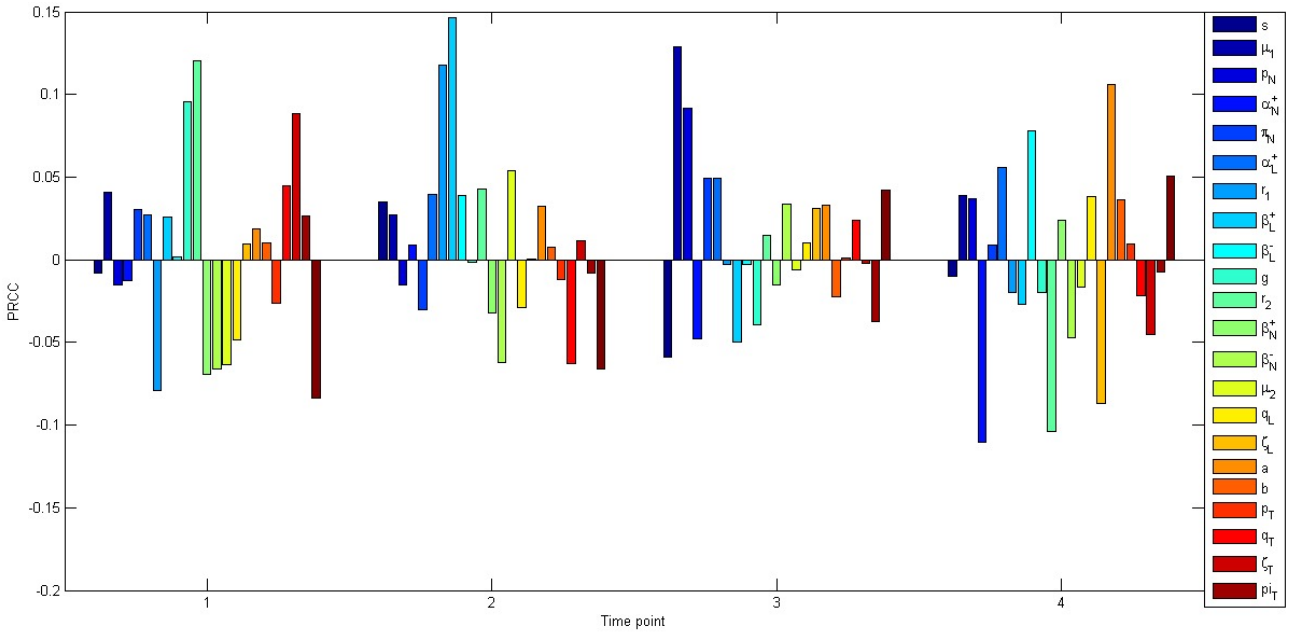

FIG. 3.10. PRCC results showing sensitivity indices of the model parameters with "naive" tumor cell population chosen as a baseline PRCC analysis variable.

Figure 3.10 shows PRCC results over fourth different points: $15, 30, 45$ and 60 days. In this analysis, different parameters become statistically significant in different time points. For instance, two parameters, the maximum CTL recruitment by immunogenic tumor cells, g, and the rate of CTLs recruitment due to CTL-"wild-type" tumor complex, r_2, were statistically significant in the first time point. In the second time point, 30 days, CTLs recruitment due to CTL-"naive" tumor complex, r_1 and the binding rate of CTLs to naive

tumor cells, β_L^+, are most influential in determining the tumor escape ($|PRCC| > 0.5$) and are statistically significant (p-value < 0.05). In 45 days, only death of NK cells, μ_1, and the proportion of NK cells that survived from NK-tumor complex formed with "wild-type" tumor cell that escaped from CTL and maintained high level of effectiveness, p_N, are most significant influential parameters. In the last in 60 days, an intrinsic tumor cell growth rate, a, the binding rate of NK cells to tumor cell that escaped from CTLs, α_L^+, and recruitment rate of CTLs due to CTL-"wild-type" tumor complex are the only parameters that account for most variability in the model.

Despite a large number of parameters the model has, we note that it is significantly more sensitive to variations to few parameters. Interestingly, at later time points, it is highly sensitive to the intrinsic tumor growth rate a, as was the model by de Pillis et al. [216]. This is very interesting because given some tumor data sets these parameters can be easily estimated, as was done in de Pillis et al. [1, 126]. One of the most interesting finding in our analysis results is that the model reveals a higher degree of sensitivity to key parameters that could be targeted with specific immunotherapies. The NK-cell based immunotherapy can be used to enhance immune surveillance against developing tumors [87]. Most interestingly, the fact that tumor-immune interactions can be observed experimentally [2, 54], our sensitivity analysis indicates that the model parameters, such as binding rate of NK cells to tumor cells or CTL recruitment, may be desirable targets for immunotherapy.

3.4.2 Local sensitivity analysis (LSA): Model implications for immunotherapy

We now provide a brief local sensitivity analysis of our model, equations (3.15) – (3.20), in order to investigate how specific parameters of interest influence model behavior. Since the model has many parameters, we only performed sensitivity analysis of parameters that are associated with model implications for immunotherapy. In particular, we focused on how specific changes in the source of NK cells, s, affect the number of "wild-type" tumor cells, T_L^1, that are susceptible to NK-cell mediated lysis after surviving their encounter with the CTLs. To perform sensitivity analysis of our model with respect to the source of NK cells,

s, we assumed that the NK cell influx parameter can be uniformly increased within the range of $\pm 10\%$ or $\pm 20\%$ of the initial parameter baseline value.

Figure 3.11 and Figure 3.12 show the effect of varying the source term in the NK cells, resulting in an increase for NK cell population and reduction of the "wild-type" tumor cells, particularly T_L^1. The NK cell source is varied in a biologically relevant range presented in Table 3.2 in order to investigate the effect of NK cell influx on tumor regression. From Figure 3.11, it can be observed when there is low boosting of NK cells, NK cell density quickly reduces to zero. That means low-level boosting of NK cells, does not increase NK cell density for longer periods of time. For instance, from Figure 3.11, it can be seen that 50% boosting of NK cells continue producing elevated NK-cell density for up to 20 days. Thus, in this simulation, it seems likely that tumor cell evasion from NK-cell surveillance would occur after 20 days. From Figure 3.12, it can also be observed

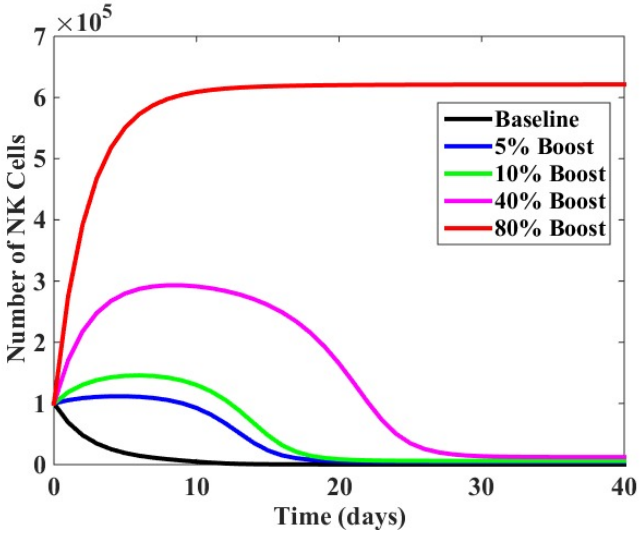

FIG. 3.11. The plot showing the effect of varying the source term of NK cells in numerical solutions. Increasing the source term of NK cells leads increased cell density of NK cells for certain period of time. Other baseline parameters for these simulations are the same as in Table 3.2, but we have values of s as indicated on the graph.

that high-level boosting of NK cells results in significant reduction of tumor cells that are potential targets for NK cell. The presence of a high number of NK cells in tumors contributes significantly to the host's anti-tumor immune responses [228]. It is important to note that Figure 3.12 does not indicate tumor eradication within 40 days, but tumor

control with different NK-cell boosting levels. This result indicates that the NK cell-based immunotherapy may be necessary (although perhaps not sufficient) to achieve an increased tumor regression or a delayed tumor growth.

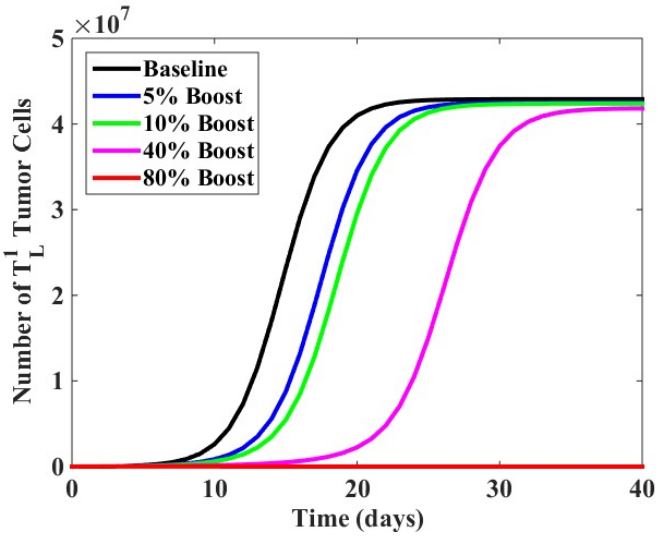

FIG. 3.12. The evolution of the "wild-type" tumor cells, T_L^1, in numerical solutions of our model, indicating the effect of varying the source term of NK cells. By increasing the source term of the NK cells does not only decrease the number of tumor cell population but also reduce time for evolution of these cells. The baseline parameters for these simulation are given in Table 3.2, with values of the source of NK cells, s, as indicated on the graph.

The above results show that the number of immune cells at the tumor site plays a significant role in cancer immune surveillance. It is important to emphasize that at each time step in our simulations, the number of immune cells at the tumor site is characterized by the intent to interact with tumor cells and/ or carry out tumor lysis. When there are few immune cells at the tumor site, we assumed that other immune cells, which are not at the tumors site, are randomly attempting to migrate into immunogenic tumor site. As can be seen in Figure 3.11 and Figure 3.12, an increment in the source of NK cells, results in depleted number of tumor cells.

These results also suggest that an infiltration of NK cells can be used as one of the biological treatment options to boost immune surveillance. Recent evidence indicates that NK-cell infiltration into tumor tissues has been associated with positive prognosis in patients [87]. Moreover, studies from human cancers demonstrate that when there are few infiltrating

NK cells into the tumor site, tumor elimination is not feasible [229, 230]. Therefore, as shown in this study, NK-cell infiltration may be an important immunotherapeutic strategy to enhance immune surveillance against tumor cells.

3.5 Discussion

In this chapter, we developed a novel mathematical model for the immune surveillance of tumors. The model describes how tumor cells evolve and survive the brief encounter with the immune system mediated by natural killer (NK) cells and the activated $CD8^+$ cytotoxic T lymphocytes (CTLs). To our knowledge, this is the first mathematical study of the tumor escape and acquisition of immune resistance to multiple immune cell populations. The key features of this model are:

(a) *The development of immunoresistance by the tumor cells:* the model successfully demonstrates that an evasion of tumor cells from their brief encounters with specific immune cells may enable tumor cells to acquire an immune-resistant phenotype through genetic mutations or epigenetic changes. After surviving an immune attack, to support their growth, tumor cells either mount a "counter-attack" or develop resistance to immune cells [2, 26, 47].

(b) *The inclusion of multiple tumor cell populations:* multiple tumor cell populations are included in this model, so that their respective evasion mechanisms can be quantified at different stages of tumor growth. To avoid CTL-mediated lysis, tumor cells usually down-regulate the major histocompatibility complex (MHC) class I molecules [30–32, 192, 213]. However, this down-regulation of MHC class I molecules renders tumor cells more susceptible to NK cell-mediated killing [32, 192]. Thus, the model qualitatively illustrates these dynamics of tumor hiding from immune cells.

The model predicts that the low NK cell number could be attributed to escape of cancer cells from the mechanisms of immune surveillance as shown in Figures 3.4 and 3.5(b). It also predicts that the development of immunoresistance by tumor cells is inevitable in tumor immune surveillance as shown in Figures 3.6 and 3.7(b). In addition to an important strategy of promoting tumor regression by focusing on increasing $CD8^+$ T cell activity [126] (i.e. to augment the negative CTL growth), our model supports boosting of NK cells. Most interestingly, an immune-boosting of NK cells may offer a better strategy for devising novel and more effective immunotherapies aimed at eliminating nascent tumor escape and reducing acquired immune resistance. Evidence from experimental studies indicates that

insufficient NK cell recruitment leads to tumor progression [231]. Additionally, the model indicates that the host immunity can only effectively control tumor growth of certain cell populations if the immune system is strong, as can be seen in Figure 3.6, otherwise tumor growth progression would be uncontrollable. Recent progress in NK cell immunobiology indicates that tumor cells can be eradicated only when immune responses are adequate [87].

The major results from this model are highlighted as follows:

An influx of the external source of NK cells might play a crucial role in enhancing NK-cell immune surveillance. The numerical simulations indicate that an infiltration of the external source of NK cells might play a crucial role when there are insufficient NK cells in the body as seen in Figure 3.11 and Figure 3.12. Increasing the source term of NK cells leads to an increased number of NK cells and consequently a decrease in the number of tumor cell populations. This could be used as an adoptive cellular immunotherapy (ACI), a treatment in which the anti-tumor leukocytes, like activated $CD8^+$ cytotoxic T lymphocytes (CTLs) or activated NK cells, are activated and cultured in large numbers in a laboratory and transferred into tumor bearing host. Advances in anti-tumor treatments such as cytokine-based immunotherapy [232] and adoptive cellular therapy [86] indicated that NK-cell based immunotherapies provide a better prognosis against tumors [87].

Immune system alone is not fully effective against progression of tumor cells. The model's simulations show that the immune system alone is not fully effective against progression of tumor cells. For example, Figure 3.6 elucidates the dynamics of tumor-immune interactions with a strong immune system, but the multi-immunoresistant tumor cell population continues to grow. It is also worthwhile to note that the NK cell population needs to be high enough, in the range of $1.0 \times 10^4 - 3.2 \times 10^4$ day^{-1} $cells$, for an effective anti-tumor response as shown in Figure 3.12. Recent evidence indicates that the presence of a high number of NK cells at the tumor site contributes significantly to the host's immune surveillance [228].

It has been suggested that low NK cell numbers in tumors increases chances of tumor escape from immune surveillance [8, 87, 188, 228, 229, 233]. This has been shown by our model as depicted in Figure 3.4 and Figure 3.5(a) – 3.5(b). In this scenario, all tumor cell populations grow uncontrollably within a short period of time. This demonstrates that the number of immune cells necessary for inhibition of tumor growth is of paramount importance [8]. The NK cells, as part of innate immunity, are the first immune effectors to attack developing tumor cells before the strong specific immunity comes into play [2, 193]. Evidence from clinical studies indicates that improved survival rate of patients with gastric carcinoma was significantly enhanced in patients with a high rate of NK infiltration than in those with a low level of NK infiltration [234]. Hence, the low number of NK cells at the tumor site, may give tumor cells a chance to evade immune surveillance.

More importantly, studies show that high levels of NK cells, particularly tumor infiltrating NK cells (TINKs), have demonstrated a favorable tumor regression in patients with colorectal carcinoma [235] and in squamous cell lung cancer [236]. This suggests that increasing NK-cell influx into tumor tissues could represent a positive prognostic outcome, as implicitly shown by the model's simulations in Figure 3.12.

Multi-immunoresistance. Finally, we note that while some tumor cell populations are decreased, naive tumor cells, T^0, and wild-type tumors that escaped from activated CD8$^+$ CTLs, T_L^1, in Figure 3.7(b), the multi-immunoresistant tumor population, T_{NL}^1, is not altered significantly. Development of the multi-immunoresistant tumor cell population is a major problem in cancer immune surveillance [47, 51].

Recent evidence shows that even-though a NK cell immunity complements a CD8$^+$ cytotoxic T lymphocytes (CTLs) immunity, poor prognosis has been observed from patients with HLA-I-defective melanoma cells [237]. This indicates that tumors are capable of deploying complex mechanisms to evade NK cell immunosurveillance as well. Experimental studies of Gulubova et al. [188] indicate that low NK cell numbers at the tumor site could be attributed to escape of metastatic cancer cells from the mechanisms of immune surveillance. This is confirmed by our simulation as indicated in Figure 3.4.

More importantly, the model simulations, depicted in Figure 3.11 and Figure 3.12, support the importance of infiltrating NK cells in tumor immune surveillance, which can be

enhanced by NK cell-based immunotherapeutic approaches like infiltration of autologous (patients' own) NK cells [87, 238].

An important drawback of the proposed model is that the multi-immunoresistant tumor population persists growing regardless of the presence of a high NK cell influx or a high recruitment of activated $CD8^+$ cytotoxic T lymphocytes (CTLs) to the tumor site. This problem can be avoided by combining immunotherapy, as indicated by external source of NK cells in our model, with other therapies like chemotherapy and/ or oncolotic virotherapy [239, 240].

Chapter 4

Oncolytic Potency and Reduced Virus Tumor-Specificity in Oncolytic Virotherapy. A Mathematical Modeling Approach

In the present chapter, we address by means of mathematical modeling the following main question: ***How can oncolytic virus infection of some normal cells in the vicinity of tumor cells enhance oncolytic virotherapy?*** To this end, we formulate a mathematical model describing the interactions between the oncolytic virus, the tumor cells, the normal cells, and the antitumoral and antiviral immune responses. The model consists of a system of delay differential equations with one (discrete) delay. We derive the model's basic reproductive number within tumor and normal cell populations and use their ratio as a metric for virus tumor-specificity. Numerical simulations are performed for different values of the basic reproduction numbers and their ratios to investigate potential trade-offs between tumor reduction and normal cells losses. A fundamental feature unravelled by the model simulations is its great sensitivity to parameters that account for most variation in the early or late stages of oncolytic virotherapy. From a clinical point of view, our findings indicate that designing an oncolytic virus that is not 100% tumor-specific can increase virus particles, which in turn, can further infect tumor cells. Moreover, our findings indicate that when infected tissues can be regenerated, oncolytic viral infection of normal cells could improve cancer treatment.

4.1 Introduction

Oncolytic virotherapy is an emerging anti-cancer treatment modality that uses Oncolytic Viruses (OVs). One of the most attractive features of the OVs is that they are either naturally occurring or genetically engineered to selectively infect, replicate in and damage tumor cells while leaving normal cells intact [96, 100]. This therapeutic approach faces a major challenge consisting of the immune system's response to the virus, which hinders oncolytic virotherapy. To date, complex dynamics of oncolytic viral tumor infection and the consequences of OV-induced immune response are poorly understood [241–243]. The immune system has often being perceived as a major impediment to successful oncolytic virus therapy by facilitating viral clearance [145, 227]. Additionally, clinical evidence [138, 244, 245] indicates that some oncolytic viruses have the ability to infect and replicate within normal cells as well, especially in the brain, where neurons are unable to replicate, and the oncolytic-induced neuronal damage could lead to undesired outcomes [102]. Evidence from both pre-clinical and clinical experiments indicates that some oncolytic viruses (OVs) can infect and replicate in normal cells surrounding the tumor [145, 246].

While this could be seen as another challenge to virotherapy, it could also be used to increase viral potency as long as the replication within normal cells is well understood and controlled. Much remains unknown about how to use normal cells to augment the oncolytic virus population[247, 248]. It is important to note that when systemically administering oncolytic virus that is not 100% tumor specific (i.e., viruses that can infect and replicate within normal cells), infection of some normal cells can occur [138, 245]. When administering oncolytic viruses intravenously, the amount of virions that effectively reach the tumor site is often reduced [249]. Note that viruses are small passive particles that reach their target cells via either radial cell-to-cell spread or diffusion across concentration gradients in soluble matters, such as blood, and propagate infection. Thus, infecting some normal cells, by oncolytic virus, surrounding the tumor may aid to increase virus population. The higher the number of infectious virions at the tumor territory, the higher the probability of infecting and destroying every single tumor cell [249, 250]. It is important to investigate how infection of the host normal cells by the OVs can enhance the oncolytic virotherapy. To normal cells, such as liver, that can be quickly self-regenerated after a trauma or disease, infection of normal cells could be tolerable if such infection is not endemic (i.e., the

infection does not persist forever) and could potentially aid to control tumor growth [251].

It is important to note that if the OV is not 100% tumor-specific and is administered intravenously, then it can infect, not only the target tumor cells, but also some healthy normal cells in the tumor site. Even though intratumoral viral injections offer direct tumor infection, they are of limited use in regions (such as the brain) where the tumor cannot be reached directly [111]. Thus, intravenous virus administration would be the only viable option in those scenarios. Numerous pre-clinical attempts have been made to enhance the oncolytic potency of some oncolytic viruses, such as recombinant VSV vectors, with limited success.

Various mathematical models have been developed to investigate the dynamics of the oncolytic viruses on tumor cells [144, 153, 239, 252]. None of the existing mathematical models, however, explicitly considers the effects of the potential adaptive immune responses against infected normal cells or against the virus itself after successful oncolytic virus propagation. For example, the mathematical models in [144, 252], describe the interactions of the immune cells with oncolytic viruses and tumor cells in virotherapy. While these two models incorporated the effects of adaptive immunity as the effector and memory immune responses, they did not consider tumor-immune interactions following successful onocolytic viral propagation. Additionally, these two models considered intratumoral injection of the oncolytic virus, while in our modeling attempt, we consider intravenous virus injection into the susceptible cell population.

Up to date, there is no mathematical model that delineates how oncolytic viruses that are not 100% tumor-specific can be used to augment oncolytic virotherapy with attenuated effects on normal cells. A recent study by Okamoto et al. [143] illustrates how infections of the normal cells by the oncolytic virus could enhance a cancer virotherapy prior to the accumulation of the adaptive immune response. They modeled how apparent competition between normal and tumor cell populations, both cell populations virally infected with a given oncolytic virus, can drive tumor cell population to extinction prior to accumulation of an adaptive immune response. While this model elucidated how infection of normal cells by oncolytic viruses can aid to increase the virus population size at the tumor site and reduce tumor burden, it did not take into account the fact that the oncolytic viral infection on the normal cells can induce unexpected and inevitable immune responses against the

infected normal cell population.

Our proposed model also aims to elucidate the tumor-normal-immune-viral dynamics $1-4$ days in the presence of immune response triggered by the escalated viral infection of normal cells. This is very important because the induction of activated $CD8^+$ T cells into the tumor site may limit subsequent oncolytic virus spread and intratumoral infection. Even though we do not model the innate immune responses, it is important to note that the innate immune response against the virally-infected cells is often active in about $2-7$ days post-infection [253].

4.2 Mathematical model formulation

The mathematical model is based on the diagram shown in Figure 4.1. The model's variables and parameters are listed in Tables 4.1 and 4.2, respectively. The model describes the interactions between normal and tumor cells in the presence of the adaptive immune responses following an initial successful viral propagation phase on both normal and tumor cell populations. It consists of a system of delay differential equations (DDEs) with one discrete delay representing the time necessary to induce tumor-specific immune response. The main objectives of the proposed model are to predict: (1) the oncolytic viral tumor-specificity that maximises tumor reduction while minimizing the undesirable toxicity on normal tissue surrounding the tumor; (2) the effects of the potential antitumoral and antiviral immune responses in oncolytic virotherapy; and (3) tumor's response to oncolytic viral infections, particularly, the model's performance to single-viral and multi-viral injections strategies. For our modeling framework, we use the basic reproductive number R_0 (see Section 4.3.1) to indicate the combined therapeutic index of the oncolytic virus that is not 100% tumor-specific as a measure of oncolytic potency of the normal and tumor cell populations. Understanding the therapeutic index for oncolytic viruses is essential for the assessment of safety and selectivity of oncolytic viruses [254].

Our proposed model uniquely characterizes the impact of the oncolytic virus that is not 100% tumor-specific on the normal and tumor cell populations and further assesses the effects of corresponding antiviral and antitumoral adaptive immune responses following a successful virus propagation in oncolytic virotherapy. Here, the oncolytic virus that is not

TABLE. 4.1. Model Variables

Variable	Description
$N_S(t)$	the total number of susceptible (uninfected) normal cell population
$T_S(t)$	the total number of susceptible (uninfected) tumor cell population
$N_I(t)$	the total number of infected normal cell population
$T_I(t)$	the total number infected tumor cell population
$V(t)$	the total number of oncolytic virions
$Y_T(t)$	the total number of tumor-specific immune cells (primed tumor antigen-specific $CD8^+$ T cells)
$Y_V(t)$	the total number of virus-specific immune cells (primed antiviral $CD8^+$ T cells)

100% tumor-specific is assumed to be a vesicular stomatitis virus (VSV), and the adaptive antitumor/antiviral immune cells are $CD8^+$ T cells. We have chosen to use VSV in our model because it is capable of infecting a wide range of cell lines, has a genome that is easy to manipulate, and is capable of producing high viral titers [244, 258, 259]. More appropriate to our model, it has potential to infect both populations of normal and tumor cells. In order to allow the VSV to infect both normal and tumor cell populations, we assume that the viral injections into the system are administered intravenously and close to the tumor. One important assumption underlying our model is that the interaction kinetics between cell population and the VSV follow mass action kinetics, and all cell populations are homogeneously mixed as assumed in [1, 260, 261]. Homogeneous mixing implies that there are no different cell types within one cell population. Mass action kinetics are the appropriate interaction kinetics when one assumes that the density of the cell populations and viral particles is proportional to the total number of cells and viral particles [262]. Alternative to the mass action infection kinetics are the kinetics that account for the possibility of virus infection saturation at higher virus concentrations (e.g., see models in [263, 264]) or the virus infections that are frequency-dependent (e.g., see models in [239, 262]). Although such virus infection kinetics may be more realistic than mass action kinetics, they may, however, not be well known and may lead to more parameters.

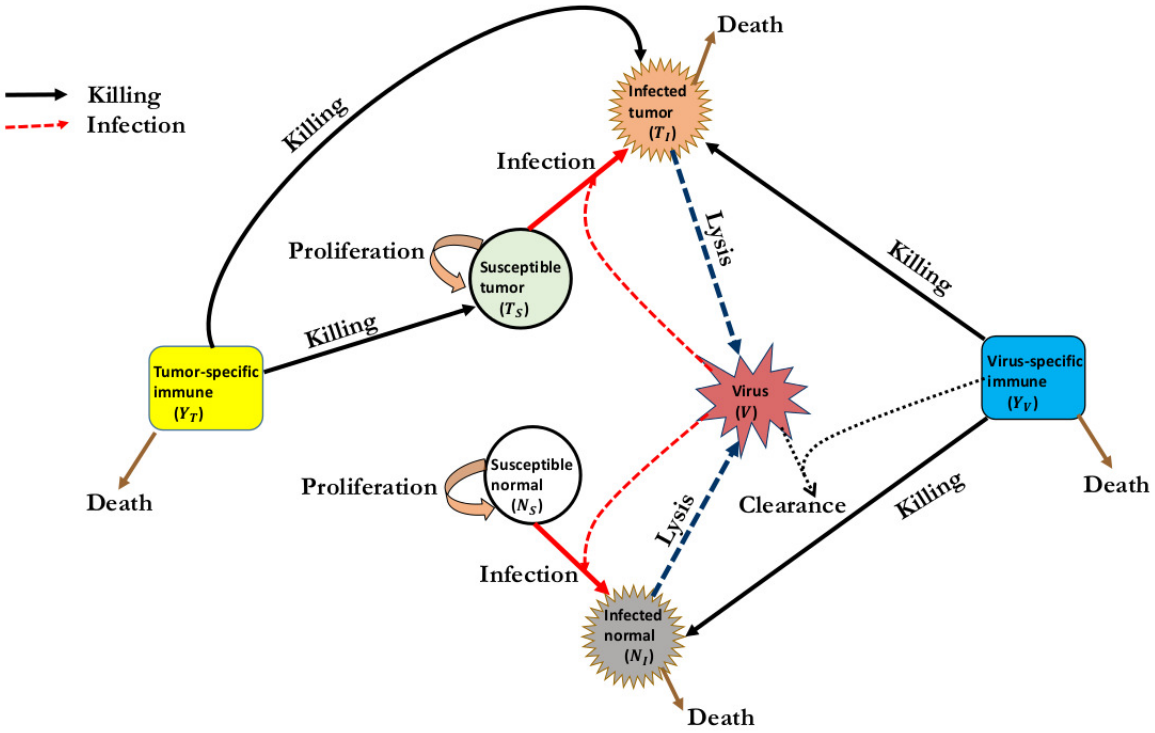

FIG. 4.1. A schematic representation of the interactions among normal cells, tumor cells, immune cells, and oncolytic viral particles. Susceptible (Uninfected) normal and tumor cells become infected by an oncolytic virus (vesicular stomatitis virus (VSV)). After successful viral propagation within the infected cells, infected cells undergo lysis (cell rupture) producing a progeny of new infectious viruses which spread and infect other susceptible cells. Debris from infected cells activates the virus-specific immune cells which then induces killing of infected cells and clearance of free virus. The tumor-specfic immune cells recognise (due to expression of tumor-associated antigens (TAAs)) and kill both uninfected and infected tumor cells.

4.2.1 Model assumptions

The biological assumptions incorporated in the model based on the discussion above and the scientific literature are as follows:

1. The susceptible (uninfected) normal and tumor cells grow logistically at the rates, r_N and r_T, up to their carrying capacities, K_N and K_T, respectively. The choice of the logistic growth for uninfected tumor cells is based on the fact that tumors grow logistically in the absence of immune response [1]. Similarly, in the absence of cancer

cells, normal cells are assumed to grow logistically [265].

2. For infected cell populations, we assume that their lifespan is much shorter than uninfected cell populations; hence, we do not need logistic growth.

3. Given that the oncolytic virus can successfully infect normal cells, we assume that normal cells, in the neighbourhood of tumor host tissue, can quickly self-renew during and after the oncolytic therapy [251].

4. To induce immune responses, oncolytic viruses are often designed to express immunostimulating cytokines, such as a granulocyte macrophage-colony stimulating factor [GM-CSF] [266] and interleukin [IL]-2 [267]. We, therefore, assume that oncolytic virus infection on both normal and tumor cell populations can induce virus-specific immune responses mediated by antiviral $CD8^+$ T cells [268].

5. We assume that tumor-specific immune cells (antitumor $CD8^+$ T cells) can recognise and kill both uninfected and infected tumor cells because tumors often express tumor-associated antigens (TAAs) [94, 269].

6. We assume that there is no virus-specific immunity prior to oncolytic virotherapy, and hence all infected cell populations, and virus-specific immune cells start at size 0. On the other hand, we assume that the initial size of the susceptible (uninfected) normal and tumor cell populations is equivalent to the size determined by the experiments at time 0 of tumor detection. Thus, we assume that tumor-specific immunity, measured by the number of antitumor $CD8^+$ T cells at the tumor site, exists at the start of oncolytic virotherapy.

7. We also assume that upon lysis of an infected cell, a progeny of new infectious oncolytic viruses bursts out of the lysed cell, and infect neighbouring uninfected cells.

4.2.2 Model equations

The model consists of the following delay differential equations (DDEs):

$$\frac{dN_S}{dt} = \underbrace{r_N N_S \left(1 - \frac{N_S + N_I}{K_N}\right)}_{\text{proliferation}} - \underbrace{\beta_N N_S V}_{\text{infection}} \tag{4.1}$$

$$\frac{dT_S}{dt} = \underbrace{r_T T_S \left(1 - \frac{T_S + T_I}{K_T}\right)}_{\text{proliferation}} - \underbrace{\beta_T T_S V}_{\text{infection}} - \underbrace{\gamma_T \frac{Y_T}{h_Y + Y_T} T_S}_{\text{killing by immune cells}} \tag{4.2}$$

$$\frac{dN_I}{dt} = \underbrace{\beta_N N_S V}_{\text{infection}} - \underbrace{\lambda_N N_I}_{\text{lysis}} - \underbrace{\gamma_V Y_V N_I}_{\text{killing by immune cells}} \tag{4.3}$$

$$\frac{dT_I}{dt} = \underbrace{\beta_T T_S V}_{\text{infection}} - \underbrace{\lambda_T T_I}_{\text{lysis}} - \underbrace{\gamma_T \frac{Y_T}{h_Y + Y_T} T_I}_{\text{killing by immune cells}} - \underbrace{\gamma_V Y_V T_I}_{\text{killing by immune cells}} \tag{4.4}$$

$$\frac{dV}{dt} = \underbrace{b_T \lambda_T T_I}_{\text{lysis}} + \underbrace{b_N \lambda_N N_I}_{\text{lysis}} - \underbrace{\omega V}_{\text{clearance}} \tag{4.5}$$

$$\frac{dY_T}{dt} = \underbrace{p_T \frac{T_S + T_I}{h_T + T_S + T_I}}_{\text{recruitment}} - \underbrace{\delta_T Y_T}_{\text{death}} \tag{4.6}$$

$$\frac{dY_V}{dt} = \underbrace{p_V \left(T_I(t-\tau) + N_I(t-\tau)\right)}_{\text{recruitment}} - \underbrace{\delta_V Y_V}_{\text{death}} \tag{4.7}$$

The initial conditions of the model are as follows at $t = 0$: $N_S = 10^{11}$ cells; $T_S = 10^6$ cells; $N_I = 0$ cells; $T_I = 0$ cells; $Y_T = Y_V = 0$ cells; $V(t) = 10^9$ plaque-forming units (PFU). (PFU is a globally accepted measurement for infectious titers (virus particles); non-infectious (defective) virions that are incapable of forming plaques cannot infect their target cells, and thus are excluded when counting the plaque-forming units.) For $\tau \leq t \leq 0$, we have constant history functions of cell concentrations on that time interval. Thus, we implicitly assume that the system was at equilibrium prior to time 0 and apply to above conditions at $t = 0$.

In equation 4.1, the first term, $r_N N_S \left(1 - \frac{N_S+N_I}{K_N}\right)$, represents a logistic growth of the normal cells with an intrinsic growth rate r_N and the carrying capacity K_N. Note, the normal cell population consists of uninfected (N_S) and infected cells (N_I). Since the uninfected normal cells can become infected with the oncolytic virus at the rate β_N, the second

term, $-\beta_N N_S V$, denotes the reduction of normal cell population due infection with the oncolytic virus.

In equation 4.2, the logistic tumor cell growth of the uninfected tumor cells is denoted by the term, $r_T T_S \left(1 - \frac{T_S+T_I}{K_T}\right)$ with the intrinsic growth rate r_T and the carrying capacity K_T. Similarly, during oncolytic virotherapy, the tumor cell population is sub-divided into two sub-populations, the uninfected cells represented by T_S and infected tumor cells denoted by T_I. The uninfected tumor cells become infected by the oncolytic virus at the rate β_T. Hence, the second term, $-\beta_T T_S V$, represents the reduction of the tumor cell population as a result of a successful viral oncolysis (i.e., viral replication and burst). Since some oncolytic viruses, such as the vesicular stomatitis virus (VSV), are capable of inducing the antitumor immune response against the infected tumor cells [90, 258], the third term, $-\gamma_T \frac{Y_T}{h_Y+Y_T} T_S$, represents the reduction of the tumor cell population by the antitumor adaptive immune response. The interaction between tumor and the tumor-specific immune cells follows the Michaelis-Menten kinetics because immune cell infiltration into the tumor is often restricted by tumor architecture [179]. Thus, γ_T denotes the rate at which tumor cells are lysed by the tumor-specific immune cells and h_Y represents the half-saturation constant of immune cells that supports half the maximum killing rate.

In equation 4.3, the first term, $\beta_N N_S V$, represents the number of normal cells that become infected with the oncolytic virus. The second term, $-\lambda_N N_I$, denotes the death of the infected normal cells at the rate λ_N. Experimental evidence indicates that death of infected normal cells may be attributed to apoptosis of the infected cells in attempt to inhibit virus propagation [91]. Therefore, we assume that the infection by the oncolytic virus also induces the adaptive antiviral immune response to infected cells [93]. The third term, $-\gamma_V Y_V N_I$, represents the number of infected normal cells lysed by the antiviral immunity with lysis rate γ_V.

In equation 4.4, the first term, $\beta_T T_S V$, represents the number of tumor cells that become infected with the virus. The second term, $-\lambda_T T_I$, denotes the death of the infected tumor cells at the OV-induced death rate λ_T. Again, since tumor architecture may hinder the adaptive antitumor immune cell infiltration [179], we consider the Michaelis-Menten kinetics for the interaction between infected tumor cells and the adaptive antitumor immune response. Hence, we model this scenario with the term $\gamma_T \frac{Y_T}{h_Y+Y_T} T_I$. The last term, $-\gamma_V Y_V T_I$, represents the number of infected tumor cells that become lysed by the virus-specific immune cells.

In equation 4.5, upon successful viral infection and replication, the infected tumor cells die and new oncolytic virus particles that are released from the infected tumor cell. Thus, b_T is the burst size for viruses from an infected tumor cell. The first term, $b_T\lambda_T T_I$, represents the production of new oncolytic virus particles released from infected tumor cells after a successful viral propagation. Similarly, the second term, $b_N\lambda_N N_I$, denotes the production of new viral particles released from the successful oncolysis of the infected normal cells. Here, b_N is the burst size for viruses from an infected normal cell. Finally, the last term, ωV, denotes the viral clearance of the free virus from the host body by virus-specific immune cells, at the clearance a rate ω.

In equation 4.6, the adaptive antitumor immune response depends of the cross-priming of the T-cells by mature antigen presenting cells (e.g. macrophages) with the antigens expressed on both infected and uninfected tumor cells [270, 271]. For simplicity, we assume that such a priming process has been successful and we do not model the kinetics of priming, instead we incorporate delay terms of immune response to viral infections. The first term, $p_T\frac{T_S+T_I}{h_T+T_S+T_I}$, represents the antitumoral immune response against the tumor cells, with the immune cell recruitment rate p_T. Since activation of antitumoral immune response, mediated by $CD8^+$ T cells, is dependent on the amount of tumor antigens, we use Michaelis-Menten term to indicate the saturation effects of the tumor-specfic immune response [126, 128]. For simplicity, we use the same half-saturation constant of tumor antigens that induce half proliferation of immune cells, h_Y, as the half-saturation constant of adaptive immune cells that supports half the maximum killing rate (to both viral- and tumor-specific $CD8^+$ T cells), h_T. Finally, the last term, $-\delta_T Y_T$, denotes that the adaptive tumor-specific immune population declines as a result of natural cell death, at the intrinsic death rate δ_T.

In equation 4.7, a delayed immune response to virus infection to both normal and tumor cells is modeled by the term $p_V\left(T_I(t-\tau)+N_I(t-\tau)\right)$, where a parameter p_V is a virus-specific proliferate rate of the antiviral immune cells due to the presence of virus particles (virus antigens) on the surface of the infected cells. Immune response to viral antigens require time necessary for cell activation and proliferation. That means, antigenic stimulation generating the antiviral immune response, mediated by T cells, require a period of time τ, which may depend on prior antigenic stimulation period $t-\tau$. Note that the delay of antiviral immune response is also crucial for enabling first round of oncolytic virus replication and subsequent release of the viral progeny [93]. The last term, $-\delta_V Y_V$, represents

the natural death, with the death rate $-\delta_V$, of the adaptive virus-specific immune cells.

4.2.3 Parameter estimation

To analyse and simulate our model, we determine the baseline parameter values from the literature that most correspond to available experimental data and biological facts. Since most of the available parameter values from the literature are reported in daily rates, we rescaled such parameter values by dividing each of them with $d*24$ hours, where d denotes the number of days, to convert daily rates to hourly rates.

Susceptible normal cells. Uninfected normal cell proliferation rate, and the normal cell carrying capacity, $r_N = 0.00275$ hr^{-1} and $K_N = 10^{11}$ cells, has been respectively taken from [143]. Since wild-type vesicular stomatitis virus can infect normal cells, the rate at which it infects normal cells, β_N, is not known precisely. However, for our modeling purpose, the hourly infection rate $\beta_N = (1.7 \times 10^{-8})/24$ virion^{-1} hr^{-1} of normal cells is rescaled from Friedman et al. [255].

Susceptible tumor cells. Similarly, we have taken the proliferation rate, $r_T = 0.003$ hr^{-1}, and the tumor cell carrying capacity, $K_T = 1.47 \times 10^{11}$ cells, from [143]. The baseline value of the rate at which VSV infects tumor cells, $\beta_T = 0.038/24$ virion^{-1} hr^{-1}, has been rescaled from the daily rate in Eftimie et al. [144]. This parameter value is within the range $(5 \times 10^{-12.5}, 5 \times 10^{14})$ virion^{-1} hr^{-1} defined in [143], where the authors found out that the range allows for tumor persistence after the delay of 7 days prior to accumulation of the adaptive immune response. The lysis rate of susceptible tumor cells by tumor-specific immune cells, $\gamma_T = 1/24$ hr^{-1}, has also been rescaled from daily rate in Eftimie et al. [144]. The half-saturation constant of the tumor-specific immune cells that maintains half the maximum killing rate, $h_T = 40$ cells, has been taken from [144].

Infected normal cells. The death rate of infected normal cells, $\lambda_N = 1/24$ cells hr^{-1}, is an *ad hoc* value and has been chosen to conform with plausible biological outcomes. The rationale for this parameter value was based on the fact that the average time for an infected cell to undergo lysis is one day [239, 255, 272]. Similarly, the lysis rate of the infected normal cells by virus-specific immune cells, $\gamma_V = 1/24$ cells hr^{-1} is also an *ad hoc* value. This value is chosen based on the reasoning that the virus-specific immune cells do

not distinguish between normal or tumor cells because they are recruited in response to viral antigens expressed by infected cells [99, 273].

Infected tumor cells. Similar to normal cells, the death rate of infected tumor cells due to VSV lysis, $\lambda_T = 1/24$ cells hr^{-1}, has been rescaled from daily rate in Eftimie et al. [144].

Oncolytic virus. The burst size of VSV from lysed infected tumor cells, $b_T = 1350$, is taken from [143]. For normal cells, we estimate that the oncolytic vesicular stomatitis virus (VSV) yields the burst size of $b_N = 1000$. This value was chosen based on the fact that VSV infection in normal cells is usually hampered by the presence of the interferon (IFN-β or $-\alpha$) [274]. Hence we chose $b_N \leq b_T$ since tumor cells are known to acquire deficiencies in antiviral inhibitory mechanisms [275, 276]. The clearance of the free virus particle by tumor-specific immune cells, $\omega = 2.5 \times 10^{-2}$ hr^{-1} was taken from [159, 255].

Tumor-specific immune cells. The hourly proliferation rate of tumor-specific immune cells in response to tumor antigens, $p_T = 0.0375/24$ hr^{-1}, was taken and rescaled from the daily rate in de Pillis et al. [126]. Assuming that the tumor-specific immune cells (i.e., tumor-specific CD8$^+$ T cells) have a half-life of 77 days as shown in [257], we estimate the hourly death rate of the tumor-specific immune cells, δ_T, to be $\delta_T = \frac{ln(2)}{(77\times24)} \approx 3.75 \times 10^{-4}$ hr^{-1}.

Virus-specific immune cells. We chose the *ad hoc* value of the proliferation rate of virus-specific immune cells in response to VSV antigens, $p_V = 0.025$ hr^{-1}, since it is the lower bound of the daily interval rate of the virus-specific immune cell proliferation rate shown by Eftimie et al. [144]. We tentatively chose this lower bound value because, during viral propagation within the infected cells, we assume that the immune response against the infected cells would be mainly driven by debris of infected cells since VSV has fast replication cycle [277]. Finally, the hourly death rate of the virus-specific immune cells, $\delta_V = 0.133/24 \approx 5.54 \times 10^{-3}$ hr^{-1} was rescaled from daily rate in Eftimie et al. [144].

4.3 Model analysis

To better understand the dynamics of the proposed model, we begin by examining the model's behavior about the steady states in the absence of the virus. This analysis is

crucial for identifying the parameters of the model that help to achieve a tumour-free state without oncolytic virotherapy. Additionally, this analysis would be important for comprehending the effect of the adaptive immune response following oncolytic virotherapy. We first present the model's virus free equilibrium points. Then we derive the model's basic reproductive number, R_0, in Section 4.3.1. The corresponding stability analysis of the model's virus free equilibrium points, in terms of R_0, is presented in Section 4.3.2. The non-trivial steady states of the model without virus (i.e., $N_I = T_I = Y_V = V = 0$) are found by equating equations (4.1 - 4.7) to zero, which results in the following virus free steady states:

$$E_N := (K_N, 0, 0, 0, 0, 0, 0) \quad \text{Tumor-free (TF) steady state,} \tag{4.8}$$

$$E_T := (0, 0, T_{S0}, 0, 0, 0, Y_{T0}) \quad \text{Tumor-only (TO) steady state} \tag{4.9}$$

(i.e., tumor without the surrounding normal cells),

$$E_{NT} := (K_N, 0, T_{S0}, 0, 0, 0, Y_{T0}) \quad \text{Co-existence steady state} \tag{4.10}$$

(i.e., tumor and the surrounding normal cells are present),

where

$$T_{S0} := \frac{-b + \sqrt{b^2 - 4ac}}{2a}, \quad \text{and} \quad Y_{T0} = \frac{p_T T_{S0}}{\delta_T \left(T_{S0} + h_T\right)}$$

with

$$\begin{aligned} a &:= r_T \xi, \quad \xi = h_Y \delta_T + p_T \\ b &:= \left(\gamma_T - r_T\right) K_T \xi + \left(h_T r_T - K_T \gamma_T\right) h_Y \delta_T \\ c &:= -K_T \delta_T h_T h_Y r_T. \end{aligned}$$

The detailed mathematical proofs of the stability analyses associated with these steady states are provided in Section 4.3.2. Before we discuss the stability analysis of the model, we first derive the model's basic reproductive number in the next section.

4.3.1 Model basic reproductive number

A basic reproductive number is defined as the average number of new infections generated by one infected cell, via cell lysis, during virotherapy in a completely susceptible cell population [278]. In general, if $R_0 > 1$, then, on average, the number of new infections

resulting from one infected cell is greater than one. Thus, viral infections will persist in both normal and tumor cell populations. If $R_0 < 1$, then, on average, the number of new infections generated by one infected cell in virotherapy is less than one. This implies that the viral infections will eventually disappear from the cell populations. Here, we provide a detailed description of the calculation of the basic reproductive number of the model. We use the next generation matrix approach [278, 279].

Proposition 1 *The basic reproductive number of model is given by*

$$R_0 = R_{0N} + R_{0T}$$

where

i. $R_{0N} := \frac{b_N \beta_N N_S}{\omega}$, *represents the basic reproductive number of the virus when introduced into a population of normal cells only*

ii. $R_{0T} := \frac{(Y_T + h_T) b_T \beta_T \lambda_T T_S}{((Y_T + h_T)\lambda_T + Y_T \gamma_T)\omega}$, *represents the basic reproductive number of the virus when introduced into a population of cancer cells only.*

Proof. By formally applying the next generation method, we determine the threshold parameter R_0 at a virus free equilibrium point $E_{NT} := (N_S, 0, T_S, 0, 0, 0, Y_T)$. The vectors of new infections and that of other transfers are respectively given by

$$f := \begin{bmatrix} \beta_N N_S V \\ \beta_T T_S V \\ 0 \end{bmatrix}$$

$$g := \begin{bmatrix} \gamma_v Y_v N_I + \lambda_N N_I \\ \gamma_v Y_v T_I + \lambda_T T_I + \frac{\gamma_T Y_T T_I}{h_Y + Y_T} \\ -b_N \lambda_N N_I - b_T \lambda_T T_I + \omega V \end{bmatrix}$$

Calculating the Jacobian matrices efvaluated at the virus free equilibrium E_{NT},

$$M = \begin{bmatrix} 0 & 0 & \beta_N N_S \\ 0 & 0 & \beta_T T_S \\ 0 & 0 & 0 \end{bmatrix}$$

$$N = \begin{bmatrix} \gamma_V Y_V + \lambda_N & 0 & 0 \\ 0 & \gamma_V Y_V + \lambda_T + \frac{\gamma_T Y_T}{h_Y + Y_T} & 0 \\ -b_N \lambda_N & -b_T \lambda_T & \omega \end{bmatrix}$$

The spectral radius of the matrix MN^{-1} is given by

$$R_0 = R_{0N} + R_{0T}$$

where

$$R_{0N} := \frac{b_N \beta_N N_S}{\omega}, \; R_{0T} := \frac{(Y_T + h_T)\, b_T \beta_T \lambda_T T_S}{((Y_T + h_T)\, \lambda_T + Y_T \gamma_T)\, \omega}.$$

■

Brief guidelines for R_0 analysis. We aim to find a threshold in which the oncolytic viruses that can exploit both normal and tumor cells, such as vesicular stomatitis virus (VSV), can infect normal cells without much toxicity on normal cell population. The major goal of every oncolytic virus is to infect and lyse as many tumor cells as possible without much toxicity on the host normal tissue. The focus of our model analysis is centred around the basic reproductive number of the model. Numerical simulations, in conjunction with the analysis of the basic reproductive numbers, aim to shed light on design and use of oncolytic viruses that are not 100% tumor-specific. In particular, we seek for R_{0N} such that

$$R_{0N} + R_{0T} \simeq 1 \;\; (\text{but}) \;\; < 1.$$

Note that if, based on the value of R_{0N},

$$\begin{aligned} &R_{0N} \simeq 0 \;\; \text{the virus cannot infect normal cells} \\ &\text{or} \quad \gg 1 \;\; (\text{the virus is too toxic on normal cells, hence not admirable.}) \end{aligned}$$

More importantly, R_{0N} should satisfy the following conditions:

$$\begin{aligned} &R_{0N} = \tilde{\alpha} R_{0T}, \quad \tilde{\alpha} \ll 1, \quad \text{where } \alpha \text{ is a small proportionality constant,} \\ &R_{0N} = \alpha(1 - R_{0T}), \quad \text{where } \alpha \text{ is a constant fraction.} \end{aligned}$$

And we also need that

$$\tilde{\alpha} = \frac{\alpha R_{0T}}{1 - R_{0T}}, \quad \text{and} \quad R_{0T} < 1.$$

With these guidelines on R_0, we investigate how the evolution of the oncolytic virus influences the treatment dynamics in Section 4.4. Now, we present the stability analysis of our model associated with the free virus steady states derived above.

4.3.2 Stability analysis of the virus free steady states

Proposition 2 *The virus free equilibrium points E_N and E_T are always unstable, while E_{NT} is locally asymptotically stable if and only if $R_0 < 1$.*

Proof. Using Maple, the characteristic equation of the linearized system around the equilibrium point $E_{NT} := (N_S, 0, T_S, 0, 0, 0, Y_T)$ is independent of the delays and is given by:

$$(\delta_v + z)\left(zK_N - K_N r_N + 2N_S r_N\right)\left(P_2 z^2 + P_1 z + P_0\right)\left(Q_3 z^3 + Q_2 z^2 + Q_1 z + Q_0\right) = 0 \tag{4.11}$$

where

$$\begin{cases} Q_3 &= Y_T + h_T \\ Q_2 &= (Y_T + h_T)\lambda_N + (Y_T + h_T)\omega + (Y_T + h_T)\lambda_T + Y_T\gamma_T \\ Q_1 &= [(Y_T + h_T)\omega + (Y_T + h_T)\lambda_T + Y_T\gamma_T - (Y_T + h_T)b_N\beta_N N_S]\lambda_N \\ & \quad + ((Y_T + h_T)\lambda_T + Y_T\gamma_T)\omega - (Y_T + h_T)b_T\beta_T\lambda_T T_S \\ Q_0 &= \left[\begin{array}{l} ((Y_T + h_T)\lambda_T + Y_T\gamma_T)\omega \\ -[((Y_T + h_T)\lambda_T + Y_T\gamma_T)b_N\beta_N N_S + (Y_T + h_T)b_T\beta_T\lambda_T T_S] \end{array}\right]\lambda_N \end{cases}$$

and

$$\begin{cases} P_2 &= \left(K_T{\delta_T}^2{T_S}^2 + 2K_T{\delta_T}^2 h_T T_S + K_T{\delta_T}^2{h_T}^2\right){h_Y}^2 \\ & \quad + \left(2K_T{T_S}^2\delta_T p_T + 2K_T T_S\delta_T h_T p_T\right)h_Y + K_T{T_S}^2{p_T}^2 \\ P_1 &= P_{13}T_S^3 + P_{12}T_S^2 + P_{11}T_S + P_{10} \\ P_0 &= P_{03}T_S^3 + P_{02}T_S^2 + P_{01}T_S + P_{00} \end{cases}$$

with

$$\begin{cases} P_{13} &= 2\xi^2 r_T = 2\xi a, \quad \xi = h_Y\delta_T + p_T \\ P_{12} &= \xi\left[(-r_T + \delta_T + \gamma_T)K_T\xi + (4h_T r_T - K_T\gamma_T)h_Y\delta_T\right] \\ &= \xi\left[B + \delta_T\left(K_T\xi + 3h_T r_T h_Y\right)\right] \\ P_{11} &= \delta_T h_T h_Y\left[(2\delta_T + \gamma_T - 2r_T)K_T\xi + (2h_T r_T - K_T\gamma_T)h_Y\delta_T\right] \\ &= \delta_T h_T h_Y\left[2b_0 + (2\delta_T - \gamma_T)K_T\xi + K_T\gamma_T h_Y\delta_T\right] \\ P_{10} &= {\delta_T}^3{h_T}^2{h_Y}^2 + \delta_T h_T h_Y C \end{cases} \tag{4.12}$$

and

$$\begin{cases} P_{03} &= 2\delta_T r_T \xi^2 \\ P_{02} &= \delta_T \xi \left[(\gamma_T - r_T)\, \xi K_T + (4h_T r_T - K_T \gamma_T)\, h_Y \delta_T \right] \\ P_{01} &= 2{\delta_T}^2 h_T h_Y \left[(\gamma_T - r_T)\, \xi K_T + (h_T r_T - K_T \gamma_T)\, h_Y \delta_T \right] \\ P_{00} &= -K_T {\delta_T}^3 {h_T}^2 {h_Y}^2 r_T \end{cases}$$

Stability of E_T:

At the virus free and tumor endemic equilibrium point, E_T, we have $N_S = 0$ reducing the term $(zK_N - K_N r_N + 2N_S r_N)$ in the characteristic equation (4.11) to $(z - r_N)\, K_N$ which has $r_N > 0$ as a root. Hence E_T is unstable, implying that the tumor would persists growing uncontrollably.

Stability of E_N:

At the virus-and-tumor free equilibrium, E_N, we have $T_S = 0$ and $N_S = K_N$ reducing the term $(P_2 z^2 + P_1 z + P_0)$ in the characteristic equation (4.11) to $K_T \delta_T^2 h_T^2 h_Y^2 \,(z + \delta_T)\,(z - r_T)$ which has a positive root r_T. Therefore, E_N is unstable. This condition means that normal cells are able to grow at an appreciable level in the absence of the tumor and virus. This result tend to highlight the significance of the ability of normal cells in continuing to maintain normal cell homeostasis in the absence of cancerous cells [280]. Note also that due to the choice of mass action infection kinetics in our model, viral replication does not affect the stability of this tumor free equilibrium.

Stability of E_{NT}:

At the virus free equilibrium with both tumor and normal cells, E_{NT}, we can see that P_2 is always positive. Let us show that P_1 and P_0 are positive.

$$\begin{aligned} P_1 = {} & 2\xi a_0 T_S^3 + \xi \left[b_0 + \delta_T \left(K_T \xi + 3 h_T r_T h_Y \right) \right] T_S^2 \\ & + \delta_T h_T h_Y \left[2b_0 + (2\delta_T - \gamma_T)\, K_T \xi + K_T \gamma_T h_Y \delta_T \right] T_S \\ & + {\delta_T}^3 {h_T}^2 {h_Y}^2 + \delta_T h_T h_Y c_0. \end{aligned}$$

Using $a_0T_S^2 + b_0T_S = -c_0 = K_T\delta_T h_T h_Y r_T$, we obtain

$$\begin{aligned}
P_1 &= \xi a_0 T_S^3 + \xi K_T \delta_T h_T h_Y r_T T_S + \left(K_T \delta_T \xi^2 + 3h_T h_Y \delta_T a_0\right) T_S^2 \\
&\quad + \delta_T h_T h_Y \left[2b_0 + \left(2\delta_T - \gamma_T\right) K_T \xi + K_T \gamma_T h_Y \delta_T\right] T_S \\
&\quad + {\delta_T}^3 {h_T}^2 {h_Y}^2 + \delta_T h_T h_Y c_0 \\
&= \xi a_0 T_S^3 + \left(K_T \delta_T \xi^2 + h_T h_Y \delta_T a_0\right) T_S^2 + 2h_T h_Y \delta_T a_0 T_S^2 \\
&\quad + 2\delta_T h_T h_Y b_0 T_S + \delta_T h_T h_Y K_T \left[\left(2\delta_T - \gamma_T\right)\xi + \gamma_T h_Y \delta_T + \xi r_T\right] T_S \\
&\quad + {\delta_T}^3 {h_T}^2 {h_Y}^2 - \delta_T h_T h_Y c_0.
\end{aligned}$$

Furthermore, since $2h_T h_Y \delta_T a_0 T_S^2 + 2\delta_T h_T h_Y b_0 T_S = -2\delta_T h_T h_Y c_0$, then

$$\begin{aligned}
P_1 &= \xi a_0 T_S^3 + \left(K_T \delta_T \xi^2 + h_T h_Y \delta_T a_0\right) T_S^2 - 3\delta_T h_T h_Y c_0 \\
&\quad + \delta_T h_T h_Y K_T \left(\left(2\delta_T + r_T - \gamma_T\right)\xi + \gamma_T h_Y \delta_T\right) T_S \\
&\quad + {\delta_T}^3 {h_T}^2 {h_Y}^2.
\end{aligned}$$

Moreover, by using $b_0 = h_T h_Y r_T \delta_T + K_T \left(\xi\left(\gamma_T - r_T\right) - h_Y \gamma_T \delta_T\right)$, we obtain

$$\begin{aligned}
P_1 &= \xi a_0 T_S^3 + \left(K_T \delta_T \xi^2 + h_T h_Y \delta_T a_0\right) T_S^2 - 3\delta_T h_T h_Y c_0 \\
&\quad + \delta_T h_T h_Y \left(2\delta_T \xi K_T + h_T h_Y r_T \delta_T - b_0\right) T_S \\
&\quad + {\delta_T}^3 {h_T}^2 {h_Y}^2 \\
&= \xi a_0 T_S^3 + \left(K_T \delta_T \xi^2 + 2h_T h_Y \delta_T a_0\right) T_S^2 - 2\delta_T h_T h_Y c_0 \\
&\quad - \delta_T h_T h_Y c_0 - h_T h_Y \delta_T a_0 T_S^2 \\
&\quad - \delta_T h_T h_Y b_0 T_S + \delta_T h_T h_Y \left(2\delta_T \xi K_T + h_T h_Y r_T \delta_T\right) T_S \\
&\quad + {\delta_T}^3 {h_T}^2 {h_Y}^2.
\end{aligned}$$

Since $-\delta_T h_T h_Y C - h_T h_Y \delta_T a_0 T_S^2 - \delta_T h_T h_Y b_0 T_S = -\delta_T h_T h_Y \left(c_0 + a_0 T_S^2 + b_0 T_S\right) = 0$, then

$$\begin{aligned}
P_1 &= \xi a_0 T_S^3 + \left(K_T \delta_T \xi^2 + 2h_T h_Y \delta_T a_0\right) T_S^2 - 2\delta_T h_T h_Y c_0 \\
&\quad + \delta_T h_T h_Y \left(2\delta_T \xi K_T + h_T h_Y r_T \delta_T\right) T_S + {\delta_T}^3 {h_T}^2 {h_Y}^2 > 0.
\end{aligned}$$

We show next that $P_0 > 0$,

$$\begin{aligned} P_0 = {} & 2\delta_T \xi a_0 T_S^3 + \delta_T \xi \left[\left(\gamma_T - r_T \right) \xi K_T + \left(4 h_T r_T - K_T \gamma_T \right) h_Y \delta_T \right] T_S^2 \\ & + 2 {\delta_T}^2 h_T h_Y \left[\left(\gamma_T - r_T \right) \xi K_T + \left(h_T r_T - K_T \gamma_T \right) h_Y \delta_T \right] T_S \\ & - K_T {\delta_T}^3 {h_T}^2 {h_Y}^2 r_T. \end{aligned}$$

Since $\left(\gamma_T - r_T \right) K_T \xi + \left(h_T r_T - K_T \gamma_T \right) h_Y \delta_T = b_0$, then

$$\begin{aligned} & \xi \left[\left(\gamma_T - r_T \right) \xi K_T + \left(4 h_T r_T - K_T \gamma_T \right) h_Y \delta_T \right] \\ & = \xi b_0 + 3 \xi h_T r_T h_Y \delta_T \\ & = \xi b_0 + 3 h_T h_Y \delta_T a_0, \end{aligned}$$

implying that

$$\begin{aligned} P_0 = {} & \delta_T \xi a_0 T_S^3 + \delta_T \xi T_S \left(a_0 T_S^3 + b_0 T_S \right) + 3 h_T h_Y \delta_T^2 a_0 T_S^2 \\ & + 2 {\delta_T}^2 h_T h_Y b_0 T_S - K_T {\delta_T}^3 {h_T}^2 {h_Y}^2 r_T. \end{aligned}$$

Therefore,

$$\begin{aligned} P_0 & > 2 h_T h_Y \delta_T^2 a_0 T_S^2 + 2 {\delta_T}^2 h_T h_Y b_0 T_S - 2 K_T {\delta_T}^3 {h_T}^2 {h_Y}^2 r_T \\ & = 2 h_T h_Y \delta_T^2 \left(a_0 T_S^2 + b_0 T_S + c_0 \right) = 0. \end{aligned}$$

Thus $P := P_2 z^2 + P_1 z + P_0 > 0$.
Concerning the polynomials Q_0, Q_1 and Q_2, we have Q_2 is always positive. Moreover, Q_1 and Q_2 can be written as

$$\begin{aligned} Q_1 : = {} & \left(\left(Y_T + h_T \right) \omega \left(1 - R_{0N} \right) + \left(Y_T + h_T \right) \lambda_T + Y_T \gamma_T \right) \lambda_N \\ & + \left(\left(Y_T + h_T \right) \lambda_T + Y_T \gamma_T \right) \omega \left(1 - R_{0T} \right) \\ Q_0 : = {} & \left(\left(\left(Y_T + h_T \right) \lambda_T + Y_T \gamma_T \right) \omega \left(1 - \left(R_{0N} + R_{0T} \right) \right) \right) \lambda_N. \end{aligned}$$

Therefore,

i. If $R_0 := R_{0N} + R_{0T} > 1$, then $Q_0 < 0$ which by Routh Hurwitz criterion [281, 282] and the fact that $Q_3 > 0$ imply that Q has at least one root with positive real parts.

ii. If $R_0 < 1$, then $Q_0 > 0$. Moreover, we have $R_{0N} < 1$ and $R_{0T} < 1$ which implies that Q_1 is also positive. Furthermore, we have $Q_2 > 0$ and $Q_3 > 0$, and

$$\begin{aligned} Q_1Q_2 &= \left[\begin{array}{l} (\omega\,(Y_T+h_T)\,(1-R_{0N}) + (Y_T+h_T)\,\lambda_T + Y_T\gamma_T)\,\lambda_N \\ +\omega\,[(Y_T+h_T)\,\lambda_T + Y_T\gamma_T]\,(1-R_{0T}) \end{array}\right] \\ &\quad \times [(Y_T+h_T)\,\lambda_N + (Y_T+h_T)\,\omega + (Y_T+h_T)\,\lambda_T + Y_T\gamma_T] \\ &> [\omega\,[(Y_T+h_T)\,\lambda_T + Y_T\gamma_T]\,(1-R_{0T})]\,[(Y_T+h_T)\,\lambda_N] \\ &> \omega\,[(Y_T+h_T)\,\lambda_T + Y_T\gamma_T]\,(1-(R_{0N}+R_{0T}))\,[(Y_T+h_T)\,\lambda_N] \\ &= Q_0Q_3. \end{aligned}$$

Thus by Routh Hurwitz, the cubic polynomial $Q := Q_3z^3 + Q_2z^2 + Q_1z + Q_0$ does not have any roots with positive real parts. Hence, E_{NT} is locally asymptotically stable if and only if $R_0 < 1$, implying that the transient infections on normal and tumor cell populations would naturally be eliminated.

■

4.4 Results

4.4.1 Numerical simulations

The numerical solutions of our model equations (4.1 - 4.7) along with the initial conditions were carried out using MATLAB *dde23*. We first investigate the system's long-term behavior. Note, at time $t < 7$, we assume that there are no virus-specific immune cells at the tumor site in order to allow the virus to infect, replicate and kill some infected cells. For all the simulations, we assumed that the susceptible tumor begins at the size measured at time $t = 0$ hours in an immunocompetent host. In experiments, tumor size is often measured in volume (mm^3), then in our model we convert tumor volume to cell population by assuming that 1 $mm^3 \approx 1 \times 10^6$ tumor cells, as has been done in [239, 260].

Comparing with previous studies. To facilitate comparison of our model findings with other mathematical models, in particular with the model by Okamoto et al. [143],

we present numerical simulations where the therapeutic dose is $V = 10^9$ pfu of the initial free virus load. As a first step in evaluating the performance and accuracy of a model in predicting tumor growth, we fit our model to the available experimental tumor data used in the model by Bajzer et al. [283], who obtained it from the in vivo experiments of human myeloma tumor xenografts implanted in immunodeficient mice [284]. The data in [283, 284] reports both the untreated and treated (when virotherapy was introduced on day 15 after the implantation of multiple myeloma xenografts in mice) tumor growth. We used the untreated tumor growth data to estimate the daily tumor growth rate (r_T) by fitting a sub-form of our model and evaluated the accuracy of the numerical simulations. The fitting of the sub-form of our model was done by minimizing the sum of square errors (SSE) between the experimental data points and the model output using the MATLAB function *lsqnonlin*. Our model fit, with a 95% confidence interval, is shown in Figure 4.2.

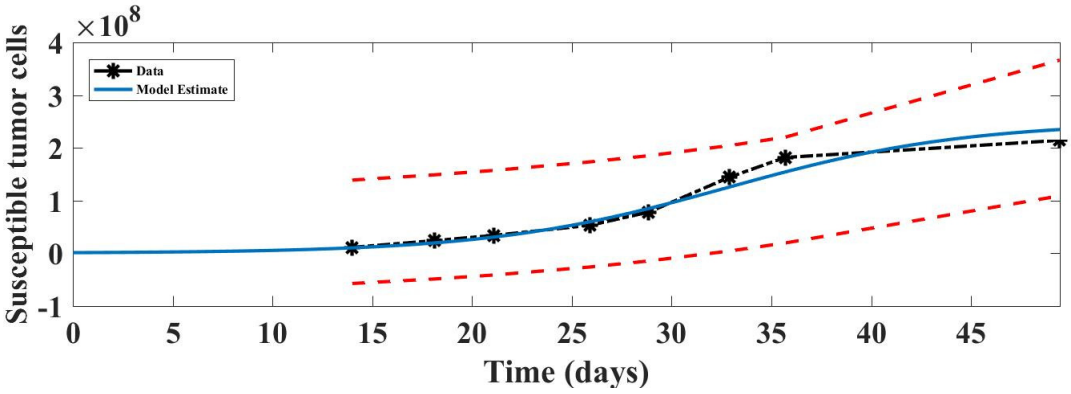

FIG. 4.2. Model fitting to experimental tumor growth data using Equation 4.2, the uninfected (susceptible) tumor cell population, T_S, and other model variables set to zero. The susceptible tumor cell population is fitted to the data with two-sided 95% confidence intervals (dashed lines) computed from exponential distribution statistics. A black dashed line is just a straight line between data points. Parameter values are $r_T = 0.00258, K_T = 3.12 \times 10^8, \beta_T = \gamma_T = 0$.

Since one of the goals of our study is to predict tumor's response to oncolytic viral infection, we observe from Figure 4.2 that the model fits (with the susceptible cell population taken as the baseline variable) the tumor growth data fairly well. This observation provides some assurance that uncertain model parameters fall within 95% confidence of the true tumor growth. We further assessed our model parameter sensitivity through a global sensitivity analysis in the subsequent section in order to gain a better understanding of the model's behavior to small variations in the parameters.

Global sensitivity analysis (GSA). For our model, we performed the GSA because a large number of parameters. Most important, we perform sensitivity analysis in order to identify key parameters that can be varied to achieve plausible oncolytic potency and reduced tumor-specificity of the oncolytic virus that is not 100% tumor-specific in oncolytic Virotherapy. Following the numerical method described in [226], we per- formed Latin hypercube sampling. We generated 1000 samples to compute the PRCC and the associated p-values with respect to virus infection at 24-hour intervals up to 96 hours. The sensitivity indices of the PRCC, ranging from -1 to $+1$, indicate the strength of the monotonic relation between the susceptible cell population and parameter of interest. A PRCC index of -1 indicates a strong negative monotonic relationship between a given parameter and the model variable(s) (i.e., susceptible normal and tumor cells in this case), while the index of $+1$ shows a strong positive monotonic relationship between the given parameter and model variable.

The GSA results: model implications for oncolytic virotherapy. We investigated the parameter sensitivity analysis with $\tau = 0$ in the equations 4.1 − 4.7. Sensitivity analysis of our model without delay (i.e., when the parameter $\tau = 0$), Equations 4.1 − 4.7. We present only two time snapshots in Figure 4.3.

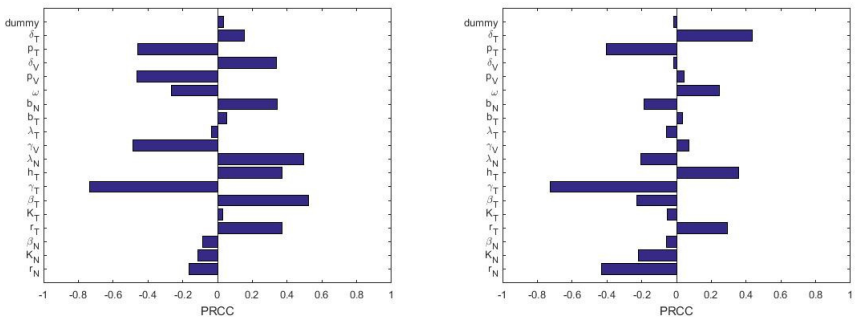

(a) 24 hours (b) 96 hours

FIG. 4.3. Sensitivity indices of the model parameters with oncolytic virus taken as a baseline PRCC analysis variable. Analysis was computed based on the baseline parameter values presented in Table 4.2, with a viral dose of $V = 10^9$ plaque-forming units (pfu). The sensitivity analysis is computed at 24 and 96 hours.

Figure 4.3 reveals high sensitivity of the model to small parameter changes at 24 and 96 hours. Most important, this global sensitivity analysis indicates which parameters account

for the most variation in the early or late stages of oncolytic virotherapy. From a treatment perspective, this is essential for identifying which parameters of the model could be the "key drivers" of the success of the virotherapy at any time point. In Figure 4.3, note that the PRCC algorithm usually assigns a PRCC value to the control variable named "dummy". This dummy parameter is not part of the model parameters, and hence, it does not affect the model results in any way. According to the PRCC algorithm, the model parameters with sensitivity index less than or equal to that of the dummy parameter are usually taken to be not significantly different from zero (with p-value > 0.01) [226].

The PRCC subplots, Figures $4.3(a) - 4.3(b)$, correspond to the times of giving the single-viral dose of $V = 10^9$ virions at the 24 and 96 hours with the initial dose given at 24-hours after the start of the tumor treatment. At time $t = 24$ hours, Figure $4.3(a)$ indicates that a number of parameters are statistically different from zero (with p-value < 0.01) The significant parameters include: the rate of VSV infection to tumor cells, β_T, half saturation constant of tumor infected cells, h_T, the death rate of infected normal cells, λ_N, death rate of the virus-specific immune cells, δ_V, the proliferation rate of tumor-specific immune cells p_T, and the lysis rate of the infected normal cells by virus-specific immune cells (γ_V).

From the treatment perspective, the result of the sensitivity analysis shows that infection of normal cells can induce an antiviral immune response that could quickly eliminate the infected cells. This suggests that oncolytic viral infection of normal cells can be useful only when the virus replicates rapidly within infected normal cells. At $t = 96$ hours, the intrinsic growth rates, r_N and r_T, of normal and tumor cells also become consistently influential on normal and tumor cell populations, respectively. Similarly, death rate of the tumor-specific immune cells, δ_T, proliferation rate of tumor-specific immune cells, p_T, and the half-saturation constant of the adaptive immune cells, h_T, also become statistically significant at later time point (i.e., time $t = 96$ hours).

Based on this global sensitivity analysis, we deduce at following treatment implications: (i) For a period of less than 4 days, apart from direct oncolysis, an oncolytic therapy should target recruiting more tumor-specific cells to augment the therapy. This could be achieved by engineering the VSV to express a tumor antigen directly [285]. Viral infections usually trigger an immune response that is essential for elimination of tumor cells [91, 227]. This sensitivity analysis indicates why it is currently not easy to treat tumors within 4 days

with oncolytic viruses, from on the onset of tumorigenesis. The precise time of oncogenesis in clinic is very difficult to determine. (ii) When designing the oncolytic viruses, such as vesicular stomatitis virus (VSV) [145] or Newcastle disease virus (NDV) [274], that are not 100% tumor-specific, it is important that such viruses replicate rapidly within normal cells since normal cells can quickly become more sensitive and inhibitory to virus replication over time. Global sensitivity analysis illustrates that the model is less sensitive to early viral infection (see Figure 4.3(a)) on the normal cell population, and becomes increasingly sensitive at later time point (Figure 4.3(b)). (iii) Tumor aggressiveness as well as the strength of the patient tumor-specific immunity may predict patient response to oncolytic virotherapy.

4.4.2 Treatment strategies

Having determined which parameters are most influential in our model, we now investigate two main dosing treatment strategies in oncolytic virotherapy: (1) single-viral dose (i.e., one viral dose administered at three different time points once), and (2) periodic dosing (i.e., one viral dose given at three successive time points). Currently, a full understanding of the best plausible protocols to administer oncolytic viruses to cancer patients is still very limited. This is partly because there are no precise clinical results for comparing two different oncolytic virotherapeutics administered through identical routes in the same types of tumor. It is important to note that a comprehensive comparison of clinical virotherapy trial regimens is time-consuming and complicated [286]. There is still no common consensus regarding:

(i) the oncolytic virus dosages (i.e., low versus high dosage. The optimum oncolytic virus dosage in the clinic is still unknown [287]; although virus inoculum is often manipulated in clinical trials in orders of magnitude ($10^3 - 10^{10}$) pfu [288]),

(ii) the appropriate dosing intervals (i.e., oncolytic virus repetitive times: hourly, weekly or monthly. A detailed review of clinical dosing intervals of various oncolytic viruses is reported in [286]),

(iii) the best virus delivery route (e.g., systemic delivery versus intratumoral delivery. Recent clinical application of oncolytic viruses in these routes is reviewed in [286, 289]),

(iv) the virus administration scheme (i.e., single- versus multiple-dose [290]. The appropriate dosing schedule of oncolytic viruses in the clinic is still not precisely defined [287]).

Although some of the above issues have explored in several studies (e.g., see reviews in [132, 291]), in the present study we address some of these challenges, in particular (ii) and (iv), from the quantitative point of view that involves the basic reproductive number, R_0, of the model. In the subsequent section, we provide brief guidelines underlining the use of R_0 analysis that conforms with plausible biological outcomes of our model. Most importantly, R_0 analysis, along with model simulations, would help to understand the qualitative behavior of the virus dynamics in our model, identify essential parameters necessary for tumor extinction or at least a controlled tumor state, and suggest possible future directions for further oncolytic virotherapy research.

Oncolytic viral infection dynamics. When designing an oncolytic virus, some important considerations include administration of variety of dosing schemes and testing different viral doses to ensure clinical safety [292]. Here, we present the results of the model with respect to the free-virus steady state as described in Section 4.3 as our initial steady state. In this steady state, it is interesting to investigate the effects of the virotherapy because:

(a) When the basic reproductive number of the model is less than one ($R_0 < 1$), then the oncolytic virus uses both normal and tumor cell populations for its replication. Note that, in general, if $R_0 > 1$, the viral infections will continue to spread in at least one cell population, as implied by the case **(i.)** in Section 4.3.2. It is essential to note that if $R_0 < 1$, viral infections will eventually disappear from both tumor and normal cell populations over time, as implied by the case **(ii.)** in Section 4.3.2. Of particular interest, we note and define the following conditions on R_{0N}:

   (i) If $R_{0N} < 1$, then the infection on normal cell population will ultimately vanish over time.

   (ii) When designing an oncolytic virus that is not 100% tumor-specific, it is important to ensure that the basic reproductive number of normal cells, R_{0N}, is less than that of tumor cells, R_{0T}. In this case, the virus would infect more tumor cells

than normal cells as evidenced by a large progeny virions from dead tumor cells [66].

(iii) $R_{0N} < R^{\star}_{0N}$, where $R^{\star}_{0N}$ is the maximum value of the basic reproductive number for the normal cell population.

(iv) Evidence suggests that the number of new virions produced from infected normal cells is somehow proportional to that produced from tumor cells [274]. Thus, we take $R_{0N} = \alpha(1 - R_{0T})$, where α is a constant fraction, as explained in **Brief guidelines for R_0 analysis** in Section 4.3.1.

(b) In the case where $R_0 < 1$, the viral infection on normal cells would invoke the immune response (T-cells or NK-cells) which may eliminate the virus-infected cells [293]. Thus, the infection of normal cells has two therapeutic outcomes:

(i) If the virus replicates and lyses infected cells quickly, then oncolytic therapy may be enhanced by production of new virions, which can then spread to uninfected tumor cells. Evidence indicates that fast replicating viruses (i.e., those that can lyse infected cells quickly), can avoid being engulfed by innate and adaptive immune cells, and have a greater opportunity to further infect uninfected cells [294].

(ii) Early removal of infected cells might inhibit success of the oncolytic therapy [153], but late immune response involvement might be necessary for clearing both infected normal and tumor (both uninfected and infected) cells [295].

(c) When the basic reproductive number of the model is greater than one ($R_0 > 1$), then the oncolytic virus endemically uses either normal or tumor cell population for its replication. From the treatment point of view, having $R_0 > 1$ is an undesirable treatment result in virotherapy because $R_0 > 1$, implies that viral infections will continue to spread in at least on cell population. Note that the basic reproductive number of the model, R_0 (see Section 4.3.1), is composed of two basic reproductive numbers, R_{0N} and R_{0T}, of normal and tumor cells, respectively. When at least one of the basic reproductive numbers is greater than unity, then the cell population corresponding to the one with the basic reproductive number greater than one would be the one in which viral infection will persists forever. Further investigation of this condition (i.e., when

$R_0 > 1$) constitutes one of the possible model extensions which will be incorporated in the future work.

Experimental dosing scenarios. Here we examine the hypothetical clinical dosing schedule of the oncolytic virus to test whether this would yield better treatment response of our hypothetical patient under single-viral dose (Scenario 1) and periodic dosing (Scenario 2). The rationale behind comparison of these treatment strategies in our model is motivated by (ii) and (iv) in **Treatment strategies**. We are interested in investigating virus dynamics for hourly dosing intervals under the two virus administration scenarios (i.e., single- versus multiple-dose). We kept the same viral dosage regimen of $V = 10^9$ pfu for all treatment scenarios. Maintaining the same virus injection dosage is often done in experimental research (e.g., see [113, 146]). Note that for all the simulations, the value of τ is fixed at 7 hours, and τ was shown not to affect the stability of the virus-free equilibrium points. Hence, we have omitted the effects of time-varying delays in the present discussions. The results of the model simulations when $R_0 < 1$ are given in Figure 4.4(a) – 4.4(b) for periodic dosing scenario, and Figure 4.5(a) – 4.5(b) for single-viral dose scenario.

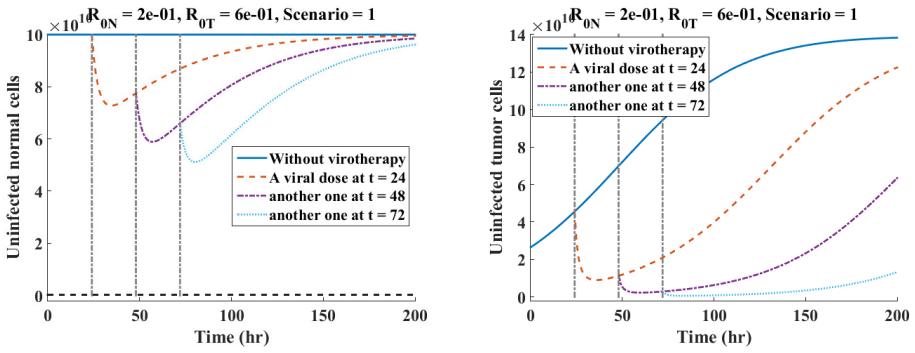

(a) (b)

FIG. 4.4. Plots of the susceptible normal and tumor cell populations when a virus is administered at three successive times, with a viral dose of $V = 10^9$ pfu. Figure 4.5(a) shows how the oncolytic virus reduces the susceptible normal cell population during multiple-viral dose scheme. Figure 4.4(b) shows how successive viral doses can lead to tumor eradication or at least keep the tumor in transient dormancy, which is followed by tumor relapse.

Given that the infected normal tissues in the neighbourhood of the tumor has capacity to self-regenerate [251], we note from Figure 4.5(a) that the susceptible normal cells re-grow to the carrying capacity when the amount of viral particles reduces. From Figure 4.4, it

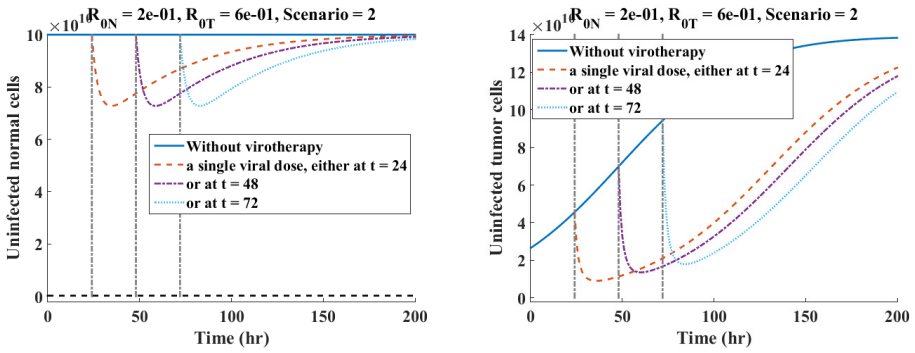

(a) (b)

FIG. 4.5. Plots of individual susceptible normal and tumor cell populations when the single dose of $V = 10^9$ pfu is administered at three different time points. Figure 4.5(a) shows a reduction and rapid self-renewing of the susceptible normal cell population during an oncolytic virotherapy. Figure 4.5(b) shows the single-viral dose scheme leads to tumor reduction, but tumor still grows after the initial reduction.

can be observed that administering the viral doses at successive time points leads to rapid reduction of both susceptible normal and tumor cell populations.

4.4.3 Tolerable normal cell depletion

In conjunction with the **Brief guidelines for R_0 analysis** in Section 4.3.1, we investigate how much should normal cells be infected by the oncolytic virus in order to maximize tumor reduction. One plausible approach in which normal cells can augment oncolytic virotherapy is to allow the virus to infect some normal cells in the tumor site, given that the basic reproductive number of the virus is less than unity (i.e., $R_0 < 1$).

In cancer treatment, white blood cell (WBC) count (which incorporates all circulating lymphocytes) is an important factor which is used to determine health status of a patient prior to treatment. Most importantly, in clinics, WBC count is a first diagnostic measure used to screen for potential virus infection [296]. In humans, the normal WBC count is in the range of approximately $5 \times 10^9 - 10^{10}$ cells/μl [296]. In our model, it is crucial to track a population of normal (healthy) cells because it is important not to deplete normal cells beyond tolerable losses. Thus, we need to determine a threshold, denoted by $\widetilde{N_S}$ cells, at which normal cells should not be depleted. However, since it often difficult

to delineate what population of normal (non-cancerous) cells constitute in clinics, in our model simulations, we link the population of normal cells with white blood cells. White blood cells are always present whenever there is infection. Since oncolytic viruses that are not 100% tumor specific can also infect non-cancerous cells (even white blood cells such as neutrophils and monocytes), we use WBC count as a measure of normal cell depletion resulting from oncolytic virus infection in the vicinity of tumor cells. More importantly, we track the normal cell population in order to determine a stage at which our hypothetical patient would no longer attain full remission from therapy. We assume the following relationship between normal cell population and WBC count:

$$\widetilde{N_S} = \alpha_1 B \quad \text{and that} \tag{4.13}$$

$$\widetilde{B} = f B_0, \tag{4.14}$$

where $\widetilde{N_S}$ denotes the total minimum number of normal (healthy) cells that should not be depleted in virotherapy, α_1 denotes a constant fraction, $\widetilde{B}$ denotes the cutoff level of white blood cell count for humans, below which treatment should cease, f denotes a constant fraction, and B_0 denotes the initial normal WBC count prior to treatment. Here, we chose $\widetilde{B} = 10^8$ cells/μl and $B_0 = 4.2 \times 10^{10}$ cells/μl are taken in [297]. Thus, we estimate $f = \widetilde{B}/B_0 = 10^8/4.2 \times 10^{10} = 2.4 \times 10^{-3}$. We estimate $\widetilde{N_S} = f N_S^0 = K_N \times (2.4 \times 10^{-3}) = 2.4 \times 10^9$ cells, where $N_S^0 = K_N$ denotes the carrying capacity of normal cells at the start of oncolytic virotherapy. Here, $\widetilde{N_S}$ serves as the level at which our hypothetical patient would no longer attain full remission if the oncolytic therapy continues.

We present results $\alpha = \frac{3}{4}$, shown in Figure 4.6 and Figure 4.7. When $\alpha = \frac{1}{2}$, we obtain Figures 4.4 with corresponding cell depletion profile shown in Tables 4.3. Note that when $\alpha = 0$, then the oncolytic virus is 100% tumor-specific since $R_0 = R_{0N} + R_{0T}$.

As we would expect, under periodic dosing scheme, whenever $R_{0N} = 3(1 - R_{0T})/4$, it is possible to drive tumor population to extinction, shown in Figure 4.8(b) and Table 4.4, while minimizing much loss of normal cell depletion, shown in Figures 4.8(a) and Table 4.4.

For all tested values of $R_0 < 1$, we note that as long as $R_{0N} = \frac{3(1-R_{0T})}{4}$, the tumor was eliminated. Also, we note that increasing values of R_{0N} slightly, the tumor can still be controlled. Most importantly, we observe that multi-viral (periodic dosing) dosing schemes

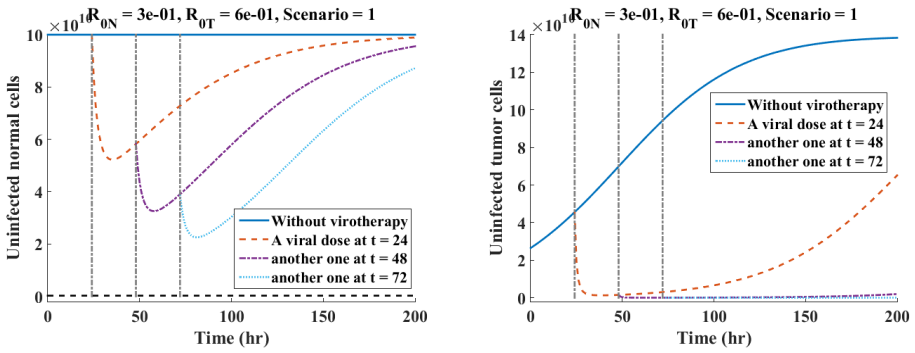

(a) (b)

FIG. 4.6. Relative comparison of cell depletion when the oncolytic virus is administered at three successive time points. Figure 4.6(a) indicates reduction of normal cell population when $R_{0N} = \frac{(1-R_{0T})}{2}$. Figure 4.6(b) shows reduction of tumor cells when $R_{0N} = \frac{3(1-R_{0T})}{4}$. The corresponding cell depletion profile is provided in Tables 4.4

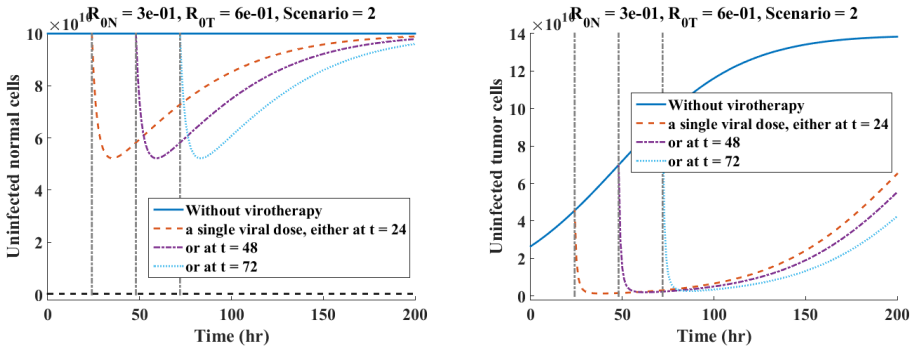

(a) (b)

FIG. 4.7. Relative comparison of cell depletion when the oncolytic virus is administered at three distinct time points. Figure 4.7(a) indicates reduction of normal cell population when $R_{0N} = \frac{3(1-R_{0T})}{4}$. Figure 4.7(b) shows reduction of tumor cells when $R_{0N} = \frac{3(1-R_{0T})}{4}$.

offers better results in terms of tumor cell depletion, shown in Figures 4.8(a) and 4.8(b). Thus, we compared minimum cell depletion for each cell population for varying values of α under scenario 1. Results are provided in Tables 4.3 and 4.4.

Notably, from Table 4.4, when R_{0N} is close to R_{0T}, tumor cell population is diametrically reduced and become eliminated between time $t = 168$ and $t = 192$ hours. We note that at time $t = 192$ hours, there are 0.057081 cells because our model is based on delay differential equations (DDEs). Numerical solutions from the DDEs can only provide some information on the average behavior of the variables of the model; thus, complete tumor

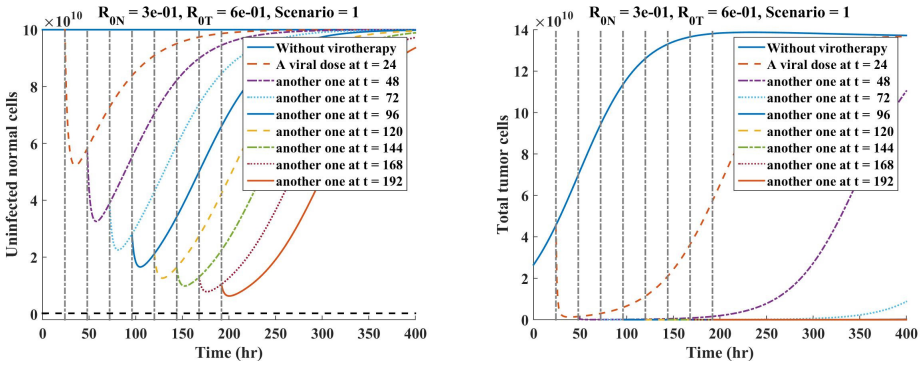

(a) (b)

FIG. 4.8. Simulation of cell depletion when $R_{0N} = \frac{3(1-R_{0T})}{4}$. Figure 4.7(a) indicates a decline in normal cell population. Figure 4.7(b) shows the tumor shrinks down to zero over time.

elimination cannot be guaranteed in our model. In principle, however, when the average number of cells is less than **one**, then we can assume that such cells are ideally eradicated. Hence the tumor cells are eradicated in this scenario. On the other hand, interestingly, we note that the population of normal cells has not reached the threshold value, $\widetilde{N_S} = K_N \times (2.4 \times 10^{-3}) = 2.4 \times 10^9$ cells, beyond which we expect our hypothetical patient not to attain complete tumor remission. Most importantly, our results indicate no toxicity to normal cells, since the minimum depletion of 6.331×10^9 normal cells, at time $t = 192$ hours, is above the threshold value, $\widetilde{N_S}$ cells. What these results suggest is that designing an oncolytic virus that is capable of exploiting a significant number of normal cells in the neighbourhood of the tumor, can plausibly drive tumor cells to extinction. Our results are more applicable the treatment scenario where tumors that cannot be reached directly.

4.5 Discussion

In this work, we set out to answer the main question of "***How can oncolytic virus infection of some normal cells in the vicinity of tumor cells enhance oncolytic virotherapy?***"To this end, we developed a delay differential equation model that describes the dynamics of the oncolytic virus that is not 100% tumor-specific on normal and tumor cell populations. A major focus of our model analysis was to explore and delineate the effects of oncolytic potency and specificity of viruses that not 100% tumor-specific in

virotherapy. We now outline all the notable features of our model analyses and simulations that provide a comprehensive picture of the model evolution and behavior on how oncolytic viruses differentially exploit the populations of normal and tumor cells during oncolytic virotherapy.

The oncolytic viral tumor-specificity. From a mathematical point of view, we sought for the solutions of the model that provide a succinct framework on the oncolytic viral tumor-specificity that maximises tumor reduction while minimizing the undesirable toxicity on normal cell population surrounding the tumor. Most importantly, the model predicts the evolution of three non-trivial virus free steady states; the tumor-free steady state in which only normal cells are ultimately present, the tumor-only steady state in which only tumor cells are present, and the co-existence steady state in which both normal and tumor cells are present. The model equilibria analysis and simulations show that the coexistence steady state plays a crucial role in controlling viral infections on normal cell population at the onset of virotherapy. In particular, they show that whenever the basic reproductive number $R_0 < 1$, infection of normal cells by the oncolytic virus may be tolerable only if such infections can aid to eliminate tumor cells (see Figure 4.8(b) and Table 4.4) that would otherwise be difficult.

We then examined differing trajectories of oncolytic virus infection on tumor cells and a limited number of normal cells. From the model simulations, Figure 4.5(a) and Figure 4.4(a), we note that normal cells quickly self-regenerate after initial reduction. The attenuated damage on normal cells has distinct treatment explanations: (a) Direct viral oncolysis is limited by early induction of antiviral immune response, (b) Virus propagation is inhibited by beta interferon (IFN-β) that is often secreted by normal cells. On the other hand, we assume that infecting a limited portion of normal cell in the tumor bed with oncolytic virus could augment oncolytic virotherapy. Given that the virus can infect and replicate in normal cells, a progeny of infectious virions produced from lysed cells can further spread and infect other uninfected tumor cells. Whenever the basic reproductive number of normal cells is less than one, $R_{ON} < 1$, viral infections on normal cells would eventually stop, coupled by the fact that normal cells often rapidly inhibit virus propagation [91]. Our findings suggest that oncolytic viral infection of normal cells can be useful only when the virus replicates rapidly within infected normal cells.

Most interestingly, our results, from Table 4.4, indicates that oncolytic viruses that are capable of exploiting some normal cells, as their replication factories, can drive tumor cells to extinction within biologically reasonable time frame. We emphasize here that such oncolytic viruses should have a higher replication preferential profile, as illustrated by respective basic reproductive numbers in our model, to tumor cells than normal cells. It can be seen from Table 4.4 and Table 4.3, that when the oncolytic virus exploits more normal cells within a given threshold, then tumor cell population is driven to extinction rapidly, as shown explicitly in Table 4.4. From clinical point of view, our theoretical results suggest that in normal cell population that can quickly self-renew (e.g., white blood cells or the liver), oncolytic virus infection on limited portion of normal cells may aid to eradicate tumor cells that would otherwise be difficult to eliminate. This is achievable and tolerable only if such viral infections are not endemic (i.e., the basic reproductive number of the virus is less than unity, $R_0 < 1$).

The effects of the potential antitumoral and antiviral immune responses in oncolytic virotherapy. Global sensitivity analysis elucidates that the model is very sensitive to a number of parameters at the initial dose (i.e., at time $t = 24$ hours). For tumor cell population, proliferation rate of uninfected tumor cells, r_T, is the most positively correlated parameter with the viral particles. At this early stage of tumor development, as the proliferation rate of susceptible tumor cells, r_T, increases, tumor density will also increase. This observation is conformable with other findings that tumor cell proliferation is a major essential factor for benign tumors, particularly the malignant tumors [298]. Note that the susceptible tumor cell population would only decrease if virus replication outpaced the intrinsic tumor growth rate. This observation is in agreement with the simulation results in Figure 4.4(b) and Figure 4.5(b) which indicates rapid reduction of the susceptible tumor cell population when the VSV doses are administered periodically (i.e., at time $t = 24$). Note that for all time points of viral dose (see Figures $4.3(a) - 4.3(b)$), lysis rate of susceptible tumor cells by tumor-specific immune cells (γ_T) is the major determinant parameter in the model. Interestingly, this result confirms the idea that a success of an oncolytic virotherapy does not only depend on direct oncolysis but also on the influence of immune response against tumor cells [90].

For normal cells, we similarly interpret the positive and negative correlations between the parameters of normal cells and the oncolytic viral particles. The sensitivity analysis reveals

that the model is highly sensitive to the lysis rate of the infected normal cells by virus-specific immune cells (γ_V) in first viral dose time point (i.e., at time $t = 24$ hours). This observation suggests that initial viral infection of normal cells, can quickly induce antiviral immune response against the infected cells.

Assessing the effectiveness of treatment strategies on tumor and normal cells after injection with oncolytic virus. We investigated the effects of two treatment strategies in oncolytic virotherapy: one single-viral dose illustrated in Figure 4.5, where viral dose is administered at three independent times, and multiple-viral doses (i.e., periodic dosing schedule) shown in Figure 4.4, where the virus is given at three successive times. The value of R_0 provides useful insights on the dynamics of oncolytic viral infection on normal and tumor cell populations because: (a) Whenever the basic reproductive number of the model is less than one ($R_0 < 1$), the oncolytic viral replication occurs in both normal and tumor cell populations; (b) When $R_0 < 1$, viral infections on normal cells might trigger antiviral immune response against the infected cells [293]. From Figure 4.5, we note that single-viral dosing strategy reduces susceptible normal cells by same amount, irrespective of the time of dosing, and the cells are rapidly self-renewing. Similarly, this strategy yields similar results with respect to tumor cells. The cell count of the susceptible cell population is quickly reduce, and followed by a rapid tumor relapse. In Figure 4.4, we note that multiple-viral dosing (i.e., periodic dosing) has a significant effect on the susceptible tumor cell population than on normal cell population. This strategy suggests that continued periodic dosing may eradicate the tumor or at least delay tumor growth. Comparing these two therapeutic strategies, we note that multiple-viral dose regime, shown Figure 4.4, offers more favorable treatment outcomes than the single-viral dose regime, shown Figure 4.5, with respect to reduction of susceptible tumor cell population.

Our model results are comparable with other mathematical models. Our model predicts that the oncolytic virus (such as VSV) that lyses infected cells fast, may drive tumor cell population to extinction rapidly. This finding is consistent with the model by Wein et al. [299] who modeled tumor-virus dynamics using a system of partial differential equations. Indeed, evidence indicates that if the oncolytic virus kills infected cells fast, then the progeny of new virions has a chance to spread and infect other uninfected tumor cells, prior to accumulation of adaptive immunity [294]. Otherwise, the induced adaptive immune response would then eradicate both infected and the remnant uninfected tumor

cells. Furthermore, our computational results also conform with results from Okamoto et al. [143] in that oncolytic virus infection of some normal cells can facilitate tumor control. Even better, our computational results, illustrated in Table 4.4 and Figure 4.8(b), indicate that tumor cell population can quickly be eradicated whenever the oncolytic virus exploits a significant amount of normal cells above a given acceptable threshold value. It is also shown that tumor burden can at least be reduced, as indicated in Table 4.3, but not completely eradicated within the given biological time frame.

Our results suggest that when designing an oncolytic virus that is not 100% tumor-specific, it is important to consider viral dosing scheduling (with respect to time and frequency of dosing) because oncolytic viral infections on normal cells might yield desirable or undesirable outcomes in virotherapy. This could be seen from Figure $4.5(a) - 4.5(b)$, for single dosing schedule, and Figure $4.4(a) - 4.4(b)$, for multiple dosing schedule, that different dosing strategies provide different outcomes. From the sensitivity analysis, our results suggest that when developing the oncolytic virus that is not 100% tumor-specific, it is important to note that viral infections on normal cells could lead to early induction of antiviral immune response that might inhibit further viral propagation.

4.6 Conclusion

In conclusion, our mathematical model shows that viral infections on normal cells can indeed augment oncolytic virotherapy if the virus replicates fast within the infected cells. Our results may be useful in the discovery of new oncolytic viruses or attenuation of known wild viral strains, such wild-type oncolytic VSV [259] or VSV variants. Results of our global sensitivity analysis have provided invaluable insights about the parameters that influence growth kinetics and tumors' response to oncolytic virus, and the adaptive immune response. Our findings support the design of oncolytic viruses that is not 100% tumor-specific, but have higher oncolytic potency towards tumor cells than normal cells, and have high capacity to recruitment adaptive antiviral and antitumoral immune responses. We believe our work opens new possibilities for designing new attenuated oncolytic viruses that can be examined in a clinical setting under complex scenarios in which tumors cannot be reached directly.

Finally, an important model extension would be to account for spatial intratumoral (within tumor) heterogeneity. It is known that that tumor heterogeneity can affect virus diffusivity within tumor cells. Another interesting possible of the model extension would be to account for variations of the immune responses towards infected and uninfected tumor cells. Currently, our model does not account for varying tumor immune responses when implementing experimental oncolytic viral dosages. Pre-existing antiviral immune responses, when treating patients who were exposed to oncolytic virotherapy before, may result in differing treatment response rates in the clinic.

.

TABLE. 4.2: Parameter values used in the model simulations

Parameter	Description	Value	Source
r_N	the intrinsic growth rate of normal cells	0.00275 hr^{-1}	[143]
K_N	the carrying capacity of normal cells	10^{11} cells	[143]
β_N	the rate at which VSV infects normal cells	$(1.7 \times 10^{-8})/24$ virion^{-1} hr^{-1}	rescaled from daily rate in Friedman et al. [255]
r_T	the intrinsic growth rate of tumor cells	0.003 hr^{-1}	[143, 256]
K_T	the carrying capacity of tumor cells	1.47×10^{12} cells	[143]
β_T	the rate at which VSV infects tumor cells	$(5 \times 10^{-12.5}$, $5 \times 10^{14})$ virion^{-1} hr^{-1}	[143]
γ_T	lysis rate of susceptible tumor cells by tumor-specific immune cells	$1/24$ hr^{-1}	rescaled from daily rate in Eftimie et al. [144]
h_Y	the half-saturation constant of immune cells	40 cells	[144]
λ_N	the death rate of infected normal cells	$1/24$ cells hr^{-1}	estimate
γ_V	lysis rate of the infected normal cells by virus-specific immune cells	$1/24$ cells^{-1} hr^{-1}	estimate
λ_T	death rate of infected tumor cells due to VSV lysis	$1/24$ cells^{-1} hr^{-1}	rescaled from daily rate in Eftimie et al. [144]
b_T	the burst size from tumor cells lysed by VSV	1350 virions cell^{-1}	[143]
b_N	the burst size from normal cells lysed by VSV	1000 virions cell^{-1}	Estimate
ω	virus clearance rate	2.5×10^{-2} hr^{-1}	[159, 255]
p_V	proliferation rate of virus-specific immune cells in response to VSV antigens	$0.025 - 0.1042$ hr^{-1}	rescaled from daily rate in Eftimie et al. [144]
δ_V	death rate of the virus-specific immune cells	5.54×10^{-3} hr^{-1}	rescaled from daily rate in Eftimie et al. [144]
p_T	proliferation rate of tumor-specific immune cells	$0.0375/24$ hr^{-1}	rescaled from daily
h_T	the half-saturation constant of tumor cells in response to tumor antigens	40 cells	[144] rate in de Pillis et al. [126]
δ_T	death rate of the tumor-specific immune cells	3.75×10^{-4} hr^{-1}	rescaled from daily rate in de Pillis et al. [257]

TABLE. 4.3. **Minimum cell reduction achievable when** $R_{0N} = (1 - R_{0T})/2$

Time (hrs)	Normal cells	Tumor cells
Without therapy, $t = 0$	1×10^{11}	2.647×10^{10}
$t = 24$	7.2764×10^{10}	9.0057×10^{9}
$t = 48$	5.889×10^{10}	2.2719×10^{9}
$t = 72$	5.1158×10^{10}	5.8419×10^{8}
$t = 96$	4.6375×10^{10}	1.5049×10^{8}
$t = 120$	4.3228×10^{10}	3.8686×10^{7}
$t = 144$	4.1055×10^{10}	9.9173×10^{6}
$t = 168$	3.9494×10^{10}	2.5356×10^{6}
$t = 192$	3.8358×10^{10}	6.4674×10^{5}

TABLE. 4.4. **Minimum cell reduction achievable when** $R_{0N} = 3(1 - R_{0T})/4$

Time (hrs)	Normal cells	Tumor cells
Without therapy, $t = 0$	1×10^{11}	2.647×10^{10}
$t = 24$	5.22×10^{10}	1.2889×10^{9}
$t = 48$	3.2569×10^{10}	4.3147×10^{7}
$t = 72$	2.2536×10^{10}	1.4405×10^{6}
$t = 96$	1.6541×10^{10}	4.7884×10^{4}
$t = 120$	1.2607×10^{10}	1.5857×10^{3}
$t = 144$	9.8565×10^{9}	5.2378×10^{1}
$t = 168$	7.8477×10^{9}	1.7291
$t = 192$	6.331×10^{9}	0.057081

Chapter 5

Mathematical Model of Oncolytic Virus Delivery by Cell Carriers

This chapter aims at answering the third question in this thesis: ***How can the use of cell carriers for the delivery of oncolytic virus particles to tumor sites affect the outcomes of oncolytic virotherapy in the presence of active immune response?***

To this end, we construct a new ordinary differential-equation based mathematical model to describe the local interactions of tumor cells with natural killer (NK) cells, cytotoxic T lymphocytes (CTLs), chimeric antigen receptor–engineered T cells (oAd-CAR T cells) and mesenchymal stem cells (oAd-MSCs) loaded with oncolytic adenovirus, and the free oncolytic adenovirus viruses within tumor microenvironment. The aim of this study is to simulate and compare the therapeutic efficacies of the mesenchymal stem cells and engineered chimeric antigen receptor–engineered T cells in delivering oncolytic viruses to tumor site in the presence of active local antitumor and antiviral immune cells. In addition to determining the efficacy of two carrier cell-based treatments, we also investigate the long-term impact of the immune response within tumor microenvironment.

Our numerical simulations suggest that, at low lysis rates, the greatest efficacy (as indicated by the virus-mediated cell deaths) is achievable with the oAd-CAR T cell based therapy than with the oAd-MSC based therapy. A combination of oAd-CAR T cell and oAd-MSC based therapies is possible extension of the current model to further investigate the synergistic effects of these therapies

Before we discuss the modeling framework herein this chapter, we first present some biological background motivating the development of our novel mathematical model.

5.1 Introduction

For most advanced or metastatic tumors, only a limited number of therapeutic options are available for cancer patients. Oncolytic virotherapy is currently considered to be one of the most promising treatment modalities against most advanced tumor cells. Tumor cells are destroyed by oncolytic viruses (OVs) that are naturally occurring or genetically engineered to preferentially infect and replicate within tumor cells, while having a limited or no toxicity to normal cells. A major obstacle with oncolytic virotherapy, however, is that when viruses cannot be injected directly into a target tumor, only a limited fraction of oncolytic viruses administered intravenously manage to migrate and reach the target tumor site. This is often due to antiviral immunity in the blood which rapidly clears the viruses [66, 112, 300–305]. Clinical evidence indicates that even for high doses of oncolytic viruses [302, 306], for the intravenous route, an efficient systemic delivery of oncolytic virus particles is still limited [109, 305, 307].

In attempt to surmount this systemic delivery obstacle, several strategies have been explored, including use of cells, that have potential to migrate towards tumor microenvironment, as delivery vehicles for oncolytic viruses. Recent evidence indicates that using carrier cells for delivering oncolytic virus particles that targets tumor cells or tumor microenvironment, is a promising treatment approach to systemic delivery [112, 247, 308–314]. Some carrier cells are used as "Trojan horses" which can internalize the OVs and allow virus replication, but have no role after successful OV delivery in tumor sites [300, 301, 315, 316]. A variety of pre-clinical and clinical studies have elucidated that different types of host immune cells are capable of recognising, migrating to and accumulating within tumors or tumor microenvirnment [301, 316–318]. In addition, various studies have demonstrated that certain types of cells, such as cytokine-induced killer (CIK) cells loaded with the vaccinia virus (VV) [308, 313], T-cells loaded with vesicular stomatitis virus (VSV) [319], dendritic cells loaded with oncolytic reovirus [301], macrophages loaded with adenovirus [317], chimeric antigen receptor (CAR)–engineered T cells loaded with vesicular stomatitis

virus (VSV) with mutations in the M protein (VSVΔM51) and "double-deleted" vaccina virus (vvDD), and mesenchymal stem cells loaded with oncolytic measles viruses [320], have potential to delivery the OVs to tumors.

Mesenchymal stem cells (MSCs) have also proven to exhibit inherent tumor-trafficking properties, and can efficiently be used to delivery the oncolytic viruses to tumor sites. Most importantly, the MSC cell-based therapies can potentiate both tumor oncolysis and anti-tumor immune responses necessary for a complete tumor elimination [92, 309]. Another important attribute of MSCs which often make them appropriate candidates for oncolytic virus delivery is that they support viral replication while loaded with the virus [280, 321, 322]. Furthermore, MSCs are capable of protecting the loaded virus from immune-mediated neutralization [320, 321, 323–328].

On one hand, the engineered CAR T cells have shown that they are also capable of delivering oncolytic viruses to tumor sites [114]. Apart from protecting the virus from neutralizing antibodies, CAR-T cells are known to retain their antitumor functions while loaded with the virus [247, 319]. This feature makes them an attractive treatment because they can destroy tumor cells prior to their lysis by the pre-loaded virus. In this study, we also investigate the efficacy of CAR-T cell based therapy in delivering oncolytic viruses to tumor site.

Despite promising pre-clinical and clinical evidence that sheds light on how carrier cells can be used as delivery vehicles for oncolytic viruses, multiple challenges remain to be fully addressed before such approaches can be applied in a clinical setting. The MSCs derived from different tissues in a patient can produce widely varying outcomes in relation to secretion of cytokines and chemokines, and immunomodulatory potential [287, 329, 330]. Hence, it becomes difficult to predict how different patients will respond to the MSC-based cell carrier therapies [329]. Moreover, MSCs can be highly heterogeneous [331, 332]; as such, it is also difficult to predict their behavior *in vivo* [112]. Thus, there is a clear need for new research to understand dynamical behavior of MSCs as carriers of oncolytic viral vectors.

5.1.1 Relevant Mathematical Models

There are several mathematical models that describe the complexity of tumor-immune cells interactions [125–130, 152]. A detailed review of some of these tumor-immune models can be found in [123, 131–134]. More recently, in [291] a succinct review of mathematical models of immunotherapy is provided. There are few mathematical models that show how cells, such as macrophages [148, 149], can be used as delivery vehicles of therapeutic agents to tumor sites. In [148], a mathematical model that describes an accumulation of engineered macrophages to hypoxic tumor sites was developed. Through model simulations, it was shown that a combination of the macrophage-based therapies and conventional chemotherapy is necessary for achieving a complete tumor eradication.

In another study, two modes of action by therapeutic drugs delivered by macrophages: either the macrophages delivered an enzyme that activates an externally applied pro-drug (the bystander model) or they directly delivered the cytotoxic factors into a hypoxic tumor site (the local model) were investigated [149]. Using the local model, it was indicated that macrophage are capable of migrating and accumulating in hypoxic sites and induce tumor cell lysis. Although the models in [148, 149] considered the use of cell-based therapies for delivery of chemotherapeutic drugs to tumor sites, none of them considered the effects of immune responses within tumor microenvironment. Here, we develop non-spatial mathematical model to investigate the comparative efficacy of delivering oncolytic viruses by either T cells or mesenchymal stem cells (MSC) to tumor site in the presence of active immune response.

5.2 Materials and methods

5.2.1 Experiments: Oncolytic virus delivery by mesenchymal stem cells

Before we turn our attention to a mathematical modeling perspective, we briefly provide information on the datasets we used for parameter estimation of the model parameters. The data was obtained via collaboration with experimental oncologists at Prof. Chae-Ok Yun's Laboratory at Hanyang University. The experiment for assessment of the mesenchymal

stem cells (MSCs) as cell carriers of an oncolytic Adenovirus (Ad) was done for both *in vitro* and *in vivo* settings.

(a) **Determining the infection of MSCs with oncolytic Adenoviral (Ad) vectors.** Fixed quantity of MSCs were seeded onto a well plate then infected with various predetermined unit of MOI (multiplicity of infection). For example, 10 MOI means that 10 infectious virus particles have been infected into one cell.

(b) **Determining the cell viability of MSCs.** The cell viability of MSCs was determined by measuring the conversion of 3-(4, 5-dimethylthiazol-2-yl)-2, 5- diphenyltetrazolium bromide (MTT) to formazan by live cells. Briefly, $1 - 2 \times 10^4$ cells were seeded into a 96 well plate at overnight and infected with oncolytic adenovirus (oAd) (at MOI of 0.5 to 50). After 2 to 7 days of incubation at 37 °C, 50 μl of MTT in phosphate buffered saline (PBS) (2 mg/ml) was added to each well. After 4 hours incubation at 37 °C, the supernatant was discarded and the precipitate was dissolved with 200 μl of dimethylsulfoxide (DMSO). Plates were then read on a microplate reader at 540 nm. All assays were performed in triplicate. Number of living cells was calculated from non-infected cells cultured and treated with MTT in the same condition, as were the experimental groups.

(c) **Assessing the replication of oncolytic Ad in MSCs.** To assess the viral production of oncolytic Ads, MSCs were seeded in 24-well plates at approximately 60% confluency and then infected with oncolytic Ad at an MOI of 0.5 to 100. After 2 or 5 days of incubation at 37 °C, supernatants and cell pellets were collected and freeze-thawed three times to harvest both extracellular and intracellular viral particles. Real-time quantitative PCR was used to assess the total number of viral genomes in each sample by quantifying Ad protein IX detected on capsid of mature virion. Samples were analyzed in triplicate, and data were processed using the SDS 19.1 software package.

(d) **Performing the *in vivo* tumor growth analysis.** To compare the antitumor effect of MSC, oAd, and oAd-MSC, the orthotopic hepatocellular carcinoma cancer model was established by injecting 1×10^6 firefly luciferase-expressing Hep3B cells into the left lobe of the liver in athymic nude mice. At 7 days post implantation, blood was harvested by retro-orbital bleeding, and the level of AFP was analyzed by enzyme-linked immunosorbent assay (ELISA) according to manufacturer's instruction. The mice were randomly divided into three groups by serum AFP level and treated

with an intravenous injection of PBS, 1×10^6 MSCs, 5×10^8 virus particles (VP) of oAd, and oAd-MSC (1×10^6 MSCs infected with 5×10^8 VP of oAd) on day 9 and 13 post tumor cell implantation ($n = 6$ per group). Optical imaging, with an IVIS SPECTRUM instrument, was conducted every week and luciferase activity was quantitatively analyzed with IGOR-PRO Living Image software.

In the next section, we present a mathematical model to assess the feasibility of delivering the oncolytic adenoviruses with the MSC to tumor site in the presence of active immune response (an aspect which was not assessed in the experiments). We additionally explore the use of an alternative carrier cell, chimeric antigen receptor–engineered T (CAR T) cells, that is known to maintain delivery and cytotoxicity activities when delivering the oncolytic viruses [114].

5.2.2 Mathematical model

In this section, we present the formulation of the mathematical model that describes the use of the mesenchymal stem cell-based and T cell-based therapies for the delivery of oncolytic viruses to tumor site. We use the model to simulate and compare the efficacy of each therapy with respect to tumor reduction. This comparison is essential for understanding the possible treatment benefits of each therapy. For our modeling perspective, we assume that the oncolytic adenovirus is successfully pre-loaded on both chimeric antigen receptor–engineered T (CAR T) cells and mesenchymal stem cells (MSCs). These carrier cells migrate to tumor sites where they deliver the oncolytic viruses via cell lysis. The carrier cell migration or trafficking occurs across complex multiple cellular networks from the injection site. In this study, however, we consider the carrier cell migration or trafficking to tumor site, but rather we focus on the interaction kinetics between the carrier cells, oncolytic virus, antitumor and antiviral immune cells, and tumor cells within tumor microenvironment. The MSC are only used as "Trojan horses" and have no other role when they are at the tumor microenvironment prior to their lysis by the oncolytic viruses. The oAd-CAR T cells, on the other hand, interact with tumor cells and may induce the death of tumor cells until they become exhausted or lysed by the pre-loaded virus. In this study, the oncolytic viruses reach the tumor site only through the delivery by either oAd-CAR T cells or oAd-MSCs. Our model consists of a system of ordinary differential equations (ODEs) describing

the interactions between the tumor cells, natural killer (NK) cells, cytotoxic T lymphocytes (CTLs), oncolytic adenovirus loaded chimeric antigen receptor–engineered T (oAd-CAR T) cells, and oncolytic adenovirus loaded mesenchymal stem cells (oAd-MSC) within tumor microenvironment.

On the other hand, we assume that there are other local immune lymphocytes within the tumor microenvironment: Natural killer (NK) cells and the activated cytotoxic T lymphocytes (CTLs). For simplicity, we assume that the oncolytic viruses can only interact with tumor cells at the tumor site, even though it is possible that viruses can also interact with immune cells as well [239]. Using this new mathematical framework, our major goals are twofolds:
(a) To assess and analyze the efficacy of either the oAd-MSCs or oAd-CAR T cells when used as delivery vehicles of oncolytic viruses, from a quantitative perspective;
(b) To investigate the possible effects of antitumoral and antiviral immune responses within tumor microenvironment before and after the delivery of oncolytic viruses at tumor site.

Model assumptions: Our model builds upon the following biological assumptions:

(i) In the absence of immune response and oncolytic virotherapy, tumor growth is characterized by logistic growth dynamics. A logistic growth function has robustly fitted tumor growth data in several previous models [152, 216, 333–336].
(ii) As part of the innate immunity, NK cells are always present in the tumor microenvironment, even in the absence of tumor cells, while CTLs are present only when a tumor is present, as done in [1, 152, 212].
(iii) We also assume that both NK cells and CTLs can actively penetrate the tumor microenvironment and kill tumor cells [17, 19, 236, 337, 338]. After a finite number of encounters with tumor cells, we assume that each NK cell and CTL will eventually cease to be effective against tumor cells, as done in [1, 131, 339].
(iv) After lysis of the carrier cells, the oncolytic viruses infect tumor cells. Since not all viruses can successfully infect tumor cells, we assume that free viruses are cleared by the antiviral immune cells within the tumor microenvironment.
(v) Finally, we assume that the tumor microenvironment is homogeneous. This assumption simplifies the model in that the geometry of the tumor microenvironment is negligible; hence, our mathematical model becomes non-spatial.

5.3 Model formulation

We present a full system of ODEs with a detailed description of how each equation of the state variable is derived in this study. A description of model variables and parameters is presented in Table 5.1 and Table 5.2, respectively. Using the mathematical framework discussed above, the model consists of the following cell populations, and the oncolytic virions.

TABLE. 5.1. Model Variables

Variable	Description
$T_u(t)$	the total number of uninfected tumor cells
$T_i(t)$	the total number of infected tumor cells
$M_i(t)$	the total number of MSC carriers in the tumor microenvironment
$V(t)$	the total number of virions released within tumor microenvironment
$E_K(t)$	the total the number of NK cells within tumor microenvironment
$E_C(t)$	the total the number of activated CTLs within tumor microenvironment
$Z(t)$	the total the number of oAd-CAR T cells within tumor microenvironment

The ODE system describing our model is given by the following equations:

$$\frac{dT_u}{dt} = \underbrace{a_T T_u \left(1 - \frac{T_u + T_i}{K_T}\right)}_{\text{tumor proliferation}} - \underbrace{\beta_T(t, t_i, MOI) T_u V}_{\text{infection}} - \underbrace{\lambda_T E_K T_u}_{\text{killing by NK}}$$
$$- \underbrace{D\left(\frac{E_C}{T_u + T_i}\right) T_u}_{\text{killing by CTL}} - \rho f(Z, T_u) \tag{5.1}$$

$$\frac{dT_i}{dt} = \underbrace{\beta_T(t, t_i, MOI) T_u V}_{\text{infection}} - \underbrace{l_v(t, t_i, MOI) T_i}_{\text{death by lysis}} - \underbrace{\lambda_T E_K T_u}_{\text{killing by NK}} - \underbrace{D\left(\frac{E_C}{T_u + T_i}\right) T_i}_{\text{killing by CTL}} \tag{5.2}$$

$$\frac{dM_i}{dt} = \underbrace{S_M(t)}_{\text{source}} - \underbrace{l_v(t, t_i, MOI) M_i}_{\text{death by lysis}} \tag{5.3}$$

$$\frac{dV}{dt} = \underbrace{l_v(t, t_i, MOI) b_M(t_i, MOI) M_i}_{\text{lysis}} + \underbrace{l_v(t, t_i, MOI) b_T T_i}_{\text{lysis}} + \underbrace{l_v(t, t_i, MOI) b_Z Z}_{\text{lysis}} - \underbrace{\omega V}_{\text{clearance}} \tag{5.4}$$

$$\frac{dE_K}{dt} = \underbrace{S_{E_K}(t)}_{\text{source}} - \underbrace{r_K \lambda_T E_K (T_u + T_i)}_{\text{inactivation}} - \underbrace{\mu_K E_K}_{\text{natural death}} \tag{5.5}$$

$$\tag{5.6}$$

$$\frac{dE_C}{dt} = \underbrace{q_C E_C \left(\frac{T_u + T_i}{h_T + T_u + T_i}\right)}_{\text{CTL proliferation}} - \underbrace{\gamma E_C}_{\text{recruitment}} - \underbrace{r_C E_C (T_u + T_i)}_{\text{inactivation}} - \underbrace{\mu_C E_C}_{\text{natural death}} \tag{5.7}$$

$$\frac{dZ}{dt} = \underbrace{S_Z(t)}_{\text{source}} - \underbrace{l_v(t, t_i, MOI) Z}_{\text{death by lysis}} \tag{5.8}$$

where

$$D(x) = \alpha \frac{x^l}{h_{E_C} + x^l}. \tag{5.9}$$

$$\rho(y) = \begin{cases} 1 & \text{if } y = \text{oAd-CAR T cell} \\ 0 & \text{otherwise} \end{cases} \tag{5.10}$$

$$f(Z, T_u) = g Z T_u \tag{5.11}$$

The Heaviside step function, $\rho(y)$, in equation (5.1) engenders death of the tumor cell if the carrier cell is the oAd-CAR T cell, and the functional response function, $f(Z, T_u)$, governs

the interactions between the tumor cells and oAd-CAR T cells. The initial conditions of the model for the *in vivo* setting are as follows: $T_{u0} = 1 \times 10^6$ cells, $T_{i0} = 0$ cells, $M_{i0} = 1 \times 10^6$ cells, $V_0 = \frac{V^\star}{M_{i0}} = \frac{2.7 \times 10^8}{1 \times 10^6} = 270$ plaque forming units (pfu), $E_{K0} = 0$ cells, $E_{C0} = 0$ cells. PFU is a generally accepted measurement for infectious titers (virus particles). Note that $V^\star$ is the number of virions recovered at day 5 post-infection of the oAd-MSCs, at 20 MOI *in vitro*, and thus may represent the tentative number of virions to be released into the tumor microenvironment for the *in vivo* setting.

The term, D in equation 5.9, represents a ratio-dependent tumor cell kill by activated CTLs, derived in [1] from the experimental data in [195]. The parameters, d and l, denote the maximum fractional tumor cell lysis by CTLs and a CTL strength scaling exponent, respectively. The parameter h_{E_C} in D represents the activated CTL toxicity constant that supports half maximum CTL killing rate.

In equation 5.1, the first term, $a_T T_u \left(1 - \frac{T_u + T_i}{K_T}\right)$, indicates that in the absence of oncolytic virus infection and immune response, the uninfected tumor cells grow logistically with an intrinsic growth rate, a_T, and with carrying capacity, K_T. The second term, $-\beta_T(t, t_i, MOI)T_u V$, denotes the infection of tumor cells by oncolytic virions (V) released within tumor microenvironment, at the infection rate, $\beta_T(t, t_i, MOI)$. Note that the infection rate, $\beta_T(t, t_i, MOI)$, depends on the time of treatment (i.e., here, the time at which the luciferase-expressing Hep3B cells were implanted into the 6 week old male nu/nu mice.), t, the time of oncolytic infection, t_i, and the multiplicity of infection, MOI. Note that $\beta_T(t, t_i, MOI) = 0$ whenever $0 \leq t < t_i$, and $\beta_T(t, t_i, MOI) > 0$ for $t_i \leq t_i^*$, where t_i^* is the terminal time of the experiment (i.e., for *in vivo* setting, t_i^* denotes the time at which mice were killed in the experiment). The third term, $-\lambda_T E_K T_u$, represents a direct NK-induced tumor cell death, with the rate of tumor cell death λ_T. The fourth term, $-DT_u$, represents tumor cell lysis by activated tumor-specific CTLs. The term D defined in equation 5.9, represents a ratio-dependent CTL-induced tumor cell death. This function form of cell lysis is a novel term derived by de Pillis et al. [1]. More information and justification of this ratio cell lysis can be found in [1] and [126]. This term has successfully been employed in number of models [216, 333–335, 340]. The last term, $\rho f(Z, T_u)$ represents the tumor-induced cell death by cytotoxic oAd-CAR T cells. For simplicity, the functional response function, $f(Z, T_u) = gZT_u$, is assumed to follow the mass-action kinetics, with a constant tumor killing rate g by the oAd-CAR T cells. This simplification is based on the notion

that these oAd-CAR T cells, loaded with oncolytic virus, are injected into the body, not recruited from the lymph node like normal $CD8^+$ T cells. Cytotoxic T cells are recruited to tumor microenvironments due to the presence of chemicals released by tumor cells [133].

In equation 5.2, an instantaneous transfer of a population of uninfected tumor cells to infected cell population is represented by the first term, $\beta_T(t, t_i, MOI)T_uV$. The oncolytic lysis of infected tumor cells is denoted by the second term, $-l_v(t, t_i, MOI)T_i$, with lysis rate $l_v(t, t_i, MOI)$. Similar to infection rate, β_T, the lysis rate, $l_v(t, t_i, MOI)$, also depends on the time of treatment, t, the time of oncolytic infection, t_i, and the multiplicity of infection, MOI. We assume that the death of the infected cells occurs very rapidly following the viral infection; hence, the intrinsic growth of infected cells is neglected. The oncolytic viral infections often foster infected tumor cells to express tumor antigens which are recognised by NK cells [96, 341, 342]. The rate at which NK cells lyse infected tumor cells is represented by the third term, $-\lambda_T E_K T_i$, where λ_T is the rate of NK-induced tumor death. The last term, DT_i, denotes the tumor cell death induced by CTLs (assumed to be similar the cell lysis of uninfected tumor cells by activated CTLs).

In equation 5.3, the first term, $S_M(t)$, represents a constant supply of MSC carrier cells into the tumor microenvironment. S_M correspond to value from the oAd-MSC data, and it reflects the total number MSCs which were infected with the oncolytic adenovirus for both *in vitro* and *in vitro* settings. The last term, $-l_v(t, t_i, MOI)M_i$, represents lysis of MSC carrier cells within tumor microenvironment by the pre-loaded replication-competent oncolytic adenovirus. Here we assume that when $t < t_i$, there are no oAd-MSCs within the tumor microenvironment.

In equation 5.4, the first term, $l_v(t, t_i, MOI)b_M M_i$, represents the production of new virions from the lysed oAd-MSCs, where $l_v(t, t_i, MOI)$ is the lysing rate of a MSC carrier. During the oncolytic virus propagation (or upon lysis) within the infected cell, a progeny of new infectious virions are released from each infected cell. Thus, b_M is the burst size for viruses from the MSC carriers. After successful virus replication within infected tumor cells, T_i, new virus particles are released and further infect the neighbouring uninfected tumor cells. Hence, the second term, $l_v(t, t_i, MOI)b_T T_i$, represents the production of new virions from the lysed infected tumor cells, with the lysis rate $l_v(t, t_i, MOI)$. The third term, $l_v(t, t_i, MOI)b_Z Z$, represents the production of new virions from oAd-CAR T cells,

with the lysis rate $l_v(t, t_i, MOI)$ and burst size b_Z. An immune induced virus inactivation and elimination is represented by the last term, ωV, where ω is the virus clearance rate within tumor microenvironment. Note that in the tumor microenvironment, free viruses are susceptible to neutralization by circulating antibodies and/or other antiviral immune cells.

In equation 5.5, as part of the innate immunity, NK cells are always present at the tumor site [2, 7, 8], and have been shown to play a vital role in immunosurveillance of tumors [4, 5, 31, 137, 196, 213]. Thus, the first term, $S_{E_K}(t)$, represents a constant supply of NK cells into the tumor microevironment, as done in previous models [1, 152]. The second term, $-r_K\lambda_T E_K(T_u + T_i)$, represents an inactivation of NK cells as a result of their interaction with tumor cells. The proportion of NK cells that gets inactivated during tumor-NK cell interactions is represented by r_K, and λ_T is the rate of NK-induced tumor death. Note that this inactivation occurs when an NK cell encounters a tumor cell several times and consequently cease to be cytotoxic and undergo apoptosis [63, 343]. This mass-action term has successfully been employed in previous models of tumor-immune interactions [1, 144, 152, 216, 333–335]. The natural death of NK cells is represented by the last term, $-\mu_K E_K$, where μ_K is the rate of NK cell death.

In equation 5.7, the first term, $q_C E_C \left(\frac{T_u+T_i}{h_T+T_u+T_i}\right)$, represents the proliferation of activated CTLs within tumor microenvironment [344, 345], where q_C is the proliferation rate of CTLs within tumor site. The CTLs, serving as a key component of the adaptive immunity, are recruited from the lymph node to the tumor microenvironment. The CTL recruitment occurs due to the presence of tumor antigens or oncolytic cell death that often exposes a plethora of tumor associated antigens. This antigenic recruitment is denoted by the term, $-\gamma E_C$, where γ is the recruitment rate of CTLs. Note that this term is negative because CTLs are present at the tumor site only when tumor cells are present, as done in [1, 152, 346]. The third term, $-r_C E_C(T_u + T_i)$, represents the CTL inactivation, at the rate r_C, as a result of their interaction with tumor cells. The last term, $-\mu_C E_C$, represents the natural death of CTLs, with the constant death rate μ_C.

In equation 5.8, a constant supply oAd-CAR T cells into the tumor microenvironment is denoted by the first term, $S_Z(t)$. The second term, $l_v(t, t_i, MOI)Z$, represents the oAd-CAR T cell death by oncolytic virus, with the lysis rate $l_v(t, t_i, MOI)$. Note that even

though the equations (5.3) and (5.8) look similar, Z and M_i differs in their genetic make-up. In addition to the loaded oncolytic virus, the chimeric antigen receptor (CAR)-T cells also have specific genes inserted into their genomes to induce a robust recognition and binding to tumor-associated antigens (TAAs) expressed on the surface of tumor cells [347].

5.4 Parameter estimation

We estimated the values of unknown parameters from the available datasets and/or by considering the plausible biological observations. The values of available parameters and their sources are presented in Table 5.2. In our model, the data-derived parameter estimates were determined by changing values of the unknown parameters until the minimum difference between model output (simulation) and the experimental data is attained as define by the sum of squares error (SSE).

The uninfected tumor. To estimate the tumor growth, $a_T = 0.41$, we used the Least-squares minimization (*leastsquares*) algorithm in *scipy.optimize* package to fit the logistic growth equation (5.1) to uninfected tumor growth data (orthotopic tumor xenografts from 6 week old male nude/nude mice), shown in Figure 5.1. Tumor carrying capacity, $K_T = 2.145 \times 10^4$, is an *ad hoc* value and was chosen to give possible biological outcomes. Note that the proliferation of uninfected tumor cells follows an exponential growth law in the early stage of tumor growth, and also that the data was collected for a short experimental duration of 60 days. This simplistic observation is consisted with other models that capture the early tumor growth dynamics [148, 239, 263, 348]. Additionally, the oAd-CAR T cell killing rate, $g = 1$ per day, is also *ad hoc* value chosen to ensure tumor cell death induced by the oAd-CAR T cells.

The MSC carriers. We used the *in vitro* MSC cell viability data to estimate the cell death dynamics of the oncolytic adenovirus. In particular, having the fixed number of MSC cells, $S_M = 1 \times 10^6$, we used equation (5.3) to fit l_v to MSC cell viability data at day 5. Figure 5.2 indicates cell viability of 5E4 MSC cells at varied incubation time points. The MSC cells were treated with various doses of oncolytic adenovirus (i.e., at different multiplicity of infection (MOI). Note 1 MOI is 1 virus per cell). By minimizing the sum of square errors (SSE) between the MSC-loaded oncolytic adenovirus (oAd-MSC) data points

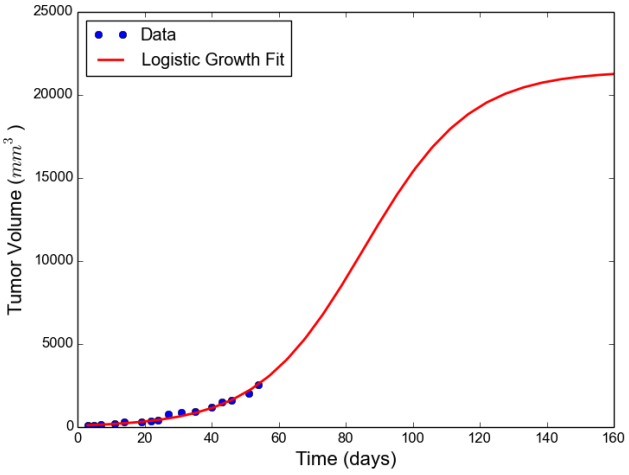

FIG. 5.1. Fit of equation (5.1) simulation to experimental uninfected tumor growth data to find the parameter a_T, with fixed $K_T = 2.145 \times 10^4\ mm^3$ and $\beta_T = \lambda_T = 0$. We convert tumor size to volume using a conversion factor of 10^6 cells to 1 mm^3, and plot the simulated tumor size from equation (5.1) in terms of volume.

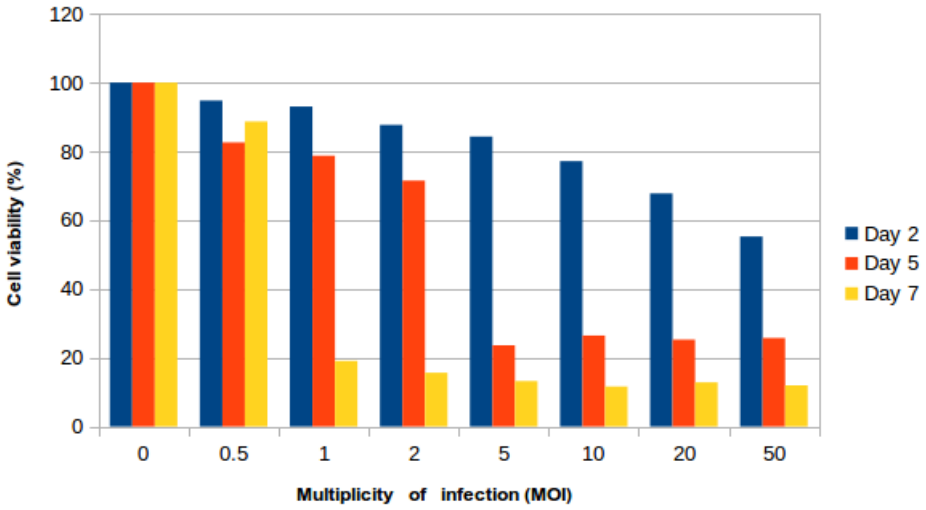

FIG. 5.2. *In vitro* cytotoxicity of naked oncolytic adenovirus in MSC. The cell viability determined at day 2, 5 and 7.

and the model simulation using the MATLAB function *lsqnonlin*, we determined various cell death for given MOIs, as shown Table 5.3.

Two fits of equation (5.3) for MOI 5 and 50 are shown in Figure 5.3.

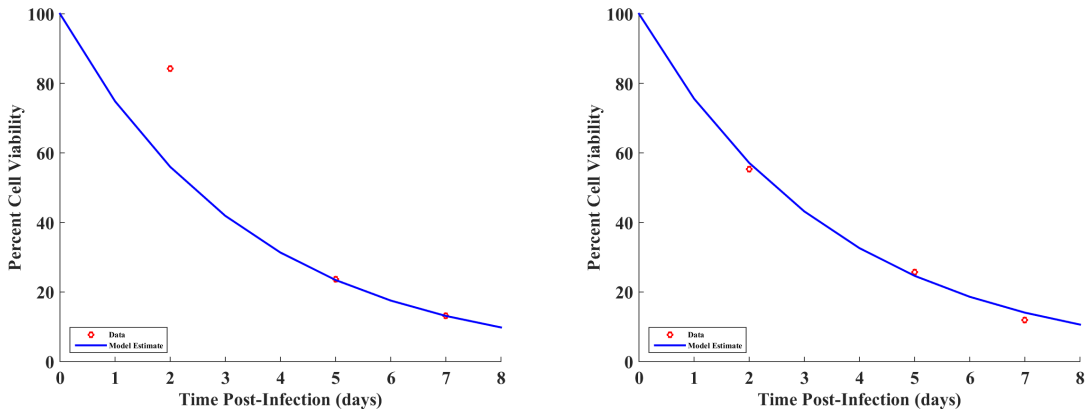

(a) 5 MOI (b) 50 MOI

FIG. 5.3. Fits of equation (5.3) simulations to MSC cell viability data to find the parameter l_v, with $S_M = 1 \times 10^6$ MSC cells/mice fixed.

The total number of infected MSC carriers, $S_M = 1 \times 10^6$ cells, is the initial number of MSCs injected at the beginning of treatment. This value is often manipulated in treatment/clinical settings, and may change from injection time point to another. In this study, $S_M = 1 \times 10^6$ cells, is kept constant throughout the injection time points.

The oncolytic virus. The virus burst sizes, $b_M(t_i, MOI)$, is determined by dividing the infectious progeny viruses produced from each infected cell by the initial number of cells [349, 350]. Thus, $b_M = \frac{V^\star}{M_{i0}} = \frac{2.7\times10^8}{1\times10^6} = 270$ plaque forming units (pfu), where $V^\star$ is the average virus yields recovered from each infected cell at day 5 post-infection of the oAd-MSCs. The infectious viruses for day 2 and 5 are given in Table 5.4.

The activated CTLs. Although the proliferation of CTLs often occur the lymph node [351], the proliferation rate of CTLs within tumor microenvironment, $q_C = 0.25$ cells day^{-1}, is an *ad hoc* value and was chosen to give possible biological outcomes. This value is assumed to be similar to the proliferation rate of immune cells in [352].

5.5 Results

In this section, we present and discuss numerical solutions of our model.

5.5.1 Numerical simulations of alternative carrier cell-based therapeutics

We now present numerical simulations of our model that illustrate main features of our model. Most importantly, we investigate some possible carrier cell-based treatment strategies that could offer effective tumor reduction. We also assess the influence of potential immune response against the oAd-MSC therapeutics as antiviral immune response and antitumor immune response mediated by oncolytic viruses. This is very important because immune responses have proven to be critical components that regulate the antitumor efficacy of the virus in clinical trials.

5.5.2 Varying lysis rate

To further investigate possible conditions that might offer enhanced oAd-MSC therapeutic efficacy, we simulated the effect of varying the lysis rate (l_v) of the oncolytic virus. Figure 5.4 indicates the results of varying lysis rate between 0.1 and 1. The results displayed in Figure 5.4 indicates that loading oncolytic viruses that high lysis rates leads to rapid destruction of the oAd-MSCs. This might pose a challenge of premature lysis of the carrier cell before reaching the target tumor cells [112]. The observation shown in Figure 5.4 imply that it could be better to load a low replicating oncolytic viruses on oAd-MSC in order to allow the oAd-MSCs to reach their target sites, as shown experimental study in [353].

5.5.3 Efficacy of oAd-MSC mediated infection against tumor growth

To investigate conditions that might enhance the oAd-MSC therapeutic efficacy, we simulated cell death profiles upon arrival of the oAd-MSCs within tumor site. The simulated dynamics are shown in Figure 5.5. The time zero (day 0) in Figure 5.5 refers to the infection time (i.e., the time the oAd-MSCs arrive within tumor microenvironment), t_i. Here,

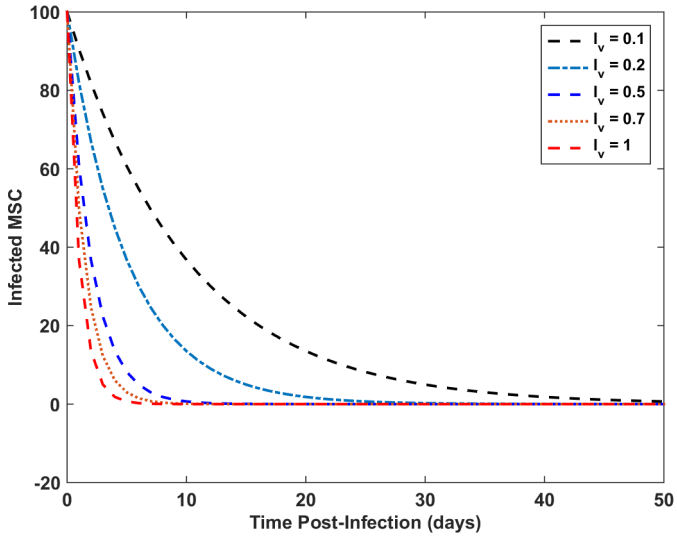

FIG. 5.4. Simulated effects of varying lysis rate on MSC-loaded oncolytic adenovirus.

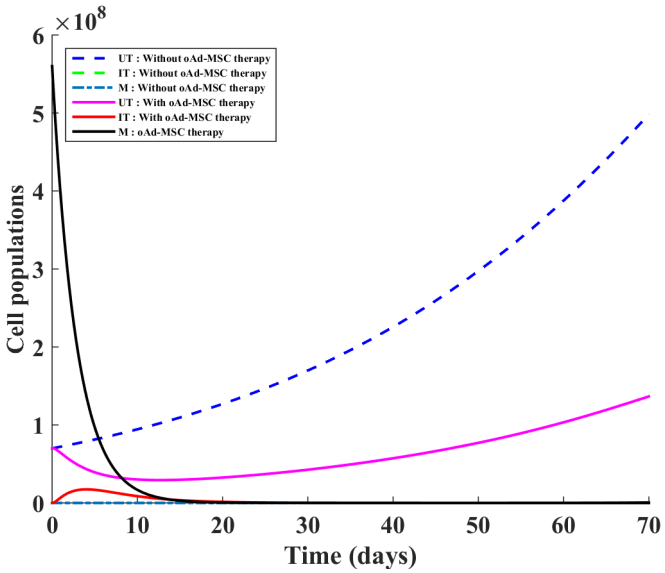

FIG. 5.5. Simulated efficacy of oAd-MSC therapy with respect to tumor growth. This indicates that oAd-MSC therapy leads to transient tumor reduction.

tumor cells are possibly infected on day 0 as the oAd-MSCs become lysed by the virus. The observation displayed in Figure 5.5 indicates that the oAd-MSC therapy leads to transient reduction of tumor burden and a quick tumor relapse. In this simulation, we set a low lysis rate, $l_v = 0.35$ day^{-1}, to allow the oAd-MSC to interact with tumor cells prior to

their lysis by the oncolytic virus. Other parameter values are as given in Table 5.2. The oAd-MSCs are, however, not cytotoxic against tumor cells as they are used as "Trojan horses" in this study. In this figure, we notice that tumor growth relapse does not reach the plateau quickly as observed when there is no therapy (dashed blue line).

5.5.4 Efficacy of oAd-CAR T cell mediated infection against tumor growth

To further investigate possible therapeutic conditions that might give rise to improved treatment outcomes, we also simulated the dynamics of the interactions of oAd-CAR T cells within tumor microenvironment. Similar to oAd-MSC based therapy, we set a low lysis rate, $l_v = 0.35$ day^{-1}, to allow the oAd-CAR T cells to interact with tumor cells prior to their lysis by the oncolytic virus. Figure 5.6 shows tumor growth versus time when the oAd-CAR T cells are within tumor site, with the first interactions or virus lysis occurring on day 0. This simulation indicates that oAd-CAR T cell therapy can possibly

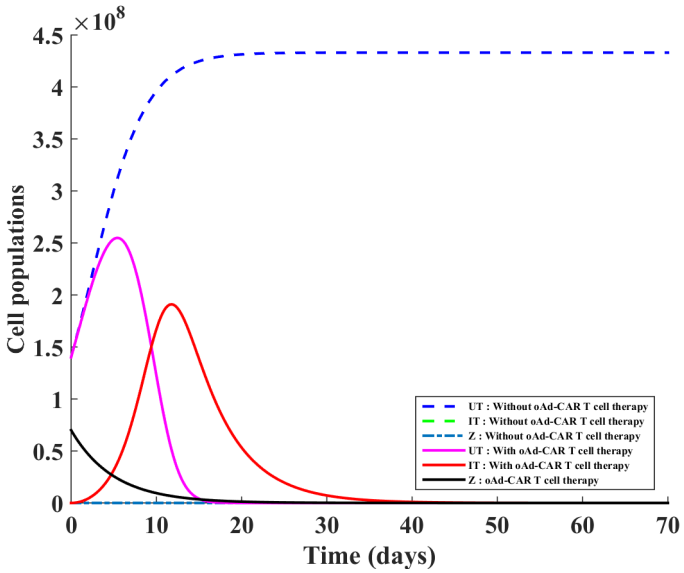

FIG. 5.6. Simulated efficacy of oAd-CAR T cell therapy with respect to tumor growth. The changed parameter value from Table 5.2 was $l_v = 0.35$ day^{-1}. Other parameter values were kept same as in the Table 5.2.

lead to tumor elimination or rapid decline in tumour burden. This is partly because the oAd-CAR T cells not only deliver oncolytic viruses, but also kill tumor cells during their

interactions. This observation is consistent with experimental outcomes reported in [114]. Similar to the observations in Figure 5.5, we see that while tumor infection increases, the oAd-CAR T cell population continually declines over time, indicating a possibility of cell death by oncolytic viruses.

5.5.5 The effect of stronger immune response

Since the immune response can have the confounding effects in oncolytic virotherapy, we considered where the presence of cytotoxic immune cells within tumor microenvironment can have any impact during the carrier cell-based therapies. To investigate the possible effects of stronger immune response, we increased the NK cell constant supply from the baseline value of $S_{E_K} = 1.30 \times 10^4$ cells in Table 5.2 by 10-fold, which gives an improved value of $S_{E_K} = 1.30 \times 10^5$ cells. We considered increasing the value of NK supply because the influx of NK supply within tumor microenvironment has been shown to enhance treatment outcomes [87, 152, 173, 232, 238, 354]. The result of our simulations with the modified NK influx is shown in Figure 5.7. In this simulation, we set a very low virus

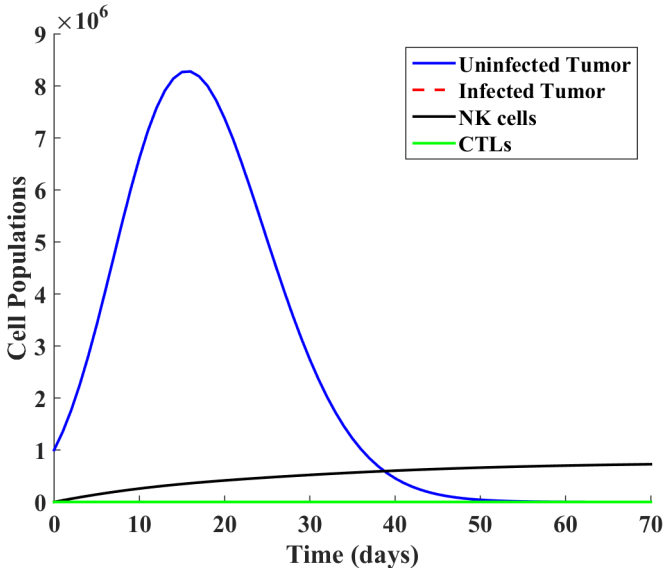

FIG. 5.7. Simulation of improved immune response within tumor microenvironment during oAd-CAR T cell therapy. The NK cell supply was set at $S_{E_K} = 1.30 \times 10^5$ cells, and a low lysis rate of $l_v = 0.035$ per day. Other parameter values are as listed in Table 5.2.

lysis rate to minimize the confounding effects of oncolytic viruses. This is essential for

minimizing early antiviral activities of NK cells which might lead to clearance of the free viruses within tumor microenvironment or infection of tumor cells during the oAd-CAR T cell therapy. Figure 5.7 indicates that increasing NK cell supply can aid to reduce tumor burden.

5.6 Discussion and conclusions

By using a quantitative approach, we investigated how the use of cell carriers in delivering oncolytic viruses to tumor microenvironment can affect tumor growth and progression. We developed a novel mathematical model that describes the local interactions of tumor cells with natural killer cells, cytotoxic T lymphocytes, chimeric antigen receptor–engineered T cells, mesenchymal stem cells, and oncolytic viruses. The aim of this study is to simulate and compare the therapeutic efficacies of the mesenchymal stem cells and engineered chimeric antigen receptor–engineered T cells in delivering oncolytic viruses to tumor site where there are active local antitumor and antiviral immune cells. Although the therapeutic benefits of the MSC-based [355] and CAR-T cell-based [114] therapies in delivering oncolytic viruses to tumor cells *in vitro* in immunodeficient mice have been previously assessed, our model results may further give useful insights into the possible *in vivo* cell dynamics in immunocompetent hosts. Our proposed simple and non-spatial mathematical model devised and analysed in this study shed light on the dynamical behaviors of tumor cells upon their interactions with either the MSCs or CAR-T cells loaded with oncolytic viruses, and the oncolytic viruses at the tumor site. The effect of local immune response, at tumor site, was also investigated to asses its influence during oncolytic virotherapy. It is important to note that the local immune response can have therapeutic benefits by clearing free viruses after all tumor cells are destroyed by oncolytic viruses. On the other hand, it can have negative treatment effects if the viruses are removed immediately after being released from the carrier cells into the tumor microenvironment. Obviously, this early antiviral may subsequently diminish the efficacy of the carrier cell-based therapies.

Although the data we used to estimate the unknown parameters in our model reports the MSC cell viability for day 2, 5 and 7 post infection of MSCs with oncolytic adenovirus at 0 to 50 multiplicity of infection (MOI) $(0, 0.5, 1, 2, 5, 10, 20,$ and $50)$, we only considered

the lysis rates associated with day 5 for illustrative purposes. The results of our parameter estimation and two snapshots of our sub-model fits are indicated in Table 5.3 and Figure 5.3, respectively. These results suggest that the MOI is an important factor that governs the cell viability of the MSC as higher MOI results in rapid destruction of the carrier cell (see Figure Figure 5.3). This finding is of relevant importance because infecting the MSCs at lower MOIs may result in insufficient viral titers released from the infected MSCs at the tumor microenvironment, while infecting the MSC at higher MOIs might destroy the carrier cells rapidly, possibly before their arrival at the tumor site during an *in vivo* treatment.

Since the efficacy of certain carrier cell types may depend on the multiplicity of infection (MOI) [114] and/or the rate at which the viruses lyse the carrier cell, we considered the effects of altering the lysis rate in Figure 5.4. From Figure 5.4, we found that high lysis rates might lead to rapid oAd-MSC destruction, which might limit the efficacy of the oAd-MSCs in delivering the oncolytic viruses to tumor sites. On the other hand, in Figure 5.6 it is shown that low lysis rates may lead to improved therapeutic outcomes when using oAd-CAR T cells in delivering the oncolytic viruses to tumor sites. Intuitively, for oAd-CAR T cell based therapy, low lysis rates may allow the oAd-CAR T cell to perform their cytotoxic activities and deliver the oncolytic viruses deep into the tumor. Similarly, our model results in Figure 5.7 indicate that high number of the natural killer cells within tumor microenvironment may augment the oncolytic virotherapy, given that the slow replicating viruses are pre-loaded on the MSCs. We do note, however, that slow replicating viruses may take a long time to reduce a large tumor [263, 264]. Our findings support the fact that use of immune carrier cells to deliver oncolytic viruses can result in improved antitumor outcomes [312].

In conclusion, our numerical simulations suggest that, at low lysis rates, the greatest efficacy (as indicated by the virus-mediated cell deaths) is achievable with the oAd-CAR T cell based therapy than with the oAd-MSC based therapy. Simulations of the combination of oAd-CAR T cell and oAd-MSC based therapies is a future work on this model to further investigate the synergistic effects of these therapies. Additionally, parameter sensitivity analysis shall be performed to assess the significance of each parameter in our model. Pre-clinical studies, however, will be necessary to quantify the tolerable toxicities associated with this combination strategy and its impact in debugging the tumor burden.

We are currently in collaboration with the experimentalists, from Prof. Chae-Ok Yun's Laboratory at Hanyang University, who will provide us with the relevant data we will be using in our future model validation.

TABLE. 5.2: Baseline parameter values used in the model simulations. The estimated values are based on day 5 of the MSC-based oncolytic virotherapy with 10 MOI.

Parameter	Description	Value	Source
a_T	the intrinsic tumor growth rate	0.41 day^{-1}	Estimate
β_T	the infection rate of tumor cells	8.9×10^{-4} virion^{-1} day^{-1}	[239]
λ_T	the rate of NK-induced tumor death	8.68×10^{-10} cell^{-1} day^{-1}	[257]
α	the maximum proportional tumor kill by CTLs	$\frac{7}{20}$ day^{-1}	[333]
l	the immune strength scaling exponent	$\frac{2}{3}$	[333]
h_{E_C}	the activated CTL toxicity constant that supports half maximum CTL killing rate	1.4	[333]
l_v	the rate of death by lysis	2.65×10^{-1} day^{-1}	Estimate
g	oAd-CAR T cell killing rate	1 day^{-1}	-
S_M	the total number of infected MSC carriers	1×10^6 cells day^{-1}	Estimate
b_M	the number of virions released from the MSC carriers	270	Estimate
b_T	the number of virions released from an infected tumor cell	3.5×10^3	[239]
ω	virus clearance rate	2.3 day^{-1}	[239]
S_{E_K}	the constant external source of NK cells	1.30×10^4 $\text{cell}\cdot\text{day}^{-1}$	[126]
r_K	the fraction of inactivated NK cells during NK-tumor interactions	1.0×10^{-7} cell^{-1} day^{-1}	[126]
q_C	the proliferation rate of CTLs within tumor site	2.4388×10^4 cells day^{-1}	–
μ_K	the natural death rate of NK cells	4.12×10^{-2} day^{-1}	[126, 152, 212]
h_T	the half-saturation constant of tumor cells	40 cells	[144]
γ	the recruitment rate of CTLs	9.0×10^{-3} day^{-1}	[216, 340]
r_C	the fraction of inactivated CTLs during CTL-tumor interactions	3.42×10^{-10} cell^{-1} day^{-1}	[126]
μ_C	the natural death rate of CTLs	2.0×10^{-2} day^{-1}	[126, 152, 212]

TABLE. 5.3. Estimates of oncolytic virus lysis rates (l_v) for various MOIs at day 5.

MOI	Model Estimate (l_v)
0	0
0.5	3.5×10^{-2}
1	4.5×10^{-2}
2	6.8×10^{-2}
5	2.9×10^{-1}
10	2.65×10^{-1}
20	2.73×10^{-1}
50	2.8×10^{-1}

TABLE. 5.4. **The virus replication profiles at various MOIs on day 2 and 5.**

MOI	Day 2 ($V^\star$)	Day 5 ($V^\star$)
0	163.349761962891	265.318542480469
0.5	1385.25170898438	498696.96875
1	2015594	2147604.25
2	1947811.625	4822552
5	4967570.5	76037696
10	6319923.5	266385744
20	13576320	210862320
50	4945146	26431380

Chapter 6

Conclusions

In this chapter, we present a summary of our work and discuss major scientific contributions in this thesis. We also outline possible future directions for immunotherapy and oncolytic virotherapy.

6.1 Summary

In this section, we summarise the accomplishment of the **three** major aims of this thesis specified in Chapter 1, which we restate below:

1. To formulate a novel differential-equation based mathematical model for the immune surveillance of tumors. The model describes how tumor cells evolve and survive the brief encounter with the immune system mediated by natural killer (NK) cells and the activated $CD8^+$ cytotoxic T lymphocytes (CTLs).
2. To develop an original delay differential equation mathematical model describing the interactions between the oncolytic virus, the tumor cells, the normal cells, and the antitumoral and antiviral immune responses. We derive the model's basic reproductive number within tumor and normal cell populations and use their ratio as a metric for virus tumor-specificity.
3. To construct a new differential-equation based mathematical model that describes the use of the mesenchymal stem cell-based and T cell-based therapies for the delivery of oncolytic viruses to tumor site. We use the model to simulate and compare the

efficacy of delivering oncolytic viruses by either type of therapy. This comparison is essential for understanding the possible treatment benefits of each therapy.

Accomplishment of aim 1:

To describe how various tumor cells evolve and survive their transient encounters with the natural killer (NK) cells and the activated $CD8^+$ cytotoxic T lymphocytes (CTLs), we constructed a novel ODE based mathematical framework presented in Chapter 3. The developed model focused specifically on unravelling complex tumor escape mechanism using a Fas/FasL system that enable tumor cells to evade their encounters with immune cells. Using our modeling approach, we were able to predict key interaction features that enable tumor escape from immune surveillance. A novel feature unravelled by our model is that survival of tumor cells from their brief encounter with a certain immune cell enable the tumor cells to acquire an immune-resistant phenotype. This immune-resistant phenotype protects the tumor cells, that survived their encounters with immune cells, from subsequent attacks by the same immune cell or immune cells of the same type. This is consistent with experimental works in [2, 26, 47]. Our simulation results indicated that increasing an external supply of NK cells might enhance NK-cell immune surveillance that is necessary for controlling tumor growth and progression.

Accomplishment of aim 2:

To examine how to increase an oncolytic potency and reduced virus tumor-specificity in oncolytic virotherapy, we built a novel DDE based mathematical model detailed in Chapter 4. In particular, the developed model focuses on how oncolytic virus infection of some normal cells in the vicinity of tumor cells can enhance oncolytic virotherapy. The model consists of a system of delay differential equations describing the interactions between the oncolytic virus, the tumor cells, the normal cells, and the antitumoral and antiviral immune responses. The basic reproductive number of the model within tumor and normal cell populations was derived and used as a measure of virus tumor-specificity. Additionally, a thorough stability analysis of the free virus steady states was performed. Interestingly, through numerical simulations, we discovered that using a certain number of normal cell can aid in amplification of virus particles, and hence lead to improved oncolysis. This is the

first mathematical model which illustrates how a controlled infection of normal cells within tumor territory can augment oncolytic virotherapy. The findings inherent in this research have important consequences for the discovery of new oncolytic virus or attenuation of wild type oncolytic virus vectors.

Accomplishment of aim 3:

To investigate how the use of mesenchymal stem cells (MSCs) or engineered chimeric antigen receptor–engineered T cells (CAR T cells) in delivering oncolytic viruses to tumor site can influence the outcomes of oncolytic virotherapy, we developed an original ODE based mathematical model presented in Chapter 5. The mathematical model describes the interactions of tumor cells with local immune cells (i.e., immune lymphocytes within tumor microenvironment), free oncolytic viruses, CAR T cells and MSCs both pre-infected with the oncolytic adenovirus. Through comparative simulations of each monotherapy, we found that at low lysis rates, the greatest efficacy (evidenced large number of virus-mediated cell death of tumor cells) is achievable with the oAd-CAR T cell based therapy than with the oAd-MSC based therapy. This observation if consistent with experimental results in [114]. From a clinical perspective, use of oAd-CAR T cells in delivering oncolytic viruses to tumor sites may constitute a favourable treatment regime since the engineered oAd-CAR T cells may not only deliver their therapeutic payloads into the tumor microenvironment, but also maintain their antitumor activities. One concern about CAR T cell therapy is a poor targeting of tumor cells. Recent reports indicates that CAR T cells also damage healthy normal cells which rarely express tumor associated antigens [356].

6.2 Contributions of this thesis

In this section, we include the major contributions of this thesis to the field of mathematical oncology as well as experimental and clinical oncology.

6.2.1 Mathematical oncology

An increasing understanding in cellular interactions between tumor cells, immune cells and oncolytic viruses has necessitated the utilization of mathematical modeling techniques to better understand the complexity of biological systems. Herein this thesis, we devised three novel mathematical models that deal with cellular interactions between tumor cells, various types of immune cells, and oncolytic viruses. The mathematical model discussed in Chapter 3 provides useful information for modeling and understanding of tumor-immune surveillance. To this end, our work developed in Chapter 3, published in the Journal of Theoretical Biology, has already been cited in 4 research works - one purely experimental and three mathematical. Mathematical models developed in Chapters 4 and 5 contain invaluable information that quantitatively indicate how increase virus particles within tumor microenvironment and how efficacious certain cell-based therapies are in delivering oncolytic viruses to tumor site, respectively. Although modeling of tumor interactions with oncolytic viruses is challenging, the mathematical models developed in this thesis provide a basic information in understanding some aspects of modeling oncolytic viruses. In general, from a modelling viewpoint, our modeling frameworks developed in this thesis are relatively straight-forward to follow, and may serve as starting points for further research related to complex cellular interactions between tumor cells, normal cells, immune cells and oncolytic viruses.

6.2.2 Clinical and experimental Oncology

Our work in Chapter 3 highlighted some important areas of clinical research that can be exploited to enhance immune surveillance. In particular, our numerical simulations have predicted how the natural killer (NK) cell-based immunotherapeutic approaches can augment tumor-immune surveillance. The numerical results contained in Chapter 4 are essential for testing our hypotheses, experimentally, related to a potential controlled use of some normal cells to enhance oncolytic virotherapy or at least control tumor cell population growth. As an example, clinical evidence indicates that a certain portion of liver can be cut without sacrificing functional ability of a liver [357]. In a similar manner, the use of some normal cells in the vicinity of tumor cells, may be invaluable for controlling tumor growth and progression. Our results clearly indicates that such approach is indeed feasible.

The research contained in Chapter 4 is helpful in discovery of new oncolytic viral vectors or attenuation of the known wild-type viral vectors. To quantify the interaction dynamics within tumor microenvironment prior to experimentation of using certain cells as carriers of oncolytic viruses, may help to cut done the costs associated with such experiments. The research presented in Chapter 5, illustrates how the use of certain cell types as cellular carriers of oncolytic viruses influences the therapeutic outcomes of cell-based therapies, particularly in immunocompetent hosts.

6.3 Future research

Our work opens new avenues of research in the field of biological and mathematical oncology. We now outline our future research to address the relevant alternative approaches motivated from the research in this thesis. One such an alternative approach includes use of tumor associated endothelial cells as oncolytic viral factories. Some oncolytic viruses have a natural preferential tropism for tumor and/or associated endothelial cells while others need to be genetically engineered to direct their specificity to tumor and/or associated endothelial cells [91, 99, 141]. Infecting tumor endothelial cells with oncolytic viruses has dual significance: (a) Viruses released from tumor endothelial cells would undoubtedly increase virus particles within tumor microenvironment; (b) Infection of tumor associated endothelial cells may cause tumor vascular collapse, thereby augmenting anti-angiogenesis treatment. To this end, we extend the model developed in Chapter 5.

Model formulation. Here, we propose a novel non-spatial mathematical model that describes the dynamics of the interactions between the respective cell populations of tumor cells, tumor endothelial cells, immune cell carriers within the tumor, and immune cell carriers circulating in the tumor vasculature. The model also considers the population of oncolytic virus particles and their potential interactions with the cell populations. The immune cell carriers extravasate from the tumor vasculature into a solid vascular tumor through an invasion-type extravasation [358]. It is important to note that carrier cells may extravasate from blood vessels to tumor cell in a variety of mechanisms. They may extravasate via leaky tumor endothelium [359, 360] or in a conventional manner in which a cell extravasates from the blood stream (i.e., through an engagement of the immune cell

carrier and endothelial adhesion molecules) [361]. Through their interaction with tumor cells, cell carriers actively penetrate into the tumor cells and form cell-in-cell structures (i.e., a phenomenon in which a cell of different type is found inside the cytoplasm of another cell) [139, 362, 363]. The formation of cell-in-cell structure appears some time after the tumor and carrier cell became in contact. Additionally, the carrier cells within the tumor also kill tumor cells. For example, HOZOT cells [139] and CIK cells [308, 309], are known to retain their cytotoxic activity against tumor cells when internalized within the tumor. For simplicity, we do not consider the effect of the volume occupied by the carrier cell inside the tumor cell, instead we simply consider the carrier cell inside the solid tumor as one of its cell constituents. To account for the effects of oncolytic virus infection on tumor cells, tumor comprises of the uninfected and infected cells, as other cell constituents. Furthermore, we omit details of the interaction dynamics regulating the immune cell carrier infiltration into the tumor, such as cognate ligand receptor binding [337] or entosis (i.e., a non-apoptotic cell migration which results in tumor cell invasion) [364].

Although ample evidence suggests that immune cells can effectively infiltrate tumor cells [17, 19, 139, 236, 337, 365, 366], there is also some evidence that some tumor-specific lymphocytes may not extravasate from the tumor vasculature [337, 338, 359, 367]. Hence, we assume that some carrier cells may be unable to extravasate from the tumor vasculature in the vicinity of the tumor. That means, we assume that the carrier cells that are unable to extravasate from tumor vasculature are "trapped" in the tortuous and disorganized tumor blood vessels, just like an observed phenomenon where the activated T cells are being held back in the tumor vasculature or microenvironment [368–370].

The model consists of the following variable: the total number of uninfected tumor cell population, $T_u(t)$, the total number of infected tumor cell population, $T_i(t)$, the total number of uninfected tumor endothelial cell population, $E_u(t)$, the total number of infected tumor endothelial cell population, $E_i(t)$, the total number of carrier cell population circulating in the tumor vasculature, $C_b(t)$, the total number of carrier cell population within the tumor, $C_T(t)$, the total number of oncolytic virions in the tumor vasculature, $V_E(t)$, and the total number of oncolytic virions within the tumor, $V_T(t)$.

The ODE system describing our model is given by the following equations:

$$\frac{dT_u}{dt} = \underbrace{a_T E_u T_u \left(1 - \frac{T_u + T_i}{K_T}\right)}_{\text{proliferation}} - \underbrace{l_v \beta_T T_i \frac{T_u}{T_i + T_u}}_{\text{infection}} - \underbrace{\delta e^{(-\mu_{C_T} T_u)} \frac{C_T}{h_T + C_T} T_u}_{\text{killing by carrier cells}} \tag{6.1}$$

$$\frac{dT_i}{dt} = \underbrace{l_v \beta_T T_i \frac{T_u}{T_i + T_u}}_{\text{infection}} - \underbrace{l_v T_i}_{\text{death by lysis}} \tag{6.2}$$

$$\frac{dE_u}{dt} = \underbrace{a_E T_u E_u \left(1 - \frac{E_u + E_i}{K_E}\right)}_{\text{proliferation}} - \underbrace{\beta_E E_u V_E}_{\text{infection}} \tag{6.3}$$

$$\frac{dE_i}{dt} = \underbrace{\beta_E E_u V_E}_{\text{infection}} - \underbrace{l_v E_i}_{\text{death by lysis}} \tag{6.4}$$

$$\frac{dC_b}{dt} = \underbrace{S}_{\text{Source}} - \underbrace{r_b q_T p_T C_b(t - \rho)}_{\text{extravasation}} \tag{6.5}$$

$$\frac{dC_T}{dt} = \underbrace{r_b q_T p_T C_b(t - \rho)}_{\text{infiltration}} - \underbrace{\delta e^{-\mu_{C_T} T_u} \frac{C_T}{h_T + C_T} T_u}_{\text{death due to tumor killing}} - \underbrace{l_v C_T}_{\text{death by lysis}} - \underbrace{\mu_{C_T} C_T}_{\text{natural death}} \tag{6.6}$$

$$\frac{dV_E}{dt} = \underbrace{l_v \beta_E E_i}_{\text{lysis}} - \underbrace{\omega V_E}_{\text{clearance}} \tag{6.7}$$

$$\frac{dV_T}{dt} = \underbrace{l_v \beta_T T_i}_{\text{lysis}} + \underbrace{l_v \beta_E E_i}_{\text{lysis}} - \underbrace{\omega V_T}_{\text{clearance}} . \tag{6.8}$$

Note that the term, p_T, in equations 6.5 and 6.6, is the function $p_T(C_b) = Max\ C_T\ e^{\left(\frac{-\mu_{Tb} C_b}{Max\ C_T}\right)}$ that describes the probability that a carrier cell from the tumor vasculature will infiltrate the tumor. The parameter $Max\ C_T$ denotes the maximum number of carrier cells that can infiltrate the tumor, and μ_{Tb} is the rate of exponential decay due to carrier cell exhaustion during extravasation and/or infiltration. The means, p_T is the probability that the carrier cell will infiltrate the tumor after extravasating the tumor vasculature. Since not every immune cell can infiltrate the tumor, we assume that there is a maximum rate at which carrier cells can enter the tumor, as has been done with the dendritic cells (DCs) in [333]. This is in agreement with clinical observations that immune cells, such as tumor-infiltrating lymphocytes (TILs), cannot infiltrate tumors unlimitedly since tumor often develop mechanisms to inhibit efficient immune cell infiltration [17, 338, 371]. Also, note that p_T decays exponentially as a function of the carrier cell concentration in the tumor vasculature. The

function $q_T = 1 - p_T$ describes the probability that a carrier cell will not extravasate the tumor vasculature.

In equation 6.1, the first term, $a_T E_u T_u \left(1 - \frac{T_u + T_i}{K_T}\right)$, indicates that in the absence of oncolytic virus infection, the uninfected tumor cells grow logistically with an intrinsic growth rate, a_T, subject to the carrying capacity of the tumor cells, K_T. In the absence of oncolytic virus infection, vascular tumor depends on the tumor vascularization (i.e., the flow of blood from the new vessels formed by angiogenesis) [360, 372–374]. For simplicity, we do not consider the subcellular events leading to tumor angiogenesis, instead, we consider the interaction of the tumor cells with the tumor endothelial cells resulting from tumor angiogenesis. The second term, $-l_v \beta_T T_i \frac{T_u}{T_i + T_u}$, denotes the infection of tumor cells by the oncolytic virus and is proportional to the oncolytic viral death by lysis. The ratio-dependent viral infection kinetics of this type has also been considered in [144, 262]. The kinetics of this type are more applicable when one assumes that the density of the infected cell population does not change with the number of the uninfected cells or virions [262]. We considered the ratio-dependent viral infection kinetics because the infection of uninfected tumor cells does not depend directly on the number of virions, but rather of the number of immune carrier cells within the tumor. The saturable immune-mediated killing mechanism of the carrier cells is defined by the term, $-\delta e^{\left(-\mu_{C_T} T_u\right)} \frac{C_T}{h_T + C_T} T_u$, where the tumor cells are killed by the immune carrier cells at the rate δ. Apart from the plausible cytotoxic killing mechanism exerted by carrier cells inside the tumor [139, 308, 309], to infiltrate into tumors, carrier cells may invade the tumor [139, 364]. Such immune carrier cell invasiveness is governed by the parameter, δ. The formation of cell-in-cell structure depends on the uninfected tumor cell concentrations at time $t - \rho$. The time delay, ρ, represents the *extravasation-infiltration* connection time: the transient time required between tumor vasculature and tumor before tumor invasion can begin. Note that the carrier cells may not only extravasate from the tumor vasculature when tumor cells and tumor endothelial cells are adjacent, but also plausibly at any point in the tumor vasculature. Thus, the time lapse from carrier cell extravasation and actual tumor invasion is endowed in the delay ρ. Hence, the encounter between the carrier cells and tumor cells, which results in the formation of cell-in-cell structures, occurs at the time of $t - \rho$. Note that we assume that the carrier cell extravasation occurs in the vicinity of tumor cells, and there are no cellular material,

such as stroma or extracellular matrix (ECM), that may impede the carrier cell trafficking and infiltration into the tumor. On the other hand, the survival probability of the carrier cells during the tumor invasion is considered by the term $e^{-\mu_{C_T} T_u}$, where μ_{C_T} is the natural death of the immune carrier cell within the tumor. Note that the probability of carrier cell survival during tumor invasion decays exponentially as a function of the concentration of uninfected tumor cells. Similar cell survival functions of this type has also been considered in [375, 376]. The parameter, h_T, denotes the half-saturation constant that supports half maximum killing of the tumor cells.

In equation 6.2, the instantaneous transfer of a subpopulation of the uninfected tumor cells to the infected cell subpopulation following the oncolytic virus infection is represented by the first term, $l_v \beta_T T_i \frac{T_u}{T_i + T_u}$. The death of the infected tumor cells, at the lysis rate l_v, via bursting of the replication-competent viral particles, is denoted by the last term, $-l_v T_i$. Here, we assume that the death of the infected cell occurs very rapidly following the virus infection, hence the intrinsic growth of infected cell is neglected.

In equation 6.3, the proliferation of the tumor endothelial cells is denoted by the term, $a_E T_u E_u \left(1 - \frac{E_u + E_i}{K_E}\right)$, in the absence of the oncolytic treatment. The parameters, a_E and K_E, define the intrinsic growth rate and the carrying capacity of the tumor endothelial cells, respectively. In this study, we assume that tumor endothelial cells grow logistically in the absence of treatment, as has been done in [377]. Upon infection with the oncolytic virus particles, the instantaneous shift of the subpopulation of the uninfected tumor endothelial cells to the infected cell subpopulation is denoted by the term, $-\beta_E E_u V_E$. The infection rate of the tumor endothelial cells by the oncolytic virions are defined by β_E. Here, we model the oncolytic virus infection with a mass action term, as done in [143]. Under this scenario, the infection rate is dependent on the number of uninfected tumor endothelial cells and the amount of oncolytic virions. We consider the mass action kinetics because the infection of the tumor endothelial cells depends on the amount of free oncolytic virus particles released from lysed carrier cells in the tumor vasculature, not on the carrier cell infiltrates. Note that tumor endothelium is also known to be prohibitive to entry of tumor-specific lymphocytes [360]. Hence we assume that the circulating carrier cells would ultimately to be destroyed by the loaded virus. After lysis, there would be free virus particles circulating in the tumor vasculature that could infect the tumor endothelial cells.

In equation 6.4, the instantaneous transfer of uninfected tumor endothelial cells to infected subpopulation is represented by the first term, $\beta_E E_u V_E$. The lysis of the infected tumor endothelial cells is defined by the last term, $-l_v E_i$, with lysis rate l_v.

In equation 6.5, the first term, S, represents the constant source of the carrier cells into the tumor vasculature from an appropriate injection site in the vicinity of the tumor. The last term, $-r_b C_b(t-\rho)$, denotes the extravasation of the carrier cells from the tumor vasculature at the rate r_b. We assume that the extravasation rate of the carrier cell from the tumor vasculature is the same as tumor infiltration rate into the tumor cells. In other words, we assume an invasion-type extravasation [358].

In equation 6.6, the carrier cell infiltration into the tumor is represented by the term $r_b C_b(t-\rho)$, where r_b is the rate of immune cell infiltration into the tumor. This term accounts for newly infiltrated carrier cells that appear in the uninfected tumor cell population, T, ρ time units after extravasation from the tumor vasculature. In this study, the rate of carrier cell infiltration, can also be regarded as the rate at which the carrier cell invades the tumor. Since the infiltration of immune cells into tumors facilitates direct cell-cell contact, some immune carrier cells may die or become deactivated during their interactions with tumor cells. Thus, the second term, $-\delta e^{-\mu_{C_T} T_u} \frac{C_T}{h_T + C_T} T_u$, denotes the carrier cell death resulting from tumor-immune cells battle. The last term, $-l_v C_T$, represents the death of the carrier cells inside the tumor due to cell lysis initiated by the loaded replication-competent oncolytic virus.

In equation 6.7, upon lysis of infected carrier cells within the tumor, some newly produced viruses could successfully infect tumor cells. Hence, the infected tumor cells, T_i, are lysed by virus particles. Thus, the first term, $l_v \beta_T T_i$, represents the production of new virions from the lysed infected tumor cells, at a rate $l_v \beta_T$ that is proportional to their lysis. Similarly, the second term, $l_v \beta_E E_i$, denotes the production of new virions from the lysed infected tumor endothelial cells, E_i, at a rate $l_v \beta_E$ that is proportional to their lysis. An immune induced [378] or non-immune induced [101] virus inactivation and elimination is represented by the last term, ωV_E, where ω is the clearance rate. Note that in the tumor vasculature, free viruses are susceptible to neutralization by circulating antibodies or other anti-virus immune cells. For simplicity, we assume that the virus clearance rate (ω) embodies the immune-induced clearance or potential inactivation by an innate immune response.

In equation 6.8, once the infected carrier cells within the tumor are lysed by the replication-competent virus, a new progeny of oncolytic virus particles would then infect neighbouring tumor cells. After successful virus replication within the infected tumor cells, T_i, new virus particles are released and further infect the neighbouring uninfected tumor cells. Thus, the first term, $l_v\beta_T T_i$, represents the production of new virions from the lysed infected tumor cells, at a rate $l_v\beta_T$ that is proportional to their lysis. Similarly, the second term, $l_v\beta_E E_i$, denotes the increase in the concentration of virus particles within the tumor as a result of the virions released from the lysed infected tumor endothelial cells, E_i, at a rate $l_v\beta_E$ that is proportional to their lysis. Virus clearance inactivation and elimination within the tumor is represented by the last term, ωV_T, where ω is the clearance rate. The virus particles within the tumor are susceptible to tumor-mediated inactivation mechanisms. For example, an inhibition of protein kinase (PKR) autophosphorylation as a resulting from activation of a ras signal transduction pathway by tumor cells leads to virus inactivation [101]. Here, we assume that the virus clearance rate (ω) embodies tumor-mediated inactivation mechanisms. Note that there are no free virus particles within tumor because the moment a virus enters a tumor cell, it becomes retained within the cell it entered only, hence it cannot infect other cells. Thus, it cannot constitute the free virus population, as in the tumor vasculature. This assumption is consistent with models in [144, 149, 283, 379].

A thorough analytical and numerical investigation of the system described by equations 6.1-6.8 may highlight the feasibility of joint battle of oncolytic viruses and the immune cell-based carrier therapies in controlling tumor growth.

6.4 Final remarks

The modeling effort in this thesis is the first attempt at relating tumor-immune surveillance to the development of tumor cell immunoresistance, use of controlled oncolytic infections of some normal cells in the vicinity of tumor cells to augment oncolytic virotherapy, and the delivery of oncolytic viruses to tumor site by the mesenchymal stem cells and the engineered antigen receptor–engineered T cells in the presence of active immune response. Mathematical modeling, in conjunction with experimental research, may provide useful insights into the dynamics of tumor-immune interactions which are pertinent in designing

effective immuno- and oncolytic viro-therapies.

The research carried out in this thesis has highlighted the importance of immune surveillance in controling tumor growth and progression, and has suggested plausible treatment regimes that can be engaged to minimize tumor escape. Our work is consistent with experimental results which indicate that the immune surveillance can be greatly enhanced through NK cell-based immunotherapeutic approaches such an infiltration of autologous (patients' own) NK cells [87, 238]. We further showed how some outstanding challenges in oncolytic virotherapy, such as insufficient infectious viral titers within tumor microenvironment, can be addressed. For example, a controlled infection of some normal cells, within the vicinity of tumor cells, by oncolytic viruses that are not 100% tumor-specific can increase the infectious virus particles within tumor microenvironment.

Since our work is purely quantitative, further experimental research is warranted to test the scientific findings and assumptions of the mathematical models developed in this thesis. We are in close collaborations with the experimental oncologists, at Prof. Chae-Ok Yun's Laboratory for Bioengineering at Hanyang University, who will provide us with the relevant data to validate the mathematical models devised in this thesis.

Bibliography

[1] de Pillis L, Radunskaya A. A mathematical model of immune response to tumor invasion. In: Computational Fluid and Solid Mechanics. ed. K.J. Bathe (Elsevier Science Ltd); 2003. p. 1661–1668.

[2] Dunn GP, Old LJ, Schreiber RD. The three Es of cancer immunoediting. Annual Review of Immunology. 2004;22:329–360.

[3] Escors D. Tumour Immunogenicity, Antigen Presentation, and Immunological Barriers in Cancer Immunotherapy. New Journal of Science. 2014;2014.

[4] Swann JB, Smyth MJ. Immune surveillance of tumors. Journal of Clinical Investigation. 2007;117(5):1137–1146.

[5] Ochsenbein AF, Klenerman P, Karrer U, Ludewig B, Pericin M, Hengartner H, et al. Immune surveillance against a solid tumor fails because of immunological ignorance. Proceedings of the National Academy of Sciences. 1999;96(5):2233–2238.

[6] Delves P, Martin S, Burton D, Roitt I. Essential Immunology. Black-well Publishing Ltd; 2006.

[7] Street SEA, Hayakawa Y, Zhan Y, Lew AM, MacGregor D, Jamieson AM, et al. Innate immune surveillance of spontaneous B cell lymphomas by natural killer cells and $\gamma\delta$ T cells. The Journal of experimental medicine. 2004;199(6):879–884.

[8] Waldhauer I, Steinle A. NK cells and cancer immunosurveillance. Oncogene. 2008;27(45):5932–5943.

[9] Smyth M, Godfrey D, Trapani J. A fresh look at tumor immunosurveillance and immunotherapy. Nature Immunology. 2001;2(4):293–299.

[10] Vivier E, Ugolini S, Blaise D, Chabannon C, Brossay L. Targeting natural killer cells and natural killer T cells in cancer. Nature Reviews Immunology. 2012;12(4):239–252.

[11] Wodarz D, Komarova N. Computational biology of cancer: lecture notes and mathematical modeling. World Scientific Publishing Company, Singapour; 2005.

[12] Kindt TJ, Goldsby RA, Osborne BA. Kuby immunology. W.H. Freeman and Company. New York; 2007.

[13] Kim R, Emi M, Tanabe K. Cancer immunoediting from immune surveillance to immune escape. Immunology. 2007;121(1):1–14.

[14] DuPage M, Jacks T. Genetically engineered mouse models of cancer reveal new insights about antitumor immune response. Current opinion in immunology. 2013;25(2):192–199.

[15] Swann MWLTJB, Koebel CM, Schreiber RD, Smyth MJ. Immune-mediated dormancy: an equilibrium with cancer. Journal of leukocyte biology. 2008;84(4):988–993.

[16] Mlecnik B, Bindea G, Pagès F, Galon J. Tumor immunosurveillance in human cancers. Cancer and metastases reviews. 2011;30(1):5–12.

[17] Pagès F, Galon J, Dieu-Nosjean MC, Tartour E, Sautès-Fridman C, Fridman WH. Immune infiltration in human tumors: a prognosis that should not be ignored. Oncogene. 2010;29(8):1093–1102.

[18] Nelson BH. The impact of T-cell immunity on ovarian cancer outcomes. Immunological reviews. 2008;222(1):101–116.

[19] Hwang WT, Adams SF, Tahirovic E, Hagemann IS, Coukos G. Prognostic significance of tumor-infiltrating T cells in ovarian cancer: a meta-analysis. Gynecologic oncology. 2012;124(2):192–198.

[20] Strauss DC, Thomas JM. Transmission of donor melanoma by organ transplantation. The Lancet oncology. 2010;11(8):790–796.

[21] Galon J, Costes A, Sanchez-Cabo F, Kirilovsky A, Mlecnik B, Lagorce-Pagès C, et al. Type, density, and location of immune cells within human colorectal tumors predict clinical outcome. Science. 2006;313(5795):1960–1964.

[22] Schreiber RD, Old LJ, Smyth MJ. Cancer immunoediting: integrating immunitys roles in cancer suppression and promotion. Science. 2011;331(6024):1565–1570.

[23] Mittal D, Gubin MM, Schreiber RD, Smyth MJ. New insights into cancer immunoediting and its three component phases–elimination, equilibrium and escape. Current opinion in immunology. 2014;27:16–25.

[24] Vesely MD, Kershaw MH, Schreiber RD, Smyth MJ. Natural innate and adaptive immunity to cancer. Annual review of immunology. 2011;29:235–271.

[25] Hanahan D, Weinberg RA. Hallmarks of cancer: The next generation. Cell. 2011;144(5):646–674.

[26] Whiteside TL. The tumor microenvironment and its role in promoting tumor growth. Oncogene. 2008;27(45):5904–5912.

[27] Mumm JB, Emmerich J, Zhang X, Chan I, Wu L, Mauze S, et al. IL-10 elicits IFNγ-dependent tumor immune surveillance. Cancer Cell. 2011;20(6):781–796.

[28] Seliger B, Cabrera T, Garrido F, Ferrone S. HLA class I antigen abnormalities and immune escape by malignant cells. Seminars in cancer biology. 2002;12(1):3–13.

[29] Stewart TJ, Abrams SI. How tumour escape mass destruction. Oncogene. 2008;27(45):5894–5903.

[30] Siddle HV, Kreiss A, Tovar C, Yuen CK, Cheng Y, Belov K, et al. Reversible epigenetic down-regulation of MHC molecules by devil facial tumour disease illustrates immune escape by a contagious cancer. Proceedings of the National Academy of Sciences. 2013;110(13):5103–5108.

[31] Bubenik J. MHC class I down-regulation: tumour escape from immune surveillance?(review). International journal of oncology. 2004;25(2):487–491.

[32] Haworth KB, Leddon JL, Chen C, Horwitz EM, Mackall CL, Cripe TP. Going back to class I: MHC and immunotherapies for childhood cancer. Pediatric blood and cancer. 2015;62(4):571–576.

[33] Wilson EB, El-Jawhari JJ, Neilson AL, Hall GD, Melcher AA, Meade JL, et al. Human tumour immune evasion via TGF-β block NK cell activation but not survival allowing therapeutic restoration of anti-tumour activity. PloS One. 2011;6(9):e22842.

[34] Thomas DA, Massagué J. TGF-β directly targets cytotoxic T cell functions during tumor evasion of immune surveillance. Cancer cell. 2005;8(5):369–380.

[35] Kawarada Y, Ganss R, Garbi N, Sacher T, Arnold B, Hämmerling GJ. NK-and CD8$^+$ T cell-mediated eradication of established tumors by peritumoral injection of CpG-containing oligodeoxynucleotides. The Journal of Immunology. 2001;167(6):5247–5253.

[36] Igney FH, Krammer PH. Immune escape of tumors: apoptosis resistance and tumor counterattack. Journal of leukocyte biology. 2002;71(6):907–920.

[37] Töpfer K, Kempe S, Müller N, Schmitz M, Bachmann M, Cartellieri M, et al. Tumor evasion from T cell surveillance. Journal of Biomedicine and Biotechnology. 2011;2011:918471.

[38] Classen CF, Falk CS, Friesen C, Fulda S, Herr I, Debatin KM. Natural killer resistance of a drug-resistant leukemia cell line, mediated by up-regulation of HLA class I expression. Haematologica. 2012;88(5):509–521.

[39] Azuma T, Yao S, Gefeng Z, Flies AS, Flies SJ, Chen L. B7-H1 is a ubiquitous anti-apoptotic receptor on cancer cells. Blood. 2008;111(7):3635–3643.

[40] Dong H, Strome SE, Salomao DR, Tamura H, Hiaro F, Flies DB, et al. Tumor-associated B7-H1 promotes T-cell apoptosis: a potential mechanism of immune evasion. Nature medicine. 2002;8(8):793–800.

[41] Karbasi A, Borhani N, Daliri K, Kazemi B, Manoochehri M. Downregulation of external death receptor genes FAS and DR5 in colorectal cancer samples positive for human papillomavirus infection. Pathology-Research and Practice. 2015;211(6):444–448.

[42] Teiti I, Florie B, Pich C, Gence R, Lajoie-Mazenc I, Rochaix P, et al. In vivo effects in melanoma of ROCK inhibition-induced FasL overexpression. Frontiers in oncology. 2015;5(156).

[43] Peter ME, Hadji A, Murmann AE, Brockway S, Putzbach W, Pattanayak A, et al. The role of CD95 and CD95 ligand in cancer. Cell Death and Differentiation. 2015;22:549–559.

[44] Méndez R, Ruiz-Cabello F, Rodriguez T, del Campo A, Paschen A, Schadendorf D, et al. Identification of different tumor escape mechanisms in several metastases from a melanoma patient undergoing immunotherapy. Cancer Immunology, Immunotherapy. 2007;56(1):88–94.

[45] Mapara MY, Sykes M. Tolerance and cancer: mechanisms of tumor evasion and strategies for breaking tolerance. Journal of clinical oncology. 2004;22(6):1136–1151.

[46] Curiel TJ. Tregs and rethinking cancer immunotherapy. Journal of clinical investigation. 2007;117(5):1167–1174.

[47] Whiteside TL, Mandapathil M, Szczepanski M, Szajnik M. Mechanisms of tumor escape from the immune system: adenosine-producing Treg, exosomes and tumor-associated TLRs. Bulletin du cancer. 2011;98(2):E25–E31.

[48] Yasumoto K, Hanagiri T, Takenoyama M. Lung cancer-associated tumor antigens and the present status of immunotherapy against non-small-cell lung cancer. General thoracic and cardiovascular surgery. 2009;57(9):449–457.

[49] Raval RR, Sharabi AB, Walker AJ, Drake CG, Sharma P. Tumor immunology and cancer immunotherapy: summary of the 2013 SITC primer. Journal for immunotherapy of cancer. 2014;2(1):1–11.

[50] Page DB, Bourla AB, Daniyan A, Naidoo J, Smith E, Smith M, et al. Tumor immunology and cancer immunotherapy: summary of the 2014 SITC primer. Journal for immunotherapy of cancer. 2015;3(1):1–10.

[51] Parsa AT, Waldron JS, Panner A, Crane CA, Parney IF, Barry JJ, et al. Loss of tumor suppressor PTEN function increases B7-H1 expression and immunoresistance in glioma. Nature medicine. 2007;13(1):84–88.

[52] Hanahan D, Weinberg RA. The hallmarks of cancer. Cell. 2000;100(1):57–70.

[53] King RJB. Cancer Biology. Prentice Hall; 2000.

[54] Pandolfi F, Cianci R, Pagliari D, Casciano F, Bagal' C, Astone A, et al. The immune response to tumors as a tool toward immunotherapy. Clinical and Developmental Immunology. 2011;2011:1–12.

[55] Weinberg RA. The Biology of Cancer. Garland Science, Taylor & Francis Group, LLC, London; 2007.

[56] Nowell PC. The clonal evolution of tumor cell populations. Science. 1976;194(4260):23–28.

[57] Kennedy KM, Dewhirst MW. Tumor metabolism of lactate: the influence and therapeutic potential for MCT and CD147 regulation. Future Oncology. 2010;6(1):127–148.

[58] Fang J, Gillies R, Gatenby R. Adaptation to hypoxia and acidosis in carcinogenesis and tumor progression. Seminars in Cancer Biology. 2008;18(5):330–337.

[59] Harris AL. Hypoxia – a key regulatory factor in tumour growth. Nature Reviews Cancer. 2002;2(1):37–47.

[60] Semenza GL. Defining the role of hypoxia-inducible factor 1 in cancer biology and therapeutics. Oncogene. 2010;29(5):625–634.

[61] Negrini S, Gorgoulis VG, Halazonetis TD. Genomic instability – an evolving hallmark of cancer. Nature reviews molecular cell biology. 2010;11(3):220–228.

[62] Luo J, Solimini NL, Elledge SJ. Genomic instability – an evolving hallmark of cancer. Cell. 2009;136(5):823–837.

[63] Marcus A, Gowen BG, Thompson TW, Iannello A, Ardolino M, Deng W, et al. Recognition of tumors by the innate immune system and natural killer cells. Advances in immunology. 2014;122:91–128.

[64] Lehmann C, Zeis M, Schmitz N, Uharek L. Impaired binding of perforin on the surface of tumor cells is a cause of target cell resistance against cytotoxic effector cells. Blood. 2000;96(2):594–600.

[65] Smyth MJ, Kelly JM, Baxter AG, Körner H, Sedgwick JD. An essential role for tumor necrosis factor in natural killer cellmediated tumor rejection in the peritoneum. The Journal of experimental medicine. 1998;188(9):1611–1619.

[66] Marchini A, Scott EM, Rommelaere J. Overcoming Barriers in Oncolytic Virotherapy with HDAC Inhibitors and Immune Checkpoint Blockade. Viruses. 2016;8(1):9.

[67] Pardoll DM. The blockade of immune checkpoints in cancer immunotherapy. Nature Reviews Cancer. 2012;12(4):252–264.

[68] Dine J, Gordon RA, Shames Y, Kasler MK, Barton-Burke M. Immune checkpoint inhibitors: An innovation in immunotherapy for the treatment and management of patients with cancer. Asia-Pacific journal of oncology nursing. 2017;4(2):127.

[69] Schadendorf D, Hodi FS, Robert C, Weber JS, Margolin K, Hamid O, et al. Pooled analysis of long-term survival data from phase II and phase III trials of ipilimumab in unresectable or metastatic melanoma. Journal of clinical oncology. 2015;33(17):1889–1894.

[70] Sharma P, Allison JP. The future of immune checkpoint therapy. Science. 2015;348(6230):56–61.

[71] Mitchison TJ. The proliferation rate paradox in antimitotic chemotherapy. Molecular biology of the cell. 2012;23(1):1–6.

[72] Housman G, Byler S, Heerboth S, Lapinska K, Longacre M, Snyder N, et al. Drug resistance in cancer: an overview. Cancers. 2014;6(3):1769–1792.

[73] Chabner BA, Bertino J, Cleary J, Ortiz T, Lane A, Supko JG, et al. Cytotoxic Agents. In: Goodman and Gilman's The Pharmacological Basis for Therapeutics. McGraw-Hill, New York; 2011. p. 1678–1682.

[74] Palma MD, Hanahan D. The biology of personalized cancer medicine: facing individual complexities underlying hallmark capabilities. Molecular oncology. 2012;6(2):111–127.

[75] Zhao Y, Butler EB, Tan M. Targeting cellular metabolism to improve cancer therapeutics. Cell death and disease. 2013;4(3):e532.

[76] Ma Y, Chapman J, Levine M, Polireddy K, Drisko J, Chen Q. High-dose parenteral ascorbate enhanced chemosensitivity of ovarian cancer and reduced toxicity of chemotherapy. Science translational medicine. 2014;6(222):222ra18–222ra18.

[77] Ito K, Ito H, Kemeny NE, Gonen M, Allen PJ, Paty PB, et al. Biliary sclerosis after hepatic arterial infusion pump chemotherapy for patients with colorectal cancer liver metastasis: incidence, clinical features, and risk factors. Annals of surgical oncology. 2012;19(5):1609–1617.

[78] Peterfreund RA, Philip JH. Critical parameters in drug delivery by intravenous infusion. Expert opinion on drug delivery. 2013;10(8):1095–1108.

[79] Findlay M, von Minckwitz G, Wardley A. Effective oral chemotherapy for breast cancer: pillars of strength. Annals of Oncology. 2008;19(2):212–222.

[80] Yamamoto E, Niimi K, Fujikake K, Nishida T, Murata M, Mitsuma A, et al. High-dose chemotherapy with autologous peripheral blood stem cell transplantation for choriocarcinoma: A case report and literature review. Molecular and Clinical Oncology. 2016;5(5):660–664.

[81] Kwan A, Mazhar D. Germ-cell cancer of the testis and related neoplasms. In: Treatment of cancer. Taylor & Francis Group, Boca Raton; 2015. p. 350–369.

[82] Lauber K, Ernst A, Orth M, Herrmann M, Belka C. Dying cell clearance and its impact on the outcome of tumor radiotherapy. Frontiers in oncology. 2012;2:116.

[83] Barcellos-Hoff MH. How tissues respond to damage at the cellular level: orchestration by transforming growth factor-β (TGF-β). The British Journal of Radiology. 2005;27 (Suppl.):123–127.

[84] Wortel RC, Witte MG, van der Heide UA, Pos FJ, Lebesque JV, van Herk M, et al. Dose–surface maps identifying local dose–effects for acute gastrointestinal toxicity after radiotherapy for prostate cancer. Radiotherapy and Oncology. 2015;117(3):515–520.

[85] Borghaei H, Smith MR, Campbell KS. Immunotherapy of cancer. European journal of pharmacology. 2009;625(1):41–54.

[86] Perica K, Varela JC, Oelke M, Schneck J. Adoptive T Cell Immunotherapy for Cancer. Rambam Maimonides medical journal. 2015;6(1):e0004.

[87] Cheng M, Chen Y, Xiao W, Sun R, Tian Z. NK cell-based immunotherapy for malignant diseases. Cellular and Molecular Immunology. 2013;10(3):230–252.

[88] Figdor CG, de Vries IJM, Lesterhuis WJ, Melief CJM. Dendritic cell immunotherapy: mapping the way. Nature medicine. 2004;10(5):475–480.

[89] Galluzzi L, Vacchelli E, Pedro BS, Buqué A, Bloy N, Castoldi F, et al. Classification of current anticancer immunotherapies. Oncotarget. 2014;5(24):12472.

[90] Lemay CG, Rintoul JL, Kus A, Paterson JM, Garcia V, Falls TJ, et al. Harnessing oncolytic virus-mediated antitumor immunity in an infected cell vaccine. Molecular Therapy. 2012;20(9):1791–1799.

[91] Russell SJ, Peng KW, Bell JC. Oncolytic virotherapy. Nature biotechnology. 2012;30(7):658–670.

[92] Atherton MJ, Lichty BD. Evolution of oncolytic viruses: novel strategies for cancer treatment. Immunotherapy. 2013;5(11):1191–1206.

[93] Cassady KA, Haworth KB, Jackson J, Markert JM, Cripe TP. To Infection and Beyond: The Multi-Pronged Anti-Cancer Mechanisms of Oncolytic Viruses. Viruses. 2016;8(2):43.

[94] Chiocca EA, Rabkin SD. Oncolytic viruses and their application to cancer immunotherapy. Cancer immunology research. 2014;2(4):295–300.

[95] Lichty BD, Breitbach CJ, Stojdl DF, Bell JC. Going viral with cancer immunotherapy. Nature Reviews Cancer. 2014;14:559–567.

[96] Workenhe ST, Mossman KL. Oncolytic virotherapy and immunogenic cancer cell death: sharpening the sword for improved cancer treatment strategies. Molecular Therapy. 2014;22(2):251–256.

[97] Kaufman HL, Kohlhapp FJ, Zloza A. Oncolytic viruses: a new class of immunotherapy drugs. Nature Reviews Drug Discovery. 2015;14(9):642–662.

[98] Angelova AL, Geletneky K, N*üe*sch JPF, Rommelaere J. Tumor selectivity of oncolytic parvoviruses: from in vitro and animal models to cancer patients. Frontiers in bioengineering and biotechnology. 2015;3:55.

[99] Bartlett DL, Liu Z, Sathaiah M, Ravindranathan R, Guo Z, He Y, et al. Oncolytic viruses as therapeutic cancer vaccines. Molecular cancer. 2013;12(1):1.

[100] Guo ZS, Thorne SH, Bartlett DL. Oncolytic virotherapy: molecular targets in tumor-selective replication and carrier cell-mediated delivery of oncolytic viruses. Biochimica et Biophysica Acta (BBA)-Reviews on Cancer. 2008;1785(2):217–231.

[101] Everts B, van der Poel HG. Replication-selective oncolytic viruses in the treatment of cancer. Cancer gene therapy. 2005;12(2):141–161.

[102] Wollmann G, Rogulin V, Simon I, Rose JK, van den Pol AN. Some attenuated variants of vesicular stomatitis virus show enhanced oncolytic activity against human glioblastoma cells relative to normal brain cells. Journal of virology. 2010;84(3):1563–1573.

[103] Verheije MH, Rottier PJM. Retargeting of Viruses to Generate Oncolytic Agents. Advances in virology. 2012;p. 1153–1174.

[104] Conrad SJ, Essani K. Oncoselectivity in Oncolytic Viruses against Colorectal Cancer. Journal of Cancer Therapy. 2014;5(13):1153–1174.

[105] Meerani S, Yao Y. Oncolytic viruses in cancer therapy. European Journal of Scientific Research. 2010;40(1):156–171.

[106] Matveeva OV, Guo ZS, Shabalina SA, Chumakov PM. Oncolysis by paramyxoviruses: multiple mechanisms contribute to therapeutic efficiency. Molecular Therapy. 2015;2:15011.

[107] Wollmann G, Ozduman K, van den Pol AN. Oncolytic Virus Therapy of Glioblastoma Multiforme–Concepts and Candidates. Cancer journal (Sudbury, Mass). 2012;18(1):69.

[108] Shilpa PS, Kaul R, Bhat S, Sultana N, Pandeshwar P. Oncolytic viruses in head and neck cancer: a new ray of hope in the management protocol. Annals of medical and health sciences research. 2014;4(3):178–184.

[109] Seymour LW, Fisher KD. Oncolytic viruses: finally delivering. British journal of cancer. 2016;114:357–361.

[110] Castleton A, Dey A, Beaton B, Patel B, Aucher A, Davis DM, et al. Human mesenchymal stromal cells deliver systemic oncolytic measles virus to treat acute lymphoblastic leukemia in the presence of humoral immunity. Blood. 2014;123(9):1327–1335.

[111] Crittenden MR, Thanarajasingam U, Vile RG, Gough MJ. Intratumoral immunotherapy: using the tumour against itself. Immunology. 2005;114(1):11–22.

[112] Kim J, Hall RR, Lesniak MS, Ahmed AU. Stem Cell-Based Cell Carrier for Targeted Oncolytic Virotherapy: Translational Opportunity and Open Questions. Viruses. 2015;7(12):6200–6217.

[113] Kim B, Han G, Toley BJ, Kim CK, Rotello VM, Forbes NS. Tuning payload delivery in tumour cylindroids using gold nanoparticles. Nature nanotechnology. 2010;5(6):465–472.

[114] VanSeggelen H, Tantalo DGM, Afsahi A, Hammill JA, Bramson JL. Chimeric antigen receptor–engineered T cells as oncolytic virus carriers. Molecular Therapy – Oncolytics. 2015;2:150014.

[115] Andtbacka RH, Kaufman HL, Collichio F, Amatruda T, Senzer N, Chesney J, et al. Talimogene laherparepvec improves durable response rate in patients with advanced melanoma. Journal of clinical oncology. 2015;33(25):2780–2788.

[116] Babiker HM, Riaz IB, Husnain M, Borad MJ. Oncolytic virotherapy including Rigvir and standard therapies in malignant melanoma. Oncolytic Virotherapy. 2017;6:11.

[117] Carrington C. Oral targeted therapy for cancer. Australian prescriber. 2015;38(5):78.

[118] O'Hare T, Corbin AS, Druker BJ. Targeted CML therapy: controlling drug resistance, seeking cure. Current opinion in genetics & development. 2006;16(1):92–99.

[119] Komarova NL, Burger JA, Wodarz D. Evolution of ibrutinib resistance in chronic lymphocytic leukemia (CLL). Proceedings of the National Academy of Sciences. 2014;111(38):13906–13911.

[120] Wodarz D, Garg N, Komarova NL, Benjamini O, Keating MJ, Wierda WG, et al. Kinetics of CLL cells in tissues and blood during therapy with the BTK inhibitor ibrutinib. Blood. 2014;123(26):4132–4135.

[121] Wang ML, Rule S, Martin P, Goy A, Auer R, Kahl BS, et al. Targeting BTK with ibrutinib in relapsed or refractory mantle-cell lymphoma. New England Journal of Medicine. 2013;369(6):507–516.

[122] Kuznetsov VA. Basic models of tumor-immune system interactions identification, analysis and predictions. In: A Survey of Models for Tumor-Immune System Dynamics. Birkhäuser, Boston; 1997. p. 237–294.

[123] Adam, John, Nicola B. A survey of models for tumor-immune system dynamics. Springer Science & Business Media; 2012.

[124] Altrock PM, Liu LL, Michor F. The mathematics of cancer: integrating quantitative models. Nature Reviews Cancer. 2015;18(12):730–745.

[125] Adam JA. The dynamic of growth-factor-modified immune response to cancer growth: one dimensional model. Mathematical Computational Modelling. 1993;17(3):83–106.

[126] de Pillis LG, Radunskaya AE, Wiseman CL. A validated mathematical model of cell-mediated immune response to tumour growth. Cancer Research. 2005;65(17):7950–7958.

[127] Banerjee S, Sarkar RP. Delay-induced model for tumour-immune interaction and control of malignant tumour growth. Biological System. 2008;91(1):268–288.

[128] Kirschner D, Panetta JC. Modeling immunotherapy of the tumor-immune interaction. Journal of Mathematical Biology. 1998;37(3):235–252.

[129] Kolev M. Mathematical modelling of the competition between tumors and immune system considering the role of the antibodies. Mathematical and Computer Modelling. 2003;37(11):1143–1152.

[130] Mallet DG, de Pillis LG. A cellular automata model of tumour-immune system interactions. Journal of Theoretical Biology. 2006;239(3):334–350.

[131] de Pillis LG, Eladdadi A, Radunskaya AE. Modeling cancer-immune responses to therapy. Journal of pharmacokinetics and pharmacodynamics. 2014;41(5):461–478.

[132] Eftimie R, Bramson JL. Interactions between the immune system and cancer: a brief review of non-spatial mathematical models. Bulletin Mathematical Biology. 2011;73(1):2–32.

[133] Eladdadi A, Kim P, Mallet D, editors. Mathematical Modeling of Tumor-Immune System Dynamics. vol. 107. Springer, Proceedings in Mathematics & Statistics; 2014.

[134] Altrock PM, Liu LL, Michor F. The Mathematics Of Cancer: Integrating Quantitative Models. Nature Review Cancer. 2015;15(12):730–745.

[135] Webb SD, Sherratt JA, Fish RG. Cells behaving badly: a theoretical model for the Fas/FasL system in tumour immunology. Mathematical Biosciences. 2002;179(2):113–129.

[136] Vianello F, Papeta N, Chen T, Kraft P, White N, Hart W, et al. Murine B16 melanomas expressing high levels of the chemokine stromal-derived factor$-1/CXCL12$ induce tumor-specific T cell chemorepulsion and escape from immune control. Journal of immunology. 2006;176(5):2902–2914.

[137] Lugini L, Cecchetti S, Huber V, Luciani F, Macchia G, Spadaro F, et al. Immune surveillance properties of human NK cell-derived exosomes. The Journal of Immunology. 2012;189(6):2833–2842.

[138] Downs-Canner S, Guo ZS, Ravindranathan R, Breitbach CJ, O'Malley ME, Jones HL, et al. Phase I Study of Intravenous Oncolytic Poxvirus (vvDD) in Patients with Advanced Solid Cancers. Molecular Therapy. 2016;24(8):1492–1501.

[139] Onishi T, Tazawa H, Hashimoto Y, Takeuchi M, Otani T, Nakamura S, et al. Tumor-specific delivery of biologics by a novel T-cell line HOZOT. Scientific Reports. 2016;6:38060.

[140] Keller BA, Bell JC. Oncolytic viruses–immunotherapeutics on the rise. Journal of Molecular Medicine. 2016;94(9):979–991.

[141] Elsedawy NB, Russell SJ. Oncolytic vaccines. Expert review of vaccines. 2013;12(10):1155–1172.

[142] Wongthida P, Diaz RM, Pulido C, Rommelfanger D, Galivo F, Kaluza K, et al. Activating systemic T-cell immunity against self tumor antigens to support oncolytic virotherapy with vesicular stomatitis virus. Human gene therapy. 2011;22(11):1343–1353.

[143] Okamoto KW, Amarasekare P, Petty IT. Modeling oncolytic virotherapy: Is complete tumor-tropism too much of a good thing? Journal of theoretical biology. 2014;358:166–178.

[144] Eftimie R, Dushoff J, Bridle BW, Bramson JL, Earn DJD. Multi-stability and multi-instability phenomena in a mathematical model of tumor-immune-virus interactions. Bulletin of mathematical biology. 2011;73(12):2932–2961.

[145] Bridle BW, Stephenson KB, Boudreau JE, Koshy S, Kazdhan N, Pullenayegum E, et al. Potentiating cancer immunotherapy using an oncolytic virus. Molecular Therapy. 2010;18(8):1430–1439.

[146] van de Ven AL, Wu M, Lowengrub J, McDougall SR, Chaplain MA, Cristini V, et al. Integrated intravital microscopy and mathematical modeling to optimize nanotherapeutics delivery to tumors. AIP advances. 2012;2(1):11208.

[147] Gasselhuber A, Dreher MR, Negussie A, Wood BJ, Rattay F, Haemmerich D. Mathematical spatio-temporal model of drug delivery from low temperature sensitive liposomes during radiofrequency tumour ablation. International Journal of Hyperthermia. 2010;26(5):499–513.

[148] Owen MR, Byrne HM, Lewis CE. Mathematical modelling of the use of macrophages as vehicles for drug delivery to hypoxic tumour sites. Journal of Theoretical Biology. 2004;226(4):377–391.

[149] Webb SD, Owen MR, Byrne HM, Murdoch C, Lewis CE. Macrophage-based anti-cancer therapy: modelling different modes of tumour targeting. Bulletin of Mathematical Biology. 2007;69(5):1747–1776.

[150] Ward JP, King JR. Mathematical modelling of avascular-tumour growth. IMA Journal of Mathematics Applied in Medicine & Biology. 1997;14(1):39–69.

[151] Ward JP, King JR. Mathematical modelling of avascular-tumour growth II: modelling growth saturation. IMA Journal of Mathematics Applied in Medicine & Biology. 1999;16(2):171–211.

[152] Mahasa KJ, Ouifki R, Eladdadi A, de Pillis L. Mathematical model of tumor–immune surveillance. Journal of Theoretical Biology. 2016;404:312–330.

[153] Wodarz D. Viruses as antitumor weapons: defining conditions for tumor remission. Cancer Research. 2001;61(8):3501–3507.

[154] Reis CL, Pacheco JM, Ennis MK, Dingli D. In silico evolutionary dynamics of tumour virotherapy. Integrative Biology. 2010;2(1):41–45.

[155] Lipniacki T, Hat B, Faeder JR, Hlavacek WS. Stochastic effects and bistability in T cell receptor signaling. Journal of theoretical Biology. 2008;254(1):110–122.

[156] Owen MR, Stamper IJ, Muthana M, Richardson GW, Dobson J, Lewis CE, et al. Mathematical modeling predicts synergistic antitumor effects of combining a macrophage-based, hypoxia-targeted gene therapy with chemotherapy. Cancer research. 2011;71(8):2826–2837.

[157] Rejniak KA, Estrella V, Chen T, Cohen AS, Lloyd MC, Morse DL. The role of tumor tissue architecture in treatment penetration and efficacy: an integrative study. Frontiers in oncology. 2013;3:111.

[158] Swat M, Thomas GL, Belmonte JM, Shirinifard A, Hmeljak D, Glazier JA. Multi-scale modeling of tissues using CompuCell3D. In: Computational Methods in Cell Biology. vol. 110. Academic Press; 2012. p. 325–366.

[159] Paiva LR, Binny C, Ferreira SC, Martins ML. A multiscale mathematical model for oncolytic virotherapy. Cancer research. 2009;69(3):1205–1211.

[160] Swat M, Thomas GL, Belmonte JM, Shirinifard A, Hmeljak D, Glazier JA. Multi-Scale Modeling of Tissues Using CompuCell3D. Computational Methods in Cell Biology, Methods in Cell Biology. 2012;110:325–366.

[161] Mahasa KJ, Eladdadi A, de Pillis L, Ouifki R. Oncolytic potency and reduced virus tumor-specificity in oncolytic virotherapy. A mathematical modelling approach. PloS one. 2017;12(9):e0184347.

[162] Organization WH. Cancer Fact sheet N^{0}297 -Updated February 2015. Accessed: 11-13-2015;Available from: http://www.who.int/mediacentre/factsheets/fs297/en/.

[163] Dunn GP, Bruce AT, Ikeda H, Old LJ, Robert D. Cancer immunoediting: from immunosurveillance to tumor escape. Nature Immunology. 2002;3(11):991–998.

[164] Al-Tameemi M, Chaplain M, d'Onofrio A. Evasion of tumours from the control of the immune system: consequences of brief encounters. Biology Direct. 2012;7(1):31–31.

[165] Baxevanis CN, Perez SA. Cancer Dormancy: A Regulatory Role for Endogenous Immunity in Establishing and Maintaining the Tumor Dormant State. Vaccines. 2015;3(3):597–619.

[166] Koebel CM, Vermi W, Swann JB, Zerafa N, Rodig SJ, Old LJ, et al. Adaptive immunity maintains occult cancer in an equilibrium state. Nature. 2007;450(7171):903–907.

[167] d'Onofrio A. Tumor evasion from immune control: strategies of a MISS to become a MASS. Chaos, Solitons and Fractals. 2007;31(2):261–268.

[168] Screpanti V, Wallin RP, Ljunggren HG, Grandien A. A central role for death receptor-mediated apoptosis in the rejection of tumors by NK cells. The Journal of Immunology. 2001;167(4):2068–2073.

[169] Langers I, Renoux VM, Thiry M, Delvenne P, Jacobs N. Natural killer cells: role in local tumor growth and metastasis. Biologics: targets and therapy. 2012;6:73–82.

[170] Cretney E, Takeda K, Yagita H, Glaccum M, Peschon JJ, Smyth MJ. Increased susceptibility to tumor initiation and metastasis in TNF-related apoptosis-inducing ligand-deficient mice. The Journal of Immunology. 2002;168(3):1356–1361.

[171] Smyth MJ, Cretney E, Takeda K, Wiltrout RH, Sedger LM, Kayagaki N, et al. Tumor necrosis factor-related apoptosis-inducing ligand (TRAIL) contributes to interferon

γ-dependent natural killer cell protection from tumor metastasis. The Journal of experimental medicine. 2001;193(6):661–670.

[172] Arase H, Arase N, Saito T. Fas-mediated cytotoxicity by freshly isolated natural killer cells. The Journal of experimental medicine. 1995;181(3):1235–1238.

[173] Sutlu T, Alici E. Natural killer cell-based immunotherapy in cancer: current insights and future prospects. Journal of internal medicine. 2009;266(2):154–181.

[174] Smyth MJ, Crowe NY, Pellicci DG, Kyparissoudis K, Kelly JM, Takeda K, et al. Sequential production of interferon-γ by NK1.1$^+$ T cells and natural killer cells is essential for the antimetastatic effect of α-galactosylceramide. Blood. 2002;99(4):1259–1266.

[175] Street SEA, Cretney E, Smyth MJ. Perforin and interferon-γ activities independently control tumor initiation, growth, and metastasis. Blood. 2001;97(1):192–197.

[176] Jyothi MD, Khar A. Interleukin-2-induced nitric oxide synthase and nuclear factor-κB activity in activated natural killer cells and the production of interferon-γ. Scandinavian journal of immunology. 2000;52(2):148–155.

[177] Seidel UJE, Schlegel P, Lang P. Natural killer cell mediated antibody-dependent cellular cytotoxicity in tumor immunotherapy with therapeutic antibodies. Frontiers in immunology. 2013;4(76). Available from: http://www.frontiersin.org/alloimmunity_and_transplantation/10.3389/fimmu.2013.00076/abstract.

[178] DiLillo DJ, Ravetch JV. Differential Fc-receptor engagement drives an anti-tumor vaccinal effect. Cell. 2015;161(5):1035–1045.

[179] Gajewski TF, Schreiber H, Fu YX. Innate and adaptive immune cells in the tumor microenvironment. Nature immunology. 2013;14(10):1014–1022.

[180] Pozzi LAM, Maciaszek JW, Rock KL. Both dendritic cells and macrophages can stimulate naive CD8 T cells in vivo to proliferate, develop effector function, and differentiate into memory cells. The Journal of Immunology. 2005;175(4):2071–2081.

[181] Palucka K, Banchereau J. Cancer immunotherapy via dendritic cells. Nature Reviews Cancer. 2012;12(4):265–277.

[182] Palucka K, Banchereau J. Cancer Immunotherapy via Dendritic Cells. In: Interaction of Immune and Cancer Cells. Springer; 2014. p. 75–89.

[183] Rousalova I, Krepela E. Granzyme B-induced apoptosis in cancer cells and its regulation (review). International journal of oncology. 2010;37(6):1361–1378.

[184] Kayagaki N, Yamaguchi N, Nakayama M, Eto H, Okumura K, Yagita H. Type I interferons (IFNs) regulate tumor necrosis factor-related apoptosis-inducing ligand (TRAIL) expression on human T cells: a novel mechanism for the antitumor effects of type I IFNs. The Journal of experimental medicine. 1999;189(9):1451–1460.

[185] Lee S, Margolin K. Cytokines in Cancer Immunotherapy. Cancer. 2011;3(4):3856–3893.

[186] Kumamoto Y, Mattei LM, Sellers S, Payne GW, Iwasaki A. $CD4^+$ T cells support cytotoxic T lymphocyte priming by controlling lymph node input. Proceedings of the National Academy of Sciences. 2011;108(21):8749–8754.

[187] Matter MS, Claus C, Ochsenbein AF. $CD4^+$ T cell help improves $CD8^+$ T cell memory by retained CD27 expression. European journal of immunology. 2008;38(7):1847–1856.

[188] Gulubova M, Manolova I, Kyurkchiev D, Julianov A, Altunkova I. Decrease in intrahepatic $CD56^+$ lymphocytes in gastric and colorectal cancer patients with liver metastases. Apmis. 2009;117(12):870–879.

[189] Jewett A, Arasteh A, Tseng HC, Behel A, Arasteh H, Yang W, et al. Strategies to rescue mesenchymal stem cells (MSCs) and dental pulp stem cells (DPSCs) from NK cell mediated cytotoxicity. The Journal of experimental medicine. 2010;5(3):e9874.

[190] Matzavinos A, Chaplain MAJ, Kuznetsov VA. Mathematical modelling of the spatio-temporal response of cytotoxic T-lymphocytes to a solid tumour. Mathematical Medicine and Biology. 2004;21(1):1–34.

[191] Joshi B, Wang X, Banerjee S, Tian H, Matzavinos A, Chaplain MAJ. On immunotherapies and cancer vaccination protocols: a mathematical modelling approach. Journal of theoretical biology. 2009;259(4):820–827.

[192] Teicher BA. Cancer drug resistance. Springer Science & Business Media; 2007.

[193] Vivier E, Tomasello E, Baratin M, Walzer T, Ugolini S. Functions of natural killer cells. Nature Immunology. 2008;9(5):503–510.

[194] Watzl C, Long EO. Exposing tumor cells to killer cell attack. Nature medicine. 2000;6(8):867–868.

[195] Diefenbach A, Jensen E, Jamieson A, Raulet D. Rae1 and H60 ligands of the NKG2D receptor stimulate tumor immunity. Nature. 2001;413(6852):165–171.

[196] Farnault L, Sanchez C, Baier C, Treut TL, Costello RT. Hematological malignancies escape from NK cell innate immune surveillance: mechanisms and therapeutic implications. Clinical and Developmental Immunology. 2012;2012:1–8.

[197] Arany Z, editor. Differentiating intracellular interactions that induce cytotoxic activity and cytokine release by NK cells. ProQuest; 2007.

[198] Itoh N, Yonehara S, Ishii AI, Yonehara M, Mizushima SI, Sameshima M, et al. The polypeptide encoded by the cDNA for human cell surface antigen Fas can mediate apoptosis. Cell. 1991;66(2):233–243.

[199] Suda T, Takahashi T, Golstein P, Nagata S. Molecular cloning and expression of the Fas ligand, a novel member of the tumor necrosis factor family. Cell. 1993;75(6):1169–1178.

[200] Krammer PH. CD95's deadly mission in the immune system. Nature. 2000;407(6805):789–795.

[201] Zeytun A, Hassuneh M, Nagarkatti M, Nagarkatti PS. Fas-Fas ligand-based interactions between tumor cells and tumor-specific cytotoxic T lymphocytes: a lethal two-way street. Blood. 1997;90(5):1952–1959.

[202] Cai Z, Yang F, Yu L, Yu Z, Jiang L, Wang Q, et al. Activated T cell exosomes promote tumor invasion via Fas signaling pathway. The Journal of Immunology. 2012;188(12):5954–5961.

[203] Khong HT, Restifo NP. Natural selection of tumor variants in the generation of "tumor escape" phenotypes. Nature immunology. 2002;3(11):999–1005.

[204] French LE, Tschopp J. Defective death receptor signaling as a cause of tumor immune escape. In Seminars in cancer biology. 2002;12(1):51–55.

[205] Hirano F, Kaneko K, Tamura H, Dong H, Wang S, Ichikawa M, et al. Blockade of B7-H1 and PD-1 by monoclonal antibodies potentiates cancer therapeutic immunity. Cancer research. 2005;65(3):1089–1096.

[206] Dong H, Strome SE, Salomao DR, Tamura H, Hirano F, Flies DB, et al. Tumor-associated B7-H1 promotes T-cell apoptosis: a potential mechanism of immune evasion. Nature medicine. 2002;8(8):793–800.

[207] Ahmad M, Rees RC, Ali SA. Escape from immunotherapy: possible mechanisms that influence tumor regression/progression. Cancer Immunology, Immunotherapy. 2004;53(10):844–854.

[208] Groth A, Klöss S, von Strandmann EP, Koehl U, Koch J. Mechanisms of tumor and viral immune escape from natural killer cell-mediated surveillance. Journal of innate immunity. 2011;3(4):344–354.

[209] Hassin D, Garber OG, Meiraz A, Schiffenbauer YS, Berke G. Cytotoxic T lymphocyte perforin and Fas ligand working in concert even when Fas ligand lytic action is still not detectable. Immunology. 2011;133(2):190–196.

[210] O'connell J, Bennett MW, O'sullivan GC, Collins JK, Shanahan F. The Fas counterattack: a molecular mechanism of tumor immune privilege. Molecular Medicine. 1997;3(5):294.

[211] Klink M. Interaction of Immune and Cancer Cells. Springer; 2014.

[212] de Pillis LG, Gu W, Radunskaya AE. Mixed immunotherapy and chemotherapy of tumours: modeling, applications and biological interpretations. Journal of Theoretical Biology. 2006;238(4):841–862.

[213] Bubenik J. MHC class I down regulation, tumour escape from immune surveillance and design of therapeutic strategies. Folia Biology (Praha). 2005;51(1):1–2.

[214] Kuznetsov VA, Makalkin IA, Taylor MA, , Perelson AS. Nonlinear dynamics of immunogenic tumors: parameter estimation and global bifurcation analysis. Bulletin of Mathematical Biology. 1994;56(2):295–321.

[215] Jenkins MR, Rudd-Schmidt JA, Lopez JA, Ramsbottom KM, Mannering SI, Andrews DM, et al. Failed CTL/NK cell killing and cytokine hypersecretion are directly linked through prolonged synapse time. The Journal of experimental medicine. 2015;212(3):307–317.

[216] de Pillis L, Fister KR, Gu W, Collins C, Daub M, Gross D, et al. Mathematical model creation for cancer chemo-immunotherapy. Computational and Mathematical Methods in Medicine. 2009;10(3):165–184.

[217] Nielsen N, Odum N, Urso B, Lanier LL, Spee P. Cytotoxicity of CD56(bright) NK cells towards autologous activated $CD4^+$ T cells is mediated through NKG2D, LFA-1 and TRAIL and dampened via CD94/NKG2A. PLoS One. 2012;7(2):e31959.

[218] Louzoun Y, Xue C, Lesinski GB, Friedman A. A mathematical model for pancreatic cancer growth and treatments. Journal of Theoretical Biology. 2014;351:74–82.

[219] Costello RT, Gastaut JA, Olive D. Tumor escape from immune surveillance. Archivum immunologiae et therapiae experimentalis. 1999;47(2):83–88.

[220] Kim R, Emi M, Tanabe K, Uchida Y, Toge T. The role of Fas ligand and transforming growth factor beta in tumor progression: molecular mechanisms of immune privilege via Fas-mediated apoptosis and potential targets for cancer therapy. Cancer. 2004;100(11):2281–2291.

[221] Mamat M, Subiyanto, Kartono A. Mathematical model of cancer treatments using immunotherapy, chemotherapy and biochemotherapy. Applied Mathematical Science. 2009;7(5):247–261.

[222] Linton AD. Introduction to medical-surgical nursing. Elsevier Health Sciences; 2015.

[223] Beerenwinkel N, Schwarz RF, Gerstung M, Markowetz F. Cancer evolution: mathematical models and computational inference. Systematic biology. 2015;1(64):e1–e25.

[224] Koh YT, García-Hernández ML, Kast WM. Tumor immune escape mechanisms. In: Cancer Drug Resistance. Springer; 2006. p. 577–602.

[225] Walker PR, Saas P, Dietrich PY. Role of Fas ligand (CD95L) in immune escape: the tumor cell strikes back. The journal of immunology. 1997;158(10):4521–4524.

[226] Marino S, Hogue IB, Ray CJ, Kirschner DE. A methodology for performing global uncertainty and sensitivity analysis in systems biology. Journal of theoretical biology. 2008;254(1):178–196.

[227] Prestwich RJ, Errington F, Diaz RM, Pandha HS, Harrington KJ, Melcher AA, et al. The case of oncolytic viruses versus the immune system: waiting on the judgment of Solomon. Human gene therapy. 2009;20(10):1119–1132.

[228] Larsen SK, Basse YGPH. NK Cells in the Tumor Microenvironment. Critical Reviews in Oncogenesis. 2014;19(1–2):91–105.

[229] Esendagli G, Bruderek K, Goldmann T, Busche A, Branscheid D, Vollmer E, et al. Malignant and non-malignant lung tissue areas are differentially populated by natural killer cells and regulatory T cells in non-small cell lung cancer. Lung cancer. 2008;59(1):32–40.

[230] Levy EM, Roberti MP, Mordoh J. Natural killer cells in human cancer: from biological functions to clinical applications. Journal of Biomedicine and Biotechnology. 2011;2011.

[231] Iannello A, Raulet DH. Immunosurveillance of senescent cancer cells by natural killer cells. Oncoimmunology. 2014;3(2):e27616.

[232] Albertsson PA, Basse PH, Hokland M, Goldfarb RH, Nagelkerke JF, Nannmark U, et al. NK cells and the tumour microenvironment: implications for NK-cell function and anti-tumour activity. Trends in immunology. 2003;24(11):603–609.

[233] Baginska J, Viry E, Paggetti J, Medves S, Berchem G, Moussay E, et al. The critical role of the tumor microenvironment in shaping natural killer cell-mediated anti-tumor immunity. Frontiers in immunology. 2013;4(490).

[234] Ishigami S, Natsugoe S, Tokuda K, Nakajo A, Che X, Iwashige H, et al. Prognostic value of intratumoral natural killer cells in gastric carcinoma. Cancer. 2000;88(3):577–583.

[235] Halama N, Braun M, Kahlert C, Spille A, Quack C, Rahbari N, et al. Natural killer cells are scarce in colorectal carcinoma tissue despite high levels of chemokines and cytokines. Clinical cancer research. 2011;17(4):678–689.

[236] Villegas FR, Coca S, Villarrubia VG, Jiménez R, Chillón MJ, Jareño J, et al. Prognostic significance of tumor infiltrating natural killer cells subset CD57 in patients with squamous cell lung cancer. Lung cancer. 2002;35(1):23–28.

[237] Anichini A, Mortarini R, Nonaka D, Molla A, Vegetti C, Montaldi E, et al. Association of antigen-processing machinery and HLA antigen phenotype of melanoma cells with survival in American Joint Committee on Cancer stage III and IV melanoma patients. Cancer research. 2006;66(12):6405–6411.

[238] Terunuma H, Deng X, Nishino N, Watanabe K. NK cell-based autologous immune enhancement therapy (AIET) for cancer. Journal of stem cells & regenerative medicine. 2013;9(1):9.

[239] Kim PS, Crivelli JJ, Choi IK, Yun CO, Wares JR. Quantitative impact of immunomodulation versus oncolysis with cytokine-expressing virus therapeutics. Mathematical biosciences and engineering. 2015;12(4):841–858.

[240] Choi JW, Lee YS, Yun CO, Kim SW. Polymeric oncolytic adenovirus for cancer gene therapy. Journal of Controlled Release. 2015;219:181–191.

[241] Workenhe ST, Verschoor ML, Mossman KL. The role of oncolytic virus immunotherapies to subvert cancer immune evasion. Future Oncology. 2015;11(4):675–689.

[242] Woller N, Gürlevik E, Ureche CI, Schumacher A, Kühnel F. Oncolytic viruses as anticancer vaccines. Harnessing Oncolytic Virus-mediated Antitumor Immunity. 2014;4(188):1–13.

[243] Alvarez-Breckenridge CA, Choi BD, Suryadevara CM, Chiocca EA. Potentiating oncolytic viral therapy through an understanding of the initial immune responses to oncolytic viral infection. Current opinion in virology. 2015;25:25–32.

[244] Lichty BD, Stojdl DF, Miller RATL, Frenkel I, Atkins H, Bell JC. Vesicular stomatitis virus: a potential therapeutic virus for the treatment of hematologic malignancy. Human gene therapy. 2004;15(9):821–831.

[245] Msaouel P, Iankov ID, Dispenzieri A, Galanis E. Attenuated oncolytic measles virus strains as cancer therapeutics. Current pharmaceutical biotechnology. 2012;13(9):1732–1741.

[246] Jha BK, Dong B, Nguyen CT, Polyakova I, Silverman RH. Suppression of antiviral innate immunity by sunitinib enhances oncolytic virotherapy. Molecular Therapy. 2013;21(9):1749–1757.

[247] Willmon C, Harrington K, Kottke T, Prestwich R, Melcher A, Vile R. Cell carriers for oncolytic viruses: Fed Ex for cancer therapy. Molecular Therapy. 2009;17(10):1667–1676.

[248] Vähä-Koskela M, Hinkkanen A. Tumor restrictions to oncolytic virus. Biomedicines. 2014;2(2):163–194.

[249] Miller AC, Russell SJ. Heterogeneous delivery is a barrier to the translational advancement of oncolytic virotherapy for treating solid tumors. Virus Adaptation and Treatment. 2014;6(1):11–31.

[250] Smith TT, Roth JC, Friedman GK, Gillespie GY. Oncolytic viral therapy: targeting cancer stem cells. Oncolytic virotherapy. 2014;3:21–33.

[251] Ribacka C, Hemminki A. Virotherapy as an approach against cancer stem cells. Current gene therapy. 2008;8(2):88–96.

[252] Macnamara C, Eftimie R. Memory versus effector immune responses in oncolytic virotherapies. Journal of theoretical biology. 2015;377:1–9.

[253] Carolan LA, Rockman S, Borg K, Guarnaccia T, Reading P, Mosse J, et al. Characterization of the Localized Immune Response in the Respiratory Tract of Ferrets following Infection with Influenza A and B Viruses. Journal of virology. 2016;90(6):2838–2848.

[254] Parato KA, Breitbach CJ, Boeuf FL, Wang J, Storbeck C, Ilkow C, et al. The oncolytic poxvirus JX-594 selectively replicates in and destroys cancer cells driven by genetic pathways commonly activated in cancers. Molecular Therapy. 2012;20(4):749–758.

[255] Friedman A, Tian JP, Fulci G, Chiocca EA, Wang J. Glioma virotherapy: effects of innate immune suppression and increased viral replication capacity. Cancer research. 2006;66(4):2314–2319.

[256] Wu JT, Byrne HM, Kirn DH, Wein LM. Modeling and analysis of a virus that replicates selectively in tumor cells. Bulletin of mathematical biology. 2001;63(4):731–768.

[257] de Pillis LG, Caldwell T, Sarapata E, Williams H. Mathematical Modeling of the Regulatory T Cell Effects on Renal Cell Carcinoma Treatment. Discrete and Continuous Dynamical Systems Series. 2013;18(4):915–943.

[258] Diaz RM, Galivo F, Kottke T, Wongthida P, Qiao J, Thompson J, et al. Oncolytic immunovirotherapy for melanoma using vesicular stomatitis virus. Cancer research. 2007;67(6):2840–2848.

[259] Hastie E, Grdzelishvili VZ. Vesicular stomatitis virus as a flexible platform for oncolytic virotherapy against cancer. Journal of General Virology. 2012;93(12):2529–2545.

[260] Rommelfanger DM, Offord CP, Dev J, Bajzer Z, Vile RG, Dingli D. Dynamics of melanoma tumor therapy with vesicular stomatitis virus: explaining the variability in outcomes using mathematical modeling. Gene therapy. 2012;19(5):543–549.

[261] Ku-Carrillo RA, Delgadillo SE, Chen-Charpentier BM. A mathematical model for the effect of obesity on cancer growth and on the immune system response. Applied Mathematical Modelling. 2016;40(7):4908–4920.

[262] Crivelli JJ, Földes J, Kim PS, Wares JR. A mathematical model for cell cycle-specific cancer virotherapy. Journal of biological dynamics. 2012;6(sup1):104–120.

[263] Wodarz D, Komarova N. Towards predictive computational models of oncolytic virus therapy: basis for experimental validation and model selection. PLoS one. 2009;4(1):e4271.

[264] Wodarz D, Chan CN, Trinité B, Komarova NL, Levy DN. On the laws of virus spread through cell populations. Journal of virology. 2014;88(22):13240–13248.

[265] Enderling H, Chaplain MAJ. Mathematical modeling of tumor growth and treatment. Current pharmaceutical design. 2014;20(30):4934–4940.

[266] Hoeller C, Michielin O, Ascierto PA, Szabo Z, Blank CU. Systematic review of the use of granulocyte–macrophage colony-stimulating factor in patients with advanced melanoma. Cancer Immunology, Immunotherapy. 2016;65(9):1015–1034.

[267] Alkayyal AA, Mahmoud AB, Auer RC. Interleukin-12-expressing oncolytic virus: A promising strategy for cancer immunotherapy. Journal of Taibah University Medical Sciences. 2016;11(3):187–193.

[268] Wiesel M, Walton S, Richter K, Oxenius A. Virusspecific CD8 T cells: activation, differentiation and memory formation. Apmis. 2009;117(5–6):356–381.

[269] Greiner J, Schmitt M, Li L, Giannopoulos K, Bosch K, Schmitt A, et al. Expression of tumor-associated antigens in acute myeloid leukemia: implications for specific immunotherapeutic approaches. Blood. 2006;108(13):4109–4117.

[270] Bridle BW, Boudreau JE, Lichty BD, Brunellière J, Koshy KSS, Bramson JL, et al. Vesicular stomatitis virus as a novel cancer vaccine vector to prime antitumor immunity amenable to rapid boosting with adenovirus. Molecular Therapy. 2009;17(10):1814–1821.

[271] Kaufman HL, Ruby CE, Hughes T, Jr CLS. Current status of granulocyte-macrophage colony-stimulating factor in the immunotherapy of melanoma. Journal for ImmunoTherapy of Cancer. 2014;2(11):1–13.

[272] Ganly I, Mautner V, Balmain A. Productive replication of human adenoviruses in mouse epidermal cells. Journal of virology. 2000;74(6):2895–2899.

[273] Sobol PT, Boudreau JE, Stephenson K, Wan Y, Lichty BD, Mossman KL. Adaptive antiviral immunity is a determinant of the therapeutic success of oncolytic virotherapy. Molecular Therapy. 2011;19(2):335–344.

[274] Krishnamurthy S, Takimoto T, Scroggs RA, Portner A. Differentially regulated interferon response determines the outcome of Newcastle disease virus infection in normal and tumor cell lines. Journal of virology. 2006;80(11):5145–5155.

[275] Stojdl DF, Lichty B, Knowles S, Marius R, Atkins H, Sonenberg N, et al. Exploiting tumor-specific defects in the interferon pathway with a previously unknown oncolytic virus. Nature medicine. 2000;6(7):821–825.

[276] Keller BA, Bell JC. Oncolytic viruses–immunotherapeutics on the rise. Journal of Molecular Medicine. 2016;94(9):979–991.

[277] Ayala-Breton C, Russell LOJ, Russell SJ, Peng KW. Faster replication and higher expression levels of viral glycoproteins give the vesicular stomatitis virus/measles virus hybrid VSV-FH a growth advantage over measles virus. Journal of virology. 2014;88(15):8332–8339.

[278] den Driessche PV, Watmough J. Reproduction numbers and sub-threshold endemic equilibria for compartmental models of disease transmission. Mathematical biosciences. 2002;180(1):29–48.

[279] Nowak M, May R. Virus dynamics: mathematical principles of immunology and virology. London: Oxford University Press; 2000.

[280] Ahmed AU, Rolle CE, Tyler MA, Han Y, Sengupta S, Wainwright DA, et al. Bone Marrow Mesenchymal Stem Cells Loaded With an Oncolytic Adenovirus Suppress the Anti-adenoviral Immune Response in the Cotton Rat Model. Molecular Therapy. 2010;18(10):1846–1856.

[281] Zi Z. Sensitivity analysis approaches applied to systems biology models. IET systems biology. 2011;5(6):336–346.

[282] Harris AL. Hypoxia–a key regulatory factor in tumour growth. Nature Reviews Cancer. 2002;2(1):38–47.

[283] Ž Bajzer, Carr T, Josić K, Russell SJ, Dingli D. Modeling of cancer virotherapy with recombinant measles viruses. Journal of theoretical Biology. 2008;252(1):109–122.

[284] Dingli D, Peng KW, Harvey ME, Greipp PR, O'Connor MK, Cattaneo R, et al. Image-guided radiovirotherapy for multiple myeloma using a recombinant measles virus expressing the thyroidal sodium iodide symporter. Blood. 2004;103(5):1641–1646.

[285] Leveille S, Goulet ML, Lichty BD, Hiscott J. Vesicular stomatitis virus oncolytic treatment interferes with tumor-associated dendritic cell functions and abrogates tumor antigen presentation. Journal of virology. 2011;85(23):12160–12169.

[286] Ruf B, Lauer UM. Assessment of current virotherapeutic application schemes:"hit hard and early" versus "killing softly"? Molecular therapy oncolytics. 2015;2:15018.

[287] Melen GJ, Franco-Luzón L, Ruano D, Á González-Murillo, Alfranca A, Casco F, et al. Influence of carrier cells on the clinical outcome of children with neuroblastoma treated with high dose of oncolytic adenovirus delivered in mesenchymal stem cells. Cancer letters. 2016;371(2):161–170.

[288] Aghi M, Martuza RL. Oncolytic viral therapies–the clinical experience. Oncogene. 2005;24(52):7802–7816.

[289] Turnbull S, West EJ, Scott KJ, Appleton E, Melcher A, Ralph C. Evidence for oncolytic virotherapy: Where have we got to and where are we going? Viruses. 2015;7(12):6291–6312.

[290] Matveeva OV, Guo ZS, Senin VM, Senina AV, Shabalina SA, Chumakov PM. Oncolysis by paramyxoviruses: preclinical and clinical studies. Molecular therapy oncolytics. 2015;2:15017.

[291] Eftimie R, Gillard JJ, Cantrell DA. Mathematical Models for Immunology: Current State of the Art and Future Research Directions. Bulletin of Mathematical Biology. 2015;78:2091–2134.

[292] Msaouel P, Dispenzieri A, Galanis E. Clinical testing of engineered oncolytic measles virus strains in the treatment of cancer: an overview. Current opinion in molecular therapeutics. 2009;11(1):43.

[293] Fiola C, Peeters B, Fournier P, Arnold A, Bucur M, Schirrmacher V. Tumor selective replication of Newcastle disease virus: association with defects of tumor cells in antiviral defence. International journal of cancer. 2006;119(2):328–338.

[294] Tollefson AE, Scaria A, Hermiston TW, Ryerse JS, Wold LJ, Wold WS. The adenovirus death protein (E3-11.6 K) is required at very late stages of infection for efficient cell lysis and release of adenovirus from infected cells. Journal of virology. 1996;70(4):2296–2306.

[295] Tong AW, Senzer N, Cerullo V, Templeton NS, Hemminki A, Nemunaitis J. Oncolytic viruses for induction of anti-tumor immunity. Current pharmaceutical biotechnology. 2012;13(9):1750–1760.

[296] Yarbro CH, Wujcik D, Gobel BH. Cancer Nursing. 7th ed. Jones and Bartlett Publishers, Sudbury; 2011.

[297] Chang W, Crowl L, Malm E, Todd-Brown K, Thomas L, Vrable M. Analyzing Immunotherapy and Chemotherapy of Tumors Through Mathematical Modeling. Department of Mathematics, Harvey-Mudd University, Claremont, Calif, USA. 2003;.

[298] Baba AI, Câtoi C. Tumor cell morphology. In: Comparative Oncology. The Publishing House of the Romanian Academy, Bucharest; 2007. p. 119–125.

[299] Wein LM, Wu JT, Kirn DH. Validation and Analysis of a Mathematical Model of a Replication-competent Oncolytic Virus for Cancer Treatment Implications for Virus Design and Delivery. Cancer research. 2003;63(6):1317–1324.

[300] Power AT, Wang J, Falls TJ, Paterson JM, Parato KA, Lichty BD, et al. Carrier cell-based delivery of an oncolytic virus circumvents antiviral immunity. Molecular Therapy. 2007;15(1):123–130.

[301] Ilett EJ, Prestwich RJ, Kottke T, Errington F, Thompson JM, Harrington KJ, et al. Dendritic cells and T cells deliver oncolytic reovirus for tumour killing despite pre-existing anti-viral immunity. Gene therapy. 2009;16(5):689–699.

[302] Adair RA, Roulstone V, Scott KJ, Morgan R, Nuovo GJ, Fuller M, et al. Cell carriage, delivery, and selective replication of an oncolytic virus in tumor in patients. Science translational medicine. 2012;4(138):138ra77–138ra77.

[303] White CL, Twigger KR, Vidal L, Bono JSD, Coffey M, Heinemann L, et al. Characterization of the adaptive and innate immune response to intravenous oncolytic reovirus (Dearing type 3) during a phase I clinical trial. Gene Therapy. 2008;15(12):911–920.

[304] Iankov ID, Blechacz B, Liu C, Schmeckpeper JD, Tarara JE, Federspiel MJ, et al. Infected cell carriers: a new strategy for systemic delivery of oncolytic measles viruses in cancer virotherapy. Molecular Therapy. 2007;15(1):114–122.

[305] Roy DG, Bell JC. Cell carriers for oncolytic viruses: current challenges and future directions. Oncolytic Virotherapy. 2013;2:47–56.

[306] Breitbach CJ, Burke J, Jonker D, Stephenson J, Haas AR, Chow LQ, et al. Intravenous delivery of a multi-mechanistic cancer-targeted oncolytic poxvirus in humans. Nature. 2011;477(7362):99–102.

[307] Miest TS, Cattaneo R. New viruses for cancer therapy: meeting clinical needs. Nature Reviews Microbiology. 2014;12(1):23–34.

[308] Thorne SH, Negrin RS, Contag CH. Synergistic antitumor effects of immune cell-viral biotherapy. Science. 2006;311(5768):1780–1784.

[309] Sampath P, Li J, Hou W, Chen H, Bartlett DL, Thorne SH. Crosstalk between immune cell and oncolytic vaccinia therapy enhances tumor trafficking and antitumor effects. Molecular Therapy. 2013;21(3):620–628.

[310] Thorne SH, Contag CH. Integrating the biological characteristics of oncolytic viruses and immune cells can optimize therapeutic benefits of cell-based delivery. Gene therapy. 2008;15(10):753–758.

[311] Ong HT, Hasegawa K, Dietz AB, Russell SJ, Peng KW. Evaluation of T cells as carriers for systemic measles virotherapy in the presence of antiviral antibodies. Gene therapy. 2007;14(4):324–333.

[312] Eisenstein S, Chen SH, Pan PY. Immune cells: More than simple carriers for systemic delivery of oncolytic viruses. Oncolytic virotherapy. 2014;3:83.

[313] Schmeel FC, Schmeel LC, Gast SM, Schmidt-Wolf IG. Adoptive immunotherapy strategies with cytokine-induced killer (CIK) cells in the treatment of hematological malignancies. International journal of molecular sciences. 2014;15(8):14632–14648.

[314] Smith GL, Benfield CT, de Motes CM, Mazzon M, Ember SW, Ferguson BJ, et al. Vaccinia virus immune evasion: mechanisms, virulence and immunogenicity. Journal of General Virology. 2013;94(11):2367–2392.

[315] Power AT, Bell JC. Cell-based delivery of oncolytic viruses: a new strategic alliance for a biological strike against cancer. Molecular Therapy. 2007;15(4):660–665.

[316] Jennings VA, Ilett EJ, Scott KJ, West EJ, Vile R, Pandha H, et al. Lymphokine-activated killer and dendritic cell carriage enhances oncolytic reovirus therapy for ovarian cancer by overcoming antibody neutralization in ascites. International Journal of Cancer. 2014;134(5):1091–1101.

[317] Muthana M, Rodrigues S, Chen YY, Welford A, Hughes R, Tazzyman S, et al. Macrophage delivery of an oncolytic virus abolishes tumor regrowth and metastasis after chemotherapy or irradiation. Cancer Research. 2013;73(2):490–945.

[318] Eisenstein S, Coakley BA, Briley-Saebo K, Ma G, Chen HM, Meseck M, et al. Myeloid-derived suppressor cells as a vehicle for tumor-specific oncolytic viral therapy. Cancer research. 2013;73(16):5003–5015.

[319] Qiao J, Wang H, Kottke T, Diaz RM, Willmon C, Hudacek A, et al. Loading of oncolytic vesicular stomatitis virus onto antigen-specific T cells enhances the efficacy of adoptive T-cell therapy of tumors. Gene therapy. 2008;15(8):604–616.

[320] Mader EK, Maeyama Y, Lin Y, Butler GW, Russell HM, Galanis E, et al. Mesenchymal stem cell carriers protect oncolytic measles viruses from antibody neutralization in an orthotopic ovarian cancer therapy model. Clinical Cancer Research. 2009;15(23):7246–7255.

[321] Sonabend AM, Ulosov IV, Tyler MA, Rivera AA, Mathis JM, Lesniak MS. Mesenchymal stem cells effectively deliver an oncolytic adenovirus to intracranial glioma. Stem Cells. 2008;26(3):831–841.

[322] Ong HT, Federspiel MJ, Guo CM, Ooi LL, Russell SJ, Peng KW, et al. Systemically delivered measles virus-infected mesenchymal stem cells can evade host immunity to inhibit liver cancer growth. Journal of hepatology. 2013;59(5):999–1006.

[323] Ahmed AU, Tyler MA, Thaci B, Alexiades NG, Han Y, Ulasov IV, et al. A comparative study of neural and mesenchymal stem cell-based carriers for oncolytic adenovirus in a model of malignant glioma. Molecular pharmaceutics. 2011;8(5):1559–1572.

[324] Komarova S, Kawakami Y, Stoff-Khalili MA, Curiel DT, Pereboeva L. Mesenchymal

progenitor cells as cellular vehicles for delivery of oncolytic adenoviruses. Molecular cancer therapeutics. 2006;5(3):755–766.

[325] Mader EK, Butler G, Dowdy SC, Mariani A, Knutson KL, Federspiel MJ, et al. Optimizing patient derived mesenchymal stem cells as virus carriers for a phase I clinical trial in ovarian cancer. Journal of translational medicine. 2013;11(1):1–14.

[326] Stoff-Khalili MA, Rivera AA, Mathis JM, Banerjee NS, Moon AS, Hess A, et al. Mesenchymal stem cells as a vehicle for targeted delivery of CRAds to lung metastases of breast carcinoma. Breast cancer research and treatment. 2007;105(2):157–167.

[327] Xia X, Ji T, Chen P, Li X, Fang Y, Gao Q, et al. Mesenchymal stem cells as carriers and amplifiers in CRAd delivery to tumors. Molecular cancer. 2011;10(1):134.

[328] Dembinski JL, Spaeth EL, Fueyo J, Gomez-Manzano C, Studeny M, Andreeff M, et al. Reduction of nontarget infection and systemic toxicity by targeted delivery of conditionally replicating viruses transported in mesenchymal stem cells. Cancer gene therapy. 2010;17(4):289–297.

[329] Aurelian L. Oncolytic viruses as immunotherapy: progress and remaining challenges. OncoTargets and therapy. 2016;9:2627–2637.

[330] Ramírez M, García-Castro J, Melen GJ, *Á* González-Murillo, Franco-Luzón L. Patient-derived mesenchymal stem cells as delivery vehicles for oncolytic virotherapy: novel state-of-the-art technology. Oncolytic Virotherapy. 2016;4:149.

[331] de Girolamo L, Lucarelli E, Alessandri G, Avanzini MA, Bernardo ME, Biagi E, et al. Mesenchymal stem/stromal cells: a new "cells as drugs" paradigm. Efficacy and critical aspects in cell therapy. Current pharmaceutical design. 2013;19(13):2459–2473.

[332] Li Z, Zhang C, Weiner LP, Zhang Y, Zhong JF. Molecular characterization of heterogeneous mesenchymal stem cells with single-cell transcriptomes. Biotechnology advances. 2013;31(2):312–317.

[333] de Pillis L, Gallegos A, Radunskaya A. A model of dendritic cell therapy for melanoma. Molecular and Cellular Oncology. 2013;3(56):1–14.

[334] de Pillis LG, Radunskaya AE, Wiseman CL. Comment on: a validated mathematical model of cell-mediated immune response to tumor growth. Cancer research. 2007;67(17):8420–8420.

[335] de Pillis LG, Gu W, Radunskaya AE. Mixed immunotherapy and chemotherapy of tumors: modeling, applications and biological interpretations. Journal of theoretical biology. 2009;238(4):841–862.

[336] Cappuccio A, Elishmereni M, Agur Z. Cancer immunotherapy by interleukin-21: potential treatment strategies evaluated in a mathematical model. Cancer Research. 2006;66(14):7293–7300.

[337] Melero I, Rouzaut A, Motz GT, Coukos G. T-cell and NK-cell infiltration into solid tumors: a key limiting factor for efficacious cancer immunotherapy. Cancer discovery. 2014;4(5):522–526.

[338] Peske JD, Woods AB, Engelhard VH. Control of CD8 T-cell Infiltration into Tumors by Vasculature and Microenvironment. Advances in cancer research. 2015;128:263–307.

[339] de Pillis LG, Radunskaya A. The dynamics of an optimally controlled tumor model: a case study. Mathematical and Computer Modelling. 2003;37(11):1221–1244.

[340] de Pillis L, Caldwell T, Sarapata E, Williams H. Mathematical Modeling of Regulatory T Cell Effects on Renal Cell Carcinoma Treatment. AIMS. 2013;18(4):915–943.

[341] Bhat R, Rommelaere J. Emerging role of Natural killer cells in oncolytic virotherapy. Immunotargets and Therapy. 2015;4:65–77.

[342] Yamano T, Kubo S, Fukumoto M, Yano A, Mawatari-Furukawa Y, Okamura H, et al. Whole cell vaccination using immunogenic cell death by an oncolytic adenovirus is effective against a colorectal cancer model. Molecular Therapy-Oncolytics. 2016;3:16031.

[343] Jewett A, Tseng HC. Tumor Induced Inactivation of Natural Killer Cell Cytotoxic Function; Implication in Growth, Expansion and Differentiation of Cancer Stem Cells. Journal of Cancer. 2011;2:443–457.

[344] Masson F, Calzascia T, Berardino-Besson WD, de Tribolet N, Dietrich PY, Walker PR. Brain microenvironment promotes the final functional maturation of tumor-specific effector CD8$^+$ T cells. The Journal of Immunology. 2007;179(2):845–853.

[345] Thompson ED, Enriquez HL, Fu YX, Engelhard VH. Tumor masses support naive T cell infiltration, activation, and differentiation into effectors. Journal of Experimental Medicine. 2010;207(8):1791–804.

[346] Poleszczuk JT, Luddy KA, Prokopiou S, Robertson-Tessi M, Moros EG, Fishman M, et al. Abscopal Benefits of Localized Radiotherapy Depend on Activated T-cell Trafficking and Distribution between Metastatic Lesions. Cancer Research. 2016;76(5):1009–1018.

[347] Yu S, Li A, Liu Q, Li T, Yuan X, Han X, et al. Chimeric antigen receptor T cells: a novel therapy for solid tumors. Journal of hematology & oncology. 2017;10(1):78.

[348] Jacobsen K, Russell L, Kaur B, Friedman A. Effects of CCN1 and Macrophage Content on Glioma Virotherapy: A Mathematical Model. Bulletin of mathematical biology. 2015;77(6):1–29.

[349] García-Castro J, Alemany R, Cascall*ó* M, Martínez-Quintanilla J, del Mar Arriero M, *Á* Lassaletta, et al. Treatment of metastatic neuroblastoma with systemic oncolytic virotherapy delivered by autologous mesenchymal stem cells: an exploratory study. Cancer gene therapy. 2010;17(7):476–483.

[350] Shashkova EV, May SM, Barry MA. Characterization of human adenovirus serotypes 5, 6, 11, and 35 as anticancer agents. Virology. 2009;394(2):311–320.

[351] Andersen MH, Schrama D, thor Straten P, Becker JC. Cytotoxic T cells. Journal of Investigative Dermatology. 2006;126(1):32–41.

[352] Wilkie KP, Hahnfeldt P. Mathematical models of immune-induced cancer dormancy and the emergence of immune evasion. Interface Focus. 2013;3(4):20130010.

[353] Ahmed AU, Thaci B, Tobias AL, Auffinger B, Zhang L, Cheng Y, et al. A Preclinical Evaluation of Neural Stem CellBased Cell Carrier for Targeted Antiglioma Oncolytic Virotherapy. JNCI Journal of the National Cancer Institute. 2013;105(13):968–977.

[354] Bhat R, Rommelaere J. Emerging role of Natural killer cells in oncolytic virotherapy. ImmunoTargets and Therapy. 2015;4:65–77.

[355] Hammer K, Kazcorowski A, Liu L, Behr M, Schemmer P, Herr I, et al. Engineered adenoviruses combine enhanced oncolysis with improved virus production by mesenchymal stromal carrier cells. International Journal of Cancer. 2015;137(4):978–990.

[356] Gross G, Eshhar Z. Therapeutic Potential of T Cell Chimeric Antigen Receptors (CARs) in Cancer Treatment: Counteracting Off-Tumor Toxicities for Safe CAR T Cell Therapy. Annual review of pharmacology and toxicology. 2016;56:59–83.

[357] Yamanaka N, Okamoto E, Kawamura E, Kato T, Oriyama T, Fujimoto J, et al. Dynamics of normal and injured human liver regeneration after hepatectomy as assessed on the basis of computed tomography and liver function. Hepatology. 1993;18(1):81–86.

[358] Kanada M, Zhang J, Yan L, Sakurai T, Terakawa S. Endothelial cell-initiated extravasation of cancer cells visualized in zebrafish. PeerJ. 2014;2:e688.

[359] Hendry SA, Farnsworth RH, Solomon B, Achen MG, Stacker SA, Fox SB. The Role of the Tumor Vasculature in the Host Immune Response: Implications for Therapeutic Strategies Targeting the Tumor Microenvironment. Frontiers in Immunology. 2016;7:621.

[360] Wagner SC, Ichim TE, Ma H, Szymanski J, Perez JA, Lopez J, et al. Cancer antiangiogenesis vaccines: Is the tumor vasculature antigenically unique? Journal of translational medicine. 2015;13(1):340.

[361] Middleton J, Patterson AM, Gardner L, Schmutz C, Ashton BA. Leukocyte extravasation: chemokine transport and presentation by the endothelium. Blood. 2002;100(12):3853–3860.

[362] He M, Wang S, Wang Y, Wang X. Modeling cell-in-cell structure into its biological significance. Cell Death and Disease. 2013;4:e630.

[363] Chen Y, Wang S, He M, Wang Y, Zhao H, Zhu H, et al. Prevalence of heterotypic tumor/immune cell-in-cell structure in vitro and in vivo leading to formation of aneuploidy. PLoS One. 2013;8(3):e59418.

[364] Overholtzer M, Mailleux AA, Mouneimne G, Normand G, Schnitt SJ, King RW, et al. A nonapoptotic cell death process, entosis, that occurs by cell-in-cell invasion. Cell. 2007;131(5):966–979.

[365] Thorne SH, Liang W, Sampath P, Schmidt T, Sikorski R, Beilhack A, et al. Targeting localized immune suppression within the tumor through repeat cycles of immune cell-oncolytic virus combination therapy. Molecular Therapy. 2010;18(9):1698–1705.

[366] Choi IK, Strauss R, Richter M, Yun CO, Lieber A. Strategies to increase drug penetration in solid tumors. Frontiers in Oncology. 2013;3(193).

[367] Lanitis E, Irving M, Coukos G. Targeting the tumor vasculature to enhance T cell activity. Current Opinion in Immunology. 2015;33:55–63.

[368] Salerno EP, Olson WC, McSkimming C, Shea S, Slingluff CL. T cells in the human metastatic melanoma microenvironment express site-specific homing receptors and retention integrins. International journal of cancer. 2014;134(3):563–574.

[369] Mikucki ME, Skitzki JJ, Frelinger JG, Odunsi K, Gajewski TF, Luster AD, et al. Unlocking tumor vascular barriers with CXCR3: Implications for cancer immunotherapy. Oncoimmunology. 2016;5(5):e1116675.

[370] Mikucki ME, Fisher DT, Matsuzaki J, Skitzki JJ, Gaulin NB, Muhitch JB, et al. Non-redundant requirement for CXCR3 signalling during tumoricidal T-cell trafficking across tumour vascular checkpoints. Nature communications. 2015;6:7458.

[371] Salgado R, Denkert C, Demaria S, Sirtaine N, Klauschen F, Pruneri G, et al. The evaluation of tumor-infiltrating lymphocytes (TILs) in breast cancer: recommendations by an International TILs Working Group 2014. Annals of Oncology. 2015;26(2):259–271.

[372] Facciabene A, Motz GT, Coukos G. T-regulatory cells: key players in tumor immune escape and angiogenesis. Cancer research. 2012;72(9):2162–2171.

[373] Tysome JR, Lemoine NR, Wang Y. Update on oncolytic viral therapy–targeting angiogenesis. OncoTargets and Therapy. 2013;6:1031–1040.

[374] Kottke T, Hall G, Pulido J, Diaz RM, Thompson J, Chong H, et al. Antiangiogenic cancer therapy combined with oncolytic virotherapy leads to regression of established tumors in mice. The Journal of clinical investigation. 2010;120(5):1551–1560.

[375] Kim PS, Lee PP, Levy D. Dynamics and Potential Impact of the Immune Response to Chronic Myelogenous Leukemia. PLoS Computational Biology. 2008;4(6):e1000095.

[376] Castillo-Montiel E, Chimal-Eguía JC, Tello JI, Piñon-Zaráte G, Herrera-Enríquez M, Castell-Rodríguez AE. Enhancing dendritic cell immunotherapy for melanoma using a simple mathematical model. Theoretical Biology and Medical Modelling. 2015;12(1):11.

[377] Yang HM. Mathematical modeling of solid cancer growth with angiogenesis. Theoretical Biology and Medical Modelling. 2012;9(1):2.

[378] Blue CE, Spiller OB, Blackbourn DJ. The relevance of complement to virus biology. Virology. 2004;319(2):176–184.

[379] Biesecker M, Kimn JH, Lu H, Dingli D, Ž Bajzer. Optimization of virotherapy for cancer. Bulletin of mathematical biology. 2010;72(2):469–489.